Scientific Excellence • Resource Protection & Conservation • Benefits for Canadians
Excellence scientifique • Protection et conservation des ressources • Bénéfices aux Canadiens

# Sea Ice Velocity Fields off Labrador and Eastern Newfoundland Derived from Satellite Imagery: 1984-1987

I.K. Peterson

Physical and Chemical Sciences Branch
Scotia-Fundy Region
Department of Fisheries and Oceans

Bedford Institute of Oceanography
P.O. Box 1006
Dartmouth, Nova Scotia
Canada B2Y 4A2

December 1990

**Canadian Technical Report of Hydrography and Ocean Sciences No. 129**

Fisheries and Oceans Pêches et Océans

Canada

## Canadian Technical Report of Hydrography and Ocean Sciences

Technical reports contain scientific and technical information that contributes to existing knowledge but which is not normally appropriate for primary literature. The subject matter is related generally to programs and interests of the Ocean Science and Surveys (OSS) sector of the Department of Fisheries and Oceans.

Technical reports may be cited as full publications. The correct citation appears above the abstract of each report. Each report is abstracted in *Aquatic Sciences and Fisheries Abstracts* and indexed in the Department's annual index to scientific and technical publications.

Technical reports are produced regionally but are numbered nationally. Requests for individual reports will be filled by the issuing establishment listed on the front cover and title page. Out of stock reports will be supplied for a fee by commercial agents.

Regional and headquarters establishments of Ocean Science and Surveys ceased publication of their various report series as of December 1981. A complete listing of these publications is published in the *Canadian Journal of Fisheries and Aquatic Sciences*, Volume 39: Index to Publications 1982. The current series, which begins with report number 1, was initiated in January 1982.

## Rapport technique canadien sur l'hydrographie et les sciences océaniques

Les rapports techniques contiennent des renseignements scientifiques et techniques qui constituent une contribution aux connaissances actuelles, mais qui ne sont pas normalement appropriés pour la publication dans un journal scientifique. Le sujet est généralement lié aux programmes et intérêts du service des Sciences et levés océaniques (SLO) du ministère des Pêches et des Océans.

Les rapports techniques peuvent être cités comme des publications complètes. Le titre exact paraît au-dessus du résumé de chaque rapport. Les rapports techniques sont résumés dans la revue *Résumés des sciences aquatiques et halieutiques*, et ils sont classés dans l'index annuel des publications scientifiques et techniques du Ministère.

Les rapports techniques sont produits à l'échelon régional, mais numérotés à l'échelon national. Les demandes de rapports seront satisfaites par l'établissement auteur dont le nom figure sur la couverture et la page du titre. Les rapports épuisés seront fournis contre rétribution par des agents commerciaux.

Les établissements des Sciences et levés océaniques dans les régions et à l'administration centrale ont cessé de publier leurs diverses séries de rapports en décembre 1981. Une liste complète de ces publications figure dans le volume 39, Index des publications 1982 du *Journal canadien des sciences halieutiques et aquatiques*. La série actuelle a commencé avec la publication du rapport numéro 1 en janvier 1982.

91-03289/

ACKNOWLEDGEMENTS

I wish to thank Linda Payzant for her help with the Image Analysis System, and Moto Ikeda and Simon Prinsenberg for reviewing the manuscript. This study was funded by the Federal Panel on Energy Research and Development, Department of Energy, Mines and Resources.

© Minister of Supply and Services 1990

Cat. No. FS 97-18/129E ISSN 0711-6764

Correct citation for this publication:

Peterson, I.K. 1990. Sea ice velocity fields off Labrador and eastern Newfoundland derived from satellite imagery: 1984-1987. Can. Tech. Rep. Hydrogr. Ocean Sci. No. 129:vi + 85 pp.

Canadian Technical Report of
Hydrography and Ocean Sciences No. 129

December 1990

# SEA ICE VELOCITY FIELDS OFF LABRADOR AND EASTERN NEWFOUNDLAND DERIVED FROM SATELLITE IMAGERY: 1984-1987

by

I.K. Peterson

Physical and Chemical Sciences
Scotia-Fundy Region
Department of Fisheries and Oceans

Bedford Institute of Oceanography
P.O. Box 1006
Dartmouth, Nova Scotia
Canada B2Y 4A2

## ABSTRACT

Peterson, I.K. 1990. Sea ice velocity fields off Labrador and eastern Newfoundland derived from satellite imagery: 1984-1987. Can. Tech. Rep. Hydrogr. Ocean Sci. No. 129:vi + 85 pp.

A data set of 92 ice velocity fields off Labrador and eastern Newfoundland has been produced for the years 1984-1987 using pairs of sequential NOAA/AVHRR visible images, 1 day apart. The digital imagery was geometrically corrected using ephemeris data. The ice velocities are in good agreement with those obtained from satellite-tracked ice beacons. The velocity fields are useful in describing the spatial variability of ice velocity on scales of tens of kilometres or more, and reveal the importance of topographic steering of the currents.

Results from a regression analysis between ice velocity and geostrophic wind, using ice velocities derived from satellite imagery were similar to those using ice velocities derived from ice beacons. Over the Labrador/Newfoundland shelf south of 54.25°N under offshore wind conditions, ice moved at 1.8-2.0% of the geostrophic wind speed, with a negligible turning angle.



## RÉSUMÉ

Peterson, I.K. 1990. Sea ice velocity fields off Labrador and eastern Newfoundland derived from satellite imagery: 1984-1987. Can. Tech. Rep. Hydrogr. Ocean Sci. No. 129:vi + 85 pp.

Un ensemble de données sur 92 champs de vitesses des glaces au large du Labrador et de l'est de Terre-Neuve a été produit pour l'intervalle de 1984 à 1987 à partir de couples d'images séquentielles du AVHRR de la NOAA prises dans le visible à des intervalles de un jour. L'imagerie numérique a fait l'objet d'une correction géométrique à l'aide de données d'éphémérides. Les vitesses des glaces concordent bien avec celles dérivées de balises des glaces poursuivies par satellites. Les champs de vitesses sont utiles pour la description de la variabilité dans l'espace de la vitesse des glaces à des échelles de dizaines de kilomètres ou plus et révèlent l'importance de l'orientation des courants par la topographie.

Les résultats d'une analyse de régression entre les vitesses des glaces et le vent géostrophique à partir des vitesses des glaces obtenues d'après l'imagerie satellite étaient similaires à ceux obtenus lorsque les vitesses des glaces étaient mesurées à l'aide de balises des glaces. Sur la plate-forme continentale du Labrador et de Terre-Neuve au sud de 54,25° de lat. N. dans des conditions de vent de terre, les glaces se déplaçaient à entre 1,8 et 2,0 % de la vitesse du vent géostrophique et avec un angle de braquage négligeable.

TABLE OF CONTENTS

Acknowledgements....ii

Abstract....iii

List of Tables....v

List of Figures....vi

1. Introduction....1

2. Methods....2

3. Ice velocity fields....2

4. Description of Imagery....3

4.1 Topographic effects....4

4.2 Undulations in the Labrador Current....4

4.3 Eddies....5

4.4 Onshore winds....5

5. Mean ice drift and wind effects....5

6. Conclusions....9

7. References....10

Appendix A. Ice velocity fields (1984-1987)....25

Appendix B. Examples of satellite imagery (1984-1987)....73

Appendix C. Geostrophic winds at 52.8°N, 54.7°W (1984-1987)....81

# LIST OF TABLES

Page

Table 1. Summary of daily ice velocity fields derived from NOAA/AVHRR imagery, showing the calendar date and Julian day of the first of the two images in the pair, the number of vectors in the velocity field (N), and the minimum and maximum latitude for the vectors. 11

Table 2. Multiple regression analysis of ice drift $(u_i, v_i)$ vs. geostrophic winds $(u_g, v_g)$, for the regression model

$u_i, v_i = b_0 + b_1 u_g + b_2 v_g + \epsilon$

where positive $u_i$ and $u_g$ are towards 70°T, and positive $v_i$ and $v_g$ are towards 340°T south of 54.25°N. North of 54.25°N, the directions are 45°T and 315°T. The last column shows the standard deviation about the regression. 12

LIST OF FIGURES

Page

Figure 1. Bathymetry off Labrador and Newfoundland (depth contours are in meters). The dots show the locations of the grid points for the geostrophic wind data set. 13

Figure 2. Mean ice drift derived from (a) satellite imagery; (b) satellite-tracked ice beacons. 14

Figure 3. Number of points used to compute the mean ice drift in Fig. 2 for (a) satellite imagery; (b) ice beacons. 15

Figure 4. Mean geostrophic wind associated with mean ice drift in Fig. 2 for (a) satellite imagery; (b) ice beacons. 18

Figure 5. Mean ice drift minus wind effect (1.7% of mean geostrophic wind, 6.8° to the right of the wind) for (a) satellite imagery; (b) ice beacons. 20

Figure 6. U (cross-shore) component and v (longshore) component of ice velocity derived from ice beacons (a,b) and from satellite imagery (c,d) vs. u and v components of geostrophic wind, for offshore wind cases south of 54.25°N. 22

## 1. INTRODUCTION

Sea ice is found over the continental shelf east of Labrador and Newfoundland from about December to July, and represents a mixture of locally formed ice, and ice advected from the north. It is a major hazard for shipping and for hydrocarbon exploration and production activities. In addition, sea ice extent may be important in controlling the number of icebergs reaching the Grand Banks from Baffin Bay, since sea ice protects icebergs from deterioration.

Changes in ice distribution are determined by ice drift and thermodynamic processes. In 1985, BIO initiated a five-year program to monitor ice drift off Labrador and eastern Newfoundland using satellite-tracked ice beacons, in order to study the variability of ice drift, and to obtain data for the development and testing of predictive models of ice motion and distribution. When ice stress is negligible, ice drift measurements can also provide information on surface currents, which is difficult to obtain in ice-infested waters by other means such as hydrographic surveys.

Results from the first three years of the ice beacon program were reported by Peterson and Symonds (1988). The beacons were deployed on drifting ice floes off Labrador by helicopter, and provided 7-10 positions per day, with a gap of about 6 hours between 0 and 6 hours GMT. A total of 28 beacons was deployed by the Bedford Institute of Oceanography in the three years (11 in 1985, 11 in 1986, and 6 in 1987). In addition, 5 beacons were deployed east of Newfoundland by Petro-Canada in 1985 (Nazarenko and Miller, 1986). The beacons remained on the ice for a period of several days to 3 months before the ice melted or the beacons were crushed.

While ice beacons provide continuous time series of ice velocity for individual ice floes, spatial and temporal resolution is limited by the low number of beacons deployed. A second method of obtaining ice drift data is by tracking ice features in sequential satellite images. This method can be used throughout most of the ice season, and using NOAA/AVHRR imagery, provides ice velocity data with a spatial resolution of a few kilometers. However, it can only be done on cloud-free days, which tend to be associated with offshore winds (Peterson and Prinsenberg, 1989).

Digital NOAA/AVHRR data for the Canadian east coast region have been archived by BIO since January 1984, for about one pass per day, at 1800 Z. This report presents ice velocity fields derived from satellite images one day

apart for the winters of 1984 through 1987. Photographs of many of the images used to compute the velocity fields are also shown. Ice velocities from the imagery are compared with those obtained from the ice beacons during the last three winters, 1985 through 1987. Finally, a short analysis of the effect of geostrophic wind on ice velocities obtained using each method is presented.

## 2. METHODS

1. Slides showing the full coverage of the imagery archived for each pass were used to select pairs of sequential images (1 day apart) which are cloud-free over a large fraction of the study area. A total of 92 image pairs was selected: 30 in 1984, 32 in 1985, 18 in 1986, and 12 in 1987 (Table 1).

2. The digital data for visible channel 2 were geometrically corrected using ephemeris data and University of Miami software. The accuracy of this procedure is about 1 km. The data were then sectorized into 2 full resolution images (0.01° latitude / pixel), centred at 49.5°N, 52°W and 54.5°N, 56°W, together extending from 47°N to 57°N. In addition, several infrared images (channel 4) were extracted for 1984, centred at 57.0°N, 54.0°W.

3. When floe sizes exceeded the resolution of the imagery (1 km), individual ice floes were tracked using animation, ie. flickering between the 2 images, with an accuracy in locating the centre of the floe of about 1 km. For smaller floe sizes, patches of floes were tracked instead, probably with an accuracy of 1-3 kilometers. Thus the accuracy of the ice velocities is ±3 cm/s. The velocity fields are plotted in Appendix A, while Appendix B shows some examples of satellite imagery from which the velocities were obtained.

4. The ice velocity fields were compared to geostrophic winds computed by the Atmospheric Environment Service from 6-hourly gridded pressure data from the Fleet Numerical Oceanographic Center (Swail, 1985). Stick plots of geostrophic winds at 52.8°N, 54.7°W for late January to late May, 1984 to 1987 are shown in Appendix C.

## 3. ICE VELOCITY FIELDS

The ice velocity fields are presented in Appendix A. For the years 1985-1987, ice velocities obtained using satellite-tracked ice beacons are also plotted (solid arrowheads). The daily geostrophic wind field for the same period is shown in the upper right hand corner, covering the same area as that in the large map. The daily wind at each grid point was calculated as

the weighted average of the wind components at 1800, 0000, 0600, 1200, and 1800 hours, with weights of 0.125, 0.25, 0.25, 0.25,and 0.125.

For example, consider the velocity fields on March 6-7, and March 10-11, 1985, when ice coverage was high, and there were several ice beacons in the study area. The imagery-derived ice velocities are in good agreement with those derived from the ice beacons, and are useful in determining the spatial scale represented by the ice beacons.

The strong response of ice drift to wind forcing is readily apparent in these examples. On March 6-7, 1985 during high northwesterly winds, there was a strong longshore ice drift of about 40 cm/s. On March 10-11, 1985, both winds and ice drift were weak, except along the shelf edge in the vicinity of the Labrador Current, where there were high along-isobath ice velocities. Other examples of velocity fields on days with weak winds, when the effects of topographic steering could be observed are:

1. April 10, April 21-27, May 21, May 29, 1984; February 17, 1985. There is an eastward flow through Hopedale Saddle.

2. April 25, May 29, 1984. There is a westward flow along the northern side and an eastward flow along the southern side of Hawke Saddle.

3. March 19, 1985. There is a clockwise gyre over Hamilton Bank, and a counterclockwise flow over Hawke Saddle.

4. April 10, 1985. There is a northwestward flow along the western edge of Hamilton Bank, with a westward flow along the northern side and an eastward flow along the southern side of Hawke Saddle.

## 4. DESCRIPTION OF IMAGERY

Photographs of many of the visible satellite images used to obtain the ice velocity fields are shown in Appendix B. Several infrared images showing ocean eddies offshore of the ice edge are also included.

A region of high uniform brightness is generally found in the visible imagery along the coast where depths are less than 100 m, and represents landfast ice, and ice which has been compressed against the coast. Off Labrador, this region is wider north of Hamilton Inlet, than to the south, where the 100 m contour is closer to shore.

In general, the drifting pack ice offshore of the landfast ice appears patchy or diffuse, because of significant concentrations of open water or thin ice. The floes are usually smaller than the resolution of the imagery (1 km),

but in the middle of the ice season (March-April), individual floes larger than 1 km are often visible.

## 4.1 Topographic effects

Features associated with the underlying bottom topography can frequently be seen, particularly during weak winds and when ice concentrations are low so that ice can freely follow the ocean currents. Examples of these are the westward (onshore) flow along the north side of a saddle, and eastward (offshore) flow along the south side:

1. April 26, 1984 (Fig. B3); March 13, 1987 (Fig. B11). A tongue of ice extends eastward along the southern side of Hawke Saddle, located at 53°N (Figure 1).

2. May 30, 1984 (Fig. B4); April 28, 1987 (Fig. B12). A tongue of ice extends westward along the northern side of Hawke Saddle.

## 4.2 Undulations in the Labrador Current

Also during weak winds, undulations in the Labrador Current can be seen between Nain Bank and northern Hamilton Bank, when the ice edge coincides with the Labrador Current. Examples are:

1. March 10 -13, 1985 (Fig. B5-7). A series of 4 undulations is visible on March 10. However, by March 11, the third undulation from the west has virtually disappeared. For the three undulations from March 10 to 13, the mean wavelength was 70 km with a range of 57-86 km, the mean amplitude was 17 km with a range of 14-24 km and the mean phase speed was 16 cm/s.

2. March 20, 1985 (Fig. B8). A series of 3 undulations, with a mean wavelength of 84 km and a mean amplitude of 22 km, is visible along northeast Hamilton Bank. If these undulations are assumed to be the same ones present on March 13, the mean phase speed is 15 cm/s.

3. April 28, 1987 (Fig. B12). An undulation with a wavelength of 73 km and an amplitude of 13 km is visible off northern Hamilton Bank.

In comparison, LeBlond (1982) reported oscillations in the Labrador Current with a mean wavelength of 73 km and mean amplitude of 15 km north of Nain Bank. However, between Hopedale Saddle and Hamilton Bank, the mean wavelength was 49 km and the mean amplitude was 13 km. The overall phase speed was 19 cm/s.

4.3 Eddies

1. April 10, 1984 (Fig. B21). A large dipole vortex is visible in the infrared imagery east of Nain Bank and offshore of the ice edge, with one large anticyclonic eddy on the south side at 57.0°N, 54.5°W, and two small cyclonic eddies on the north side at 57.9°N, 55.0°W and 57.7°N, 55.5°W.

2. April 19, 1984 (Fig. B22). A warm-core eddy centered at 56.6°N, 54.0°W, probably anticyclonic, is visible in the infrared imagery.

3. April 26-27, 1984 (Fig. B23). A series of about 4 cyclonic vortices is visible in the ice field roughly along the 3000 m isobath, between 55°N and 59°N. There is also a fast-growing vortex dipole at 55.1°N, 53.5°W. Two cyclonic vortices can be seen along the ice edge south of Belle Isle Bank (Fig. B13). In the infrared imagery, two anticyclonic warm-core rings are visible at 56.5°N, 53.8°W and 56.9°N, 52.5°W (Peterson, 1987).

4. May 30, 1984 (Fig. B24). In the infrared imagery, a series of about 6 cyclonic vortices is visible along the 3000 m isobath, between 55°N and 59°N.

5. March 10-13, 1985 (Fig. B5-7). A dipole vortex can be seen extending westward along the northern edge of Belle Isle Bank.

6. April 14, 1987 (Fig. B19). A cyclonic arc of ice is visible north of Notre Dame Bank.

4.4 Onshore winds

April 1, 1984 (Fig. B1); Feb 26, 1987 (Fig. B10). These examples show reduced ice extent and high ice concentration following strong onshore winds. As the winds change direction, the ice gradually sloughs off the coast, and breaks into smaller floes (April 10, 1984 (Fig. B2)).

5. MEAN ICE DRIFT AND WIND EFFECTS

The mean ice drift for the winters of 1984 through 1987 was computed by averaging the data for each velocity field into 0.25° latitude by 0.5° longitude squares, and then averaging over all velocity fields (Figure 2). For comparison, the mean ice drift was also calculated from the 33 ice beacons deployed in 1985 to 1987 by computing daily mean ice velocities from linearly interpolated positions at 2100 hours GMT, and then averaging the data into 0.25° latitude by 0.5° longitude squares. The number of points from which the the means were calculated are plotted in Figure 3.

The vector mean winds corresponding to the mean ice velocities for the

imagery data and beacon data are shown in Figure 4. For the imagery data, the mean wind field is quite uniform over the region and is westerly to northwesterly, corresponding to the wind direction most favourable for cloud-free conditions (Peterson and Prinsenberg, 1989). However, the mean wind field for the beacon data is much more variable spatially. There is a tendency for the mean wind to be onshore near the coast, and offshore far from the coast, simply because that is the required wind direction to bring the beacon there. Along the coast of southern Labrador, the mean winds when the ice beacons were there are strong and southward, while over the centre of the Northeast Newfoundland shelf (51°N, 52°W), the mean winds are weak.

Following Thorndike and Colony (1982), the response of ice drift to geostrophic wind can be examined using a regression model of the form

$$U_i = |A| \, e^{i\theta} \, U_g + U_w + \epsilon \qquad (1)$$

where $U_i$ and $U_g$ are daily ice velocities and geostrophic winds (complex), $|A|$ is the scaling factor and $\theta$ is the turning angle. The coefficient (complex) $U_w$ is termed the mean current.

At high geostrophic wind speeds, air stress and water stress roughly balance each other, and the free-drift response can be approximated by

$$U_i = (\rho_a c_a / \rho_w c_w)^{1/2} U_a e^{i(\alpha-\beta)} + U_w \qquad (2)$$

where $\rho_a$, $c_a$, $\rho_w$, $c_w$ are the density and drag coefficients for air and water respectively, and $\alpha$ and $\beta$ are turning angles associated with the atmosphere and ocean boundary layers. For the estimates of these parameters given in Thorndike and Colony (1982), the scaling factor $(\rho_a c_a / \rho_w c_w)^{1/2}$ and turning angle $(\alpha-\beta)$ in (2) are 1.5% and 1°. At low wind speeds, the Coriolis force becomes important, so that the turning angle decreases to a minimum of about -66°.

Using mean winds and ice velocities for the ice beacons (Fig. 2b and 4b), regression coefficients in equation (1) were estimated. The scaling factor $|A|$ and turning angle $\theta$ were 1.71% and -6.8° ($r^2$= 0.36), implying that in the absence of a current, ice drifts at 1.71% of the geostrophic wind speed, 6.8° to the right of the wind.

This approach gives equal weight to each grid square, whereas in the original data, most of the points were near the coast. The regression coefficients calculated here are within the range of those calculated for individual buoy tracks in 1985 and 1986 (Peterson and Symonds, 1988). In this earlier study, $|A|$ ranged from 1.1% - 2.3%, $\theta$ from -8 to 23°, and $r^2$ was 0.42

to 0.60.

The scaling factor found here is somewhat larger than that predicted by a free-drift response (1.5%), perhaps because the geostrophic winds used appear to underestimate the true geostrophic wind by 20% (Peterson and Symonds, 1988). Also, the drag coefficent $c_a$ decreases with increasing ice concentration (Anderson, 1987), and ice concentrations are generally higher in the central Arctic than off Labrador and Newfoundland. A large scaling factor may also result from the formation of a coastal jet by longshore winds. The small turning angle ($-6.8^\circ$) is in agreement with that predicted by a free-drift response.

In Fig. 5, the wind effect has been subtracted from the mean ice velocity for both the ice beacons and the imagery, using a scaling factor of 1.71% and a turning angle of $-6.8^\circ$. The effect of topographic steering can clearly be seen, particularly for the imagery.

To study the response of ice drift to wind in more detail, the analysis was confined to the Labrador/Newfoundland shelf, i.e. cases in the Gulf of St. Lawrence, Strait of Belle Isle, and the main core of the Labrador Current were eliminated. Cases along the coast where depths are less than 100 m were also ignored, since landfast ice is often found in these areas. Because of ice stress, the response of ice drift to geostrophic wind is expected to vary with wind direction relative to the longshore direction, and with ice concentration. Therefore the data set was divided into cases north and south of $54.25^\circ$N, the north having higher ice concentrations and a narrower shelf. Onshore and offshore wind cases were considered separately, with an assumed longshore direction of $315^\circ$N in the north and $340^\circ$N in the south. Also, since the response may differ in the longshore vs. cross-shore direction because of wind-generated coastal jets, the regression analysis was done separately for cross-shore and longshore ice velocity components (Table 2).

Low internal ice stress is most likely to be encountered south of $54.25^\circ$N with offshore winds. For this case, the response in the south to offshore winds was similar for the imagery and the beacons, with gains of 1.4-1.5% in the offshore direction, and 2.0-2.1% in the longshore direction. Because of spatial and temporal autocorrelation, the number of degrees of freedom is much less than the number of data points. For the beacons, the number of degrees of freedom is assumed to be the total number of days on which there was beacon data, divided by half to correct for autocorrelation (124/2 = 62), while for

the imagery it was assumed to be the number of velocity fields (92). Using the reduced numbers of degrees of freedom, differences in ice response in the longshore and offshore directions are not statistically significant. Any difference in the cross-shore and longshore directions would most likely occur close to shore. If complex regression coefficients are calculated (equation 1), then the scaling factors and turning angles are 1.82% and 3.75° ($r^2$=0.37) for the imagery and 1.96% and -0.51° ($r^2$=0.54) for the beacons, with a residual current of 7-8 cm/s southwards in both cases.

Each velocity component was plotted against the corresponding geostrophic wind component for the offshore wind cases south of 54.25°N (Fig. 6). Cross-components were not plotted because of the small turning angles involved. Note that the wind speeds are lower for the imagery data than for the beacon data. For the u components, both offshore and onshore wind cases were plotted, but the regression line shown was computed for offshore wind cases only (Fig. 5a,c). For the v components, only offshore wind cases are shown (Fig. 5b,d). The y-intercepts in Fig. 5 correspond to a southward residual current of 5-7 cm/s. There is also the suggestion of a non-linear relationship between geostrophic wind and longshore ice velocity for the beacon data (Fig. 5d).

In general, estimated gains are lower for onshore wind cases and for cases north of 54.25°N (Table 2). As ice piles up against the shore during onshore winds, internal ice stress increases and opposes the ice drift.

The unexplained variance on the shelf south of 54.25°N for offshore wind cases is 172 $cm^2/s^2$ (76 $cm^2/s^2$ offshore and 96 $cm^2/s^2$ longshore) for the imagery, and 285 $cm^2/s^2$ (124 $cm^2/s^2$ offshore and 161 $cm^2/s^2$ longshore) for the beacons (Table 2). The error due to positioning can only account for 21 $cm^2/s^2$ for the imagery assuming a standard deviation of 2 km in both the east-west and north-south directions. For the beacons, the error due to positioning can account for 0.2 $cm^2/s^2$, assuming a standard deviation of 0.2 km in both east-west and north-south directions. In comparison, Petrie and Isenor (1985) found that wind could account for only 10-15% of the variability of daily mean surface currents on the Grand Banks measured with ocean drifters, leaving an unexplained variance of 107 $cm^2/s^2$ (58 $cm^2/s^2$ east-west and 49 $cm^2/s^2$ north-south). However, about 63% of the variance of currents in their study (67 $cm^2/s^2$) could be attributed to error in the position fixes, which was 5 km (standard deviation).

The unexplained variance due to error in the wind estimates can be evaluated using observed winds from ice beacons equipped with anemometers. On-ice wind records longer than 20 days were obtained from 3 ice beacons in 1985-1987: #2341 in 1985, #2525 in 1986, and #3121 in 1987 (Peterson and Symonds, 1988). The r.m.s. errors in geostrophic wind with respect to the observed 2 m winds calculated for the three beacons using complex regression are 5.1 m/s, 5.0 m/s and 5.7 m/s, with $r^2$ values of 0.74 to 0.84. These errors correspond to a variance for estimated ice velocity of about 90 $cm^2/s^2$, using a scaling factor of 1.8%. Thus error in wind estimates can account for half the unexplained variance for the imagery and a third of the unexplained variance for the beacons. Other sources of error are spatial variations in ocean currents, inertial oscillations, eddies, and wind-driven longshore currents near the coast. Also, the air-ice drag coefficient varies with floe size, ice roughness and concentration (Anderson, 1987).

## 6. CONCLUSIONS

1. A data set of 92 daily ice velocity fields off Labrador and eastern Newfoundland has been produced for the years 1984-1987 using sequential NOAA/AVHRR visible images. The digital imagery was geometrically corrected using ephemeris data, with an accuracy of about 1 km.

2. The ice velocities are in good agreement with those obtained from satellite-tracked ice beacons, but their means correspond to different wind conditions.

3. The velocity fields are useful in describing the spatial variability of ice velocity on scales of tens of kilometres or more, and reveal the importance of topographic steering of the currents.

4. Photographs of visible satellite imagery show the effects of topographic steering and onshore winds on ice distribution. The ice also reveals the presence of eddies and undulations in the Labrador Current. Examples of infrared imagery show ocean eddies offshore of the ice edge.

5. Results from a regression analysis between ice velocity and geostrophic wind, using ice velocities derived from satellite imagery were similar to those using ice velocities derived from ice beacons. Over the Labrador/Newfoundland shelf south of 54.25°N, under offshore wind conditions, ice moved at about 1.8-2.0% of the geostrophic wind speed, with a negligible

turning angle. The residual current accounts for a southward ice drift of 7-8 cm/s, or 6-7 km/day. For onshore winds, and cases north of 54.25°N, the gains were less, presumably due to internal ice stress.

## 7. REFERENCES

Anderson, R.J. 1987. Wind stress measurements over rough ice during the 1984 Marginal Ice Zone Experiment. J. Geophys. Res. 92:6933-6941.

LeBlond, P.H. 1982. Satellite observations of Labrador Current undulations. Atmosphere-Ocean 20:129-142.

Nazarenko, D.M. and J.D. Miller. 1986. Sea ice drift measurements using satellite-tracked beacons. In Proceedings of the Canadian East Coast Workshop on Sea Ice, January 7-9, 1986. Can. Tech. Rep. Hydrogr. Ocean Sci. No. 73:583-597.

Peterson ,I.K. 1987. A snapshot of the Labrador Current inferred from ice floe movement in NOAA satellite imagery. Atmosphere-Ocean 25:402-415.

Peterson, I.K. and S.J. Prinsenberg. 1989. Observations of sea ice drift off Newfoundland using satellite imagery and ice beacons. Proceedings of IGARSS '89 Vol. 4:2359-2362.

Peterson, I.K. and G. Symonds. 1988. Ice floe trajectories off Labrador and eastern Newfoundland: 1985-1987. Can. Tech. Rep. Hydrogr. Ocean Sci. No. 104:v+101 pp.

Petrie, B. and A. Isenor. 1985. The near-surface circulation and exchange in the Newfoundland Grand Banks region. Atmosphere-Ocean 23:209-227.

Swail, V.R. 1985. Geostrophic wind climatology of Canadian marine areas. Canadian Climate Centre Report No. 85-9.

Thorndike, A.S. and R. Colony, 1982. Sea ice motion in response to geostrophic winds. J. Geophys. Res. 87:5845-5852.

Table 1. Summary of daily ice velocity fields derived from NOAA/AVHRR imagery, showing the calendar date and Julian day of the first of the two images in the pair, the number of vectors in the velocity field (N), and the minimum and maximum latitude for the vectors.

| Date of 1st Image | Jday | N | Min. Lat. | Max. Lat. |
|---|---|---|---|---|
| FEB 10 1984 | 41 | 63 | 51.77 | 56.85 |
| MAR 2 1984 | 62 | 21 | 51.25 | 52.94 |
| MAR 8 1984 | 68 | 91 | 48.22 | 55.98 |
| MAR 13 1984 | 73 | 96 | 49.10 | 56.90 |
| MAR 18 1984 | 78 | 60 | 51.84 | 56.19 |
| MAR 29 1984 | 89 | 11 | 54.40 | 56.77 |
| MAR 30 1984 | 90 | 7 | 54.12 | 56.30 |
| MAR 31 1984 | 91 | 14 | 51.48 | 56.74 |
| APR 1 1984 | 92 | 47 | 48.82 | 57.01 |
| APR 2 1984 | 93 | 77 | 49.98 | 56.89 |
| APR 3 1984 | 94 | 41 | 48.14 | 56.94 |
| APR 4 1984 | 95 | 33 | 47.90 | 53.27 |
| APR 10 1984 | 101 | 70 | 53.56 | 56.93 |
| APR 16 1984 | 107 | 40 | 51.87 | 57.01 |
| APR 17 1984 | 108 | 40 | 51.14 | 56.98 |
| APR 18 1984 | 109 | 71 | 50.06 | 56.71 |
| APR 19 1984 | 110 | 59 | 47.86 | 56.57 |
| APR 20 1984 | 111 | 7 | 55.32 | 56.76 |
| APR 21 1984 | 112 | 43 | 54.54 | 56.99 |
| APR 22 1984 | 113 | 86 | 49.62 | 56.89 |
| APR 23 1984 | 114 | 85 | 50.85 | 57.02 |
| APR 24 1984 | 115 | 88 | 51.35 | 57.01 |
| APR 25 1984 | 116 | 130 | 50.62 | 56.91 |
| APR 26 1984 | 117 | 139 | 49.73 | 56.96 |
| APR 27 1984 | 118 | 66 | 50.00 | 56.94 |
| MAY 11 1984 | 132 | 96 | 47.55 | 55.32 |
| MAY 21 1984 | 142 | 11 | 55.59 | 56.96 |
| MAY 27 1984 | 148 | 65 | 50.09 | 54.85 |
| MAY 28 1984 | 149 | 60 | 49.72 | 54.73 |
| MAY 29 1984 | 150 | 83 | 51.43 | 56.98 |
| FEB 17 1985 | 48 | 60 | 52.77 | 56.73 |
| FEB 24 1985 | 55 | 63 | 50.82 | 56.87 |
| MAR 6 1985 | 65 | 90 | 47.30 | 56.86 |
| MAR 7 1985 | 66 | 57 | 47.33 | 56.93 |
| MAR 10 1985 | 69 | 302 | 47.20 | 57.01 |
| MAR 11 1985 | 70 | 130 | 49.13 | 56.72 |
| MAR 12 1985 | 71 | 138 | 48.38 | 56.99 |
| MAR 18 1985 | 77 | 40 | 51.31 | 55.10 |
| MAR 19 1985 | 78 | 132 | 50.27 | 56.92 |
| MAR 25 1985 | 84 | 108 | 47.98 | 56.90 |
| MAR 31 1985 | 90 | 51 | 49.16 | 53.95 |
| APR 1 1985 | 91 | 38 | 50.15 | 56.89 |
| APR 2 1985 | 92 | 15 | 50.44 | 56.82 |
| APR 3 1985 | 93 | 41 | 49.51 | 56.53 |
| APR 4 1985 | 94 | 35 | 47.64 | 55.86 |
| APR 5 1985 | 95 | 80 | 47.26 | 56.88 |
| APR 8 1985 | 98 | 69 | 48.27 | 54.54 |
| APR 9 1985 | 99 | 37 | 49.75 | 54.84 |
| APR 10 1985 | 100 | 96 | 49.71 | 56.72 |
| APR 13 1985 | 103 | 47 | 48.17 | 56.81 |
| APR 22 1985 | 112 | 23 | 47.89 | 54.63 |
| APR 27 1985 | 117 | 25 | 50.25 | 55.52 |
| APR 30 1985 | 120 | 21 | 49.49 | 56.14 |
| MAY 1 1985 | 121 | 43 | 49.31 | 54.49 |
| MAY 2 1985 | 122 | 65 | 49.84 | 54.52 |
| MAY 6 1985 | 126 | 66 | 49.26 | 56.06 |
| MAY 11 1985 | 131 | 19 | 50.23 | 53.98 |
| MAY 12 1985 | 132 | 10 | 50.79 | 52.98 |
| MAY 13 1985 | 133 | 14 | 50.76 | 51.85 |
| MAY 14 1985 | 134 | 5 | 50.72 | 51.90 |
| MAY 24 1985 | 144 | 61 | 50.08 | 56.79 |
| MAY 27 1985 | 147 | 42 | 49.54 | 56.22 |
| FEB 14 1986 | 45 | 28 | 48.40 | 54.16 |
| MAR 1 1986 | 60 | 12 | 52.91 | 56.64 |
| MAR 2 1986 | 61 | 12 | 53.25 | 56.15 |
| MAR 3 1986 | 62 | 33 | 48.54 | 56.43 |
| MAR 4 1986 | 63 | 57 | 49.04 | 56.50 |
| MAR 9 1986 | 68 | 17 | 49.14 | 54.77 |
| MAR 13 1986 | 72 | 27 | 47.47 | 53.02 |
| MAR 14 1986 | 73 | 38 | 50.95 | 55.51 |
| MAR 15 1986 | 74 | 49 | 50.79 | 56.86 |
| MAR 16 1986 | 75 | 71 | 47.98 | 56.73 |
| MAR 17 1986 | 76 | 95 | 47.11 | 56.85 |
| MAR 18 1986 | 77 | 43 | 47.21 | 51.88 |
| APR 4 1986 | 94 | 42 | 47.85 | 55.41 |
| APR 5 1986 | 95 | 70 | 48.06 | 56.16 |
| APR 6 1986 | 96 | 50 | 49.66 | 56.48 |
| APR 7 1986 | 97 | 64 | 49.37 | 56.91 |
| APR 8 1986 | 98 | 70 | 47.03 | 56.91 |
| APR 18 1986 | 108 | 41 | 48.11 | 56.68 |
| JAN 30 1987 | 30 | 37 | 49.70 | 56.95 |
| FEB 6 1987 | 37 | 27 | 50.51 | 56.73 |
| FEB 7 1987 | 38 | 52 | 51.11 | 56.94 |
| FEB 12 1987 | 43 | 42 | 48.23 | 53.21 |
| FEB 26 1987 | 57 | 15 | 51.09 | 56.03 |
| MAR 10 1987 | 69 | 38 | 47.00 | 53.71 |
| MAR 13 1987 | 72 | 52 | 49.84 | 56.92 |
| MAR 14 1987 | 73 | 36 | 52.42 | 56.94 |
| MAR 31 1987 | 90 | 48 | 48.02 | 54.88 |
| APR 13 1987 | 103 | 67 | 48.27 | 54.94 |
| APR 27 1987 | 117 | 89 | 49.25 | 56.65 |
| MAY 2 1987 | 122 | 36 | 49.98 | 54.61 |

Table 2. Multiple regression analysis of ice drift ($u_i$,$v_i$) vs. geostrophic winds ($u_g$,$v_g$), for the regression model

$u_i, v_i = b_0 + b_1 u_g + b_2 v_g + \epsilon$

where positive $u_i$ and $u_g$ are towards 70°T, and positive $v_i$ and $v_g$ are towards 340°T south of 54.25°N. North of 54.25°N, the directions are 45°T and 315°T. The last column shows the standard deviation about the regression.

| | $r^2$ | $b_0$ | $b_1$ | $b_2$ | s.d.($\epsilon$) |
|---|---|---|---|---|---|
| South of 54.25°N, offshore winds | | | | | |
| Imagery (N = 2034) | | | | | |
| $u_i$ | 0.23 | -2.37 | 1.42 | -0.02 | 9 |
| $v_i$ | 0.47 | -5.74 | 0.15 | 2.02 | 10 |
| Beacons (N = 340) | | | | | |
| $u_i$ | 0.35 | 0.57 | 1.54 | 0.14 | 11 |
| $v_i$ | 0.63 | -6.71 | 0.02 | 2.09 | 13 |
| South of 54.25°n, onshore winds | | | | | |
| Imagery (N = 845) | | | | | |
| $u_i$ | 0.11 | -1.24 | 0.76 | 0.19 | 9 |
| $v_i$ | 0.37 | -7.78 | -0.01 | 1.37 | 10 |
| Beacons (N = 228) | | | | | |
| $u_i$ | 0.06 | -2.91 | 0.59 | 0.03 | 12 |
| $v_i$ | 0.57 | -7.54 | 0.14 | 1.88 | 16 |
| North of 54.25°N, offshore winds | | | | | |
| Imagery (N = 480) | | | | | |
| $u_i$ | 0.07 | -0.06 | 0.82 | -0.15 | 8 |
| $v_i$ | 0.18 | -4.74 | -0.26 | 1.06 | 10 |
| Beacons (N = 84) | | | | | |
| $u_i$ | 0.41 | -2.33 | 1.90 | 0.13 | 8 |
| $v_i$ | 0.40 | -10.41 | 0.46 | 1.28 | 13 |
| North of 54.25°n, onshore winds | | | | | |
| Imagery (N = 321) | | | | | |
| $u_i$ | 0.09 | 0.29 | 0.83 | -0.08 | 8 |
| $v_i$ | 0.28 | -7.32 | 0.36 | 1.28 | 11 |
| Beacons (N = 92) | | | | | |
| $u_i$ | 0.27 | 3.73 | 1.05 | -0.12 | 13 |
| $v_i$ | 0.44 | -15.75 | 0.05 | 1.87 | 18 |

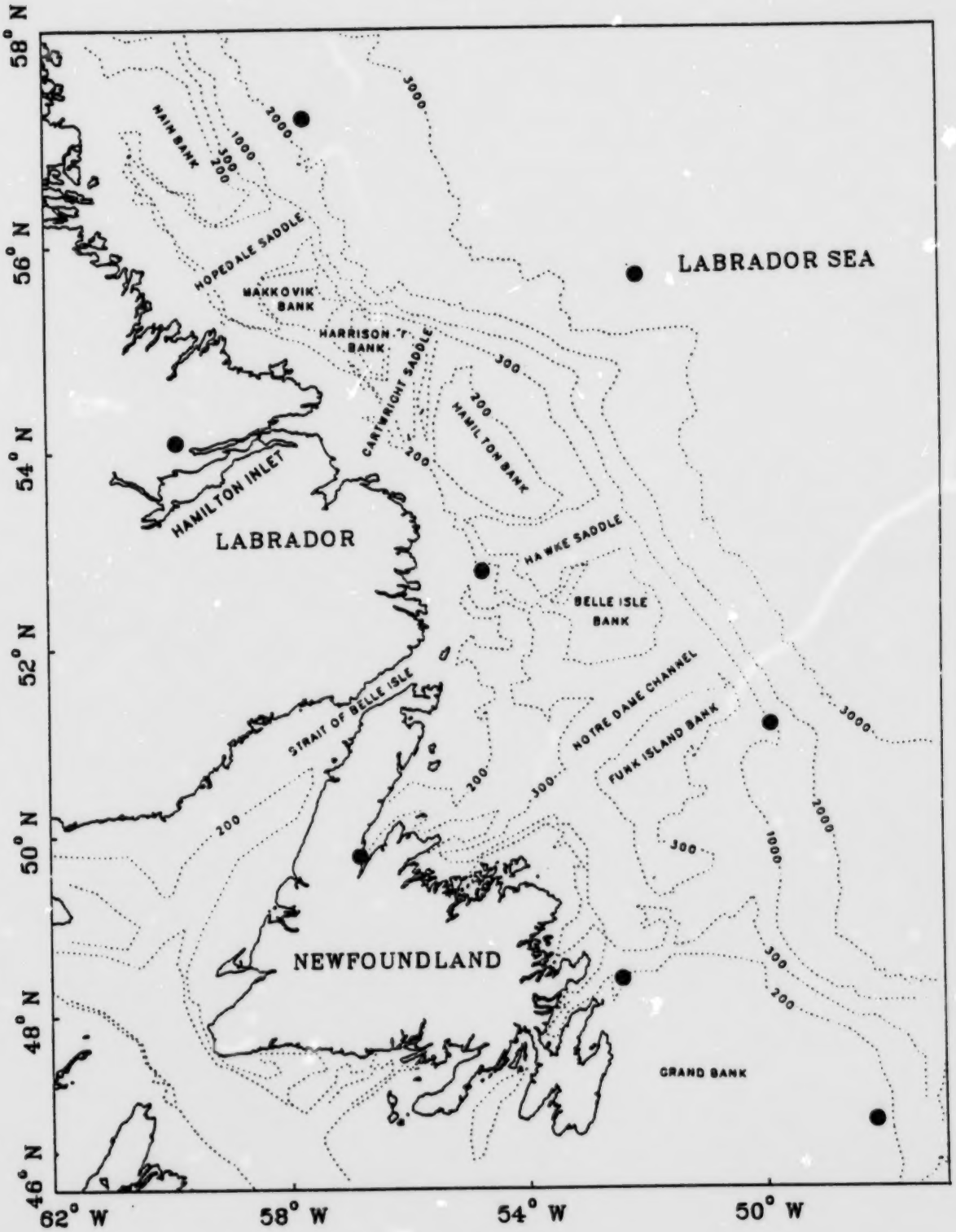


Figure 1. Bathymetry off Labrador and Newfoundland (depth contours are in meters). The dots show the locations of the grid points for the geostrophic wind data set.

# MEAN OF ICE VELOCITY (IMAGERY)

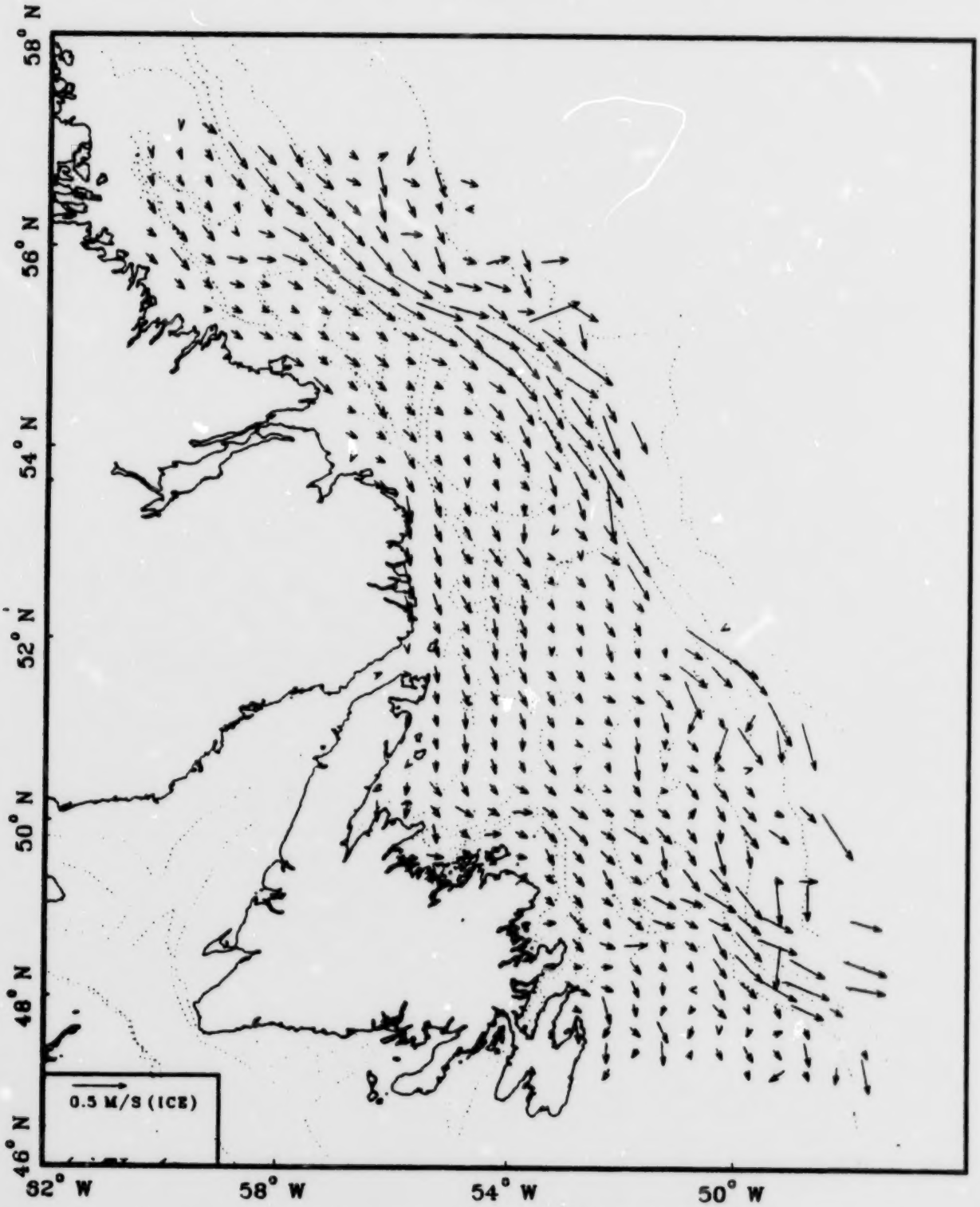


Figure 2(a). Mean ice drift derived from satellite imagery.

# MEAN OF ICE VELOCITY (BEACONS)

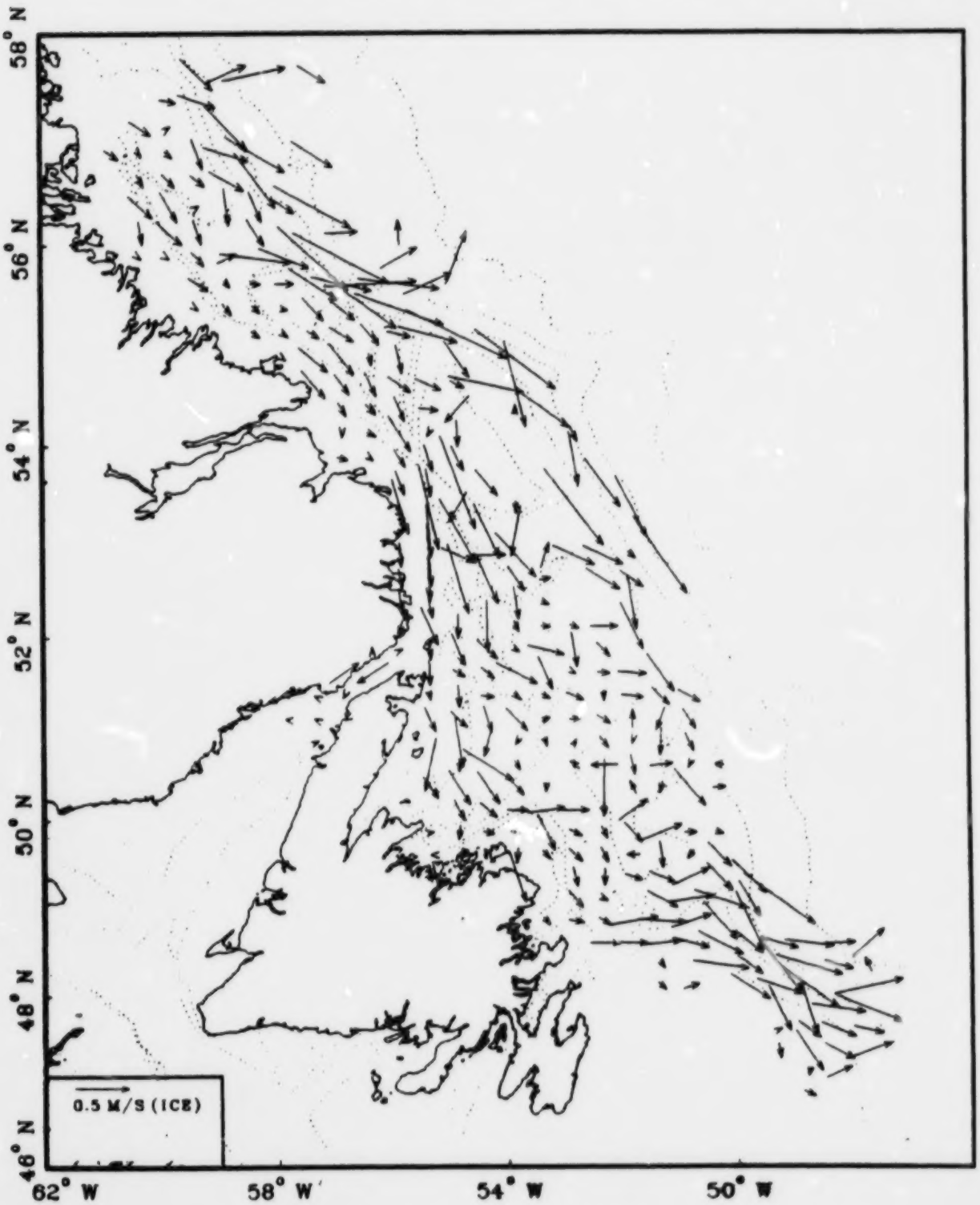


Figure 2(b). Mean ice drift derived from satellite-tracked ice beacons.

# NUMBER OF POINTS (IMAGERY)

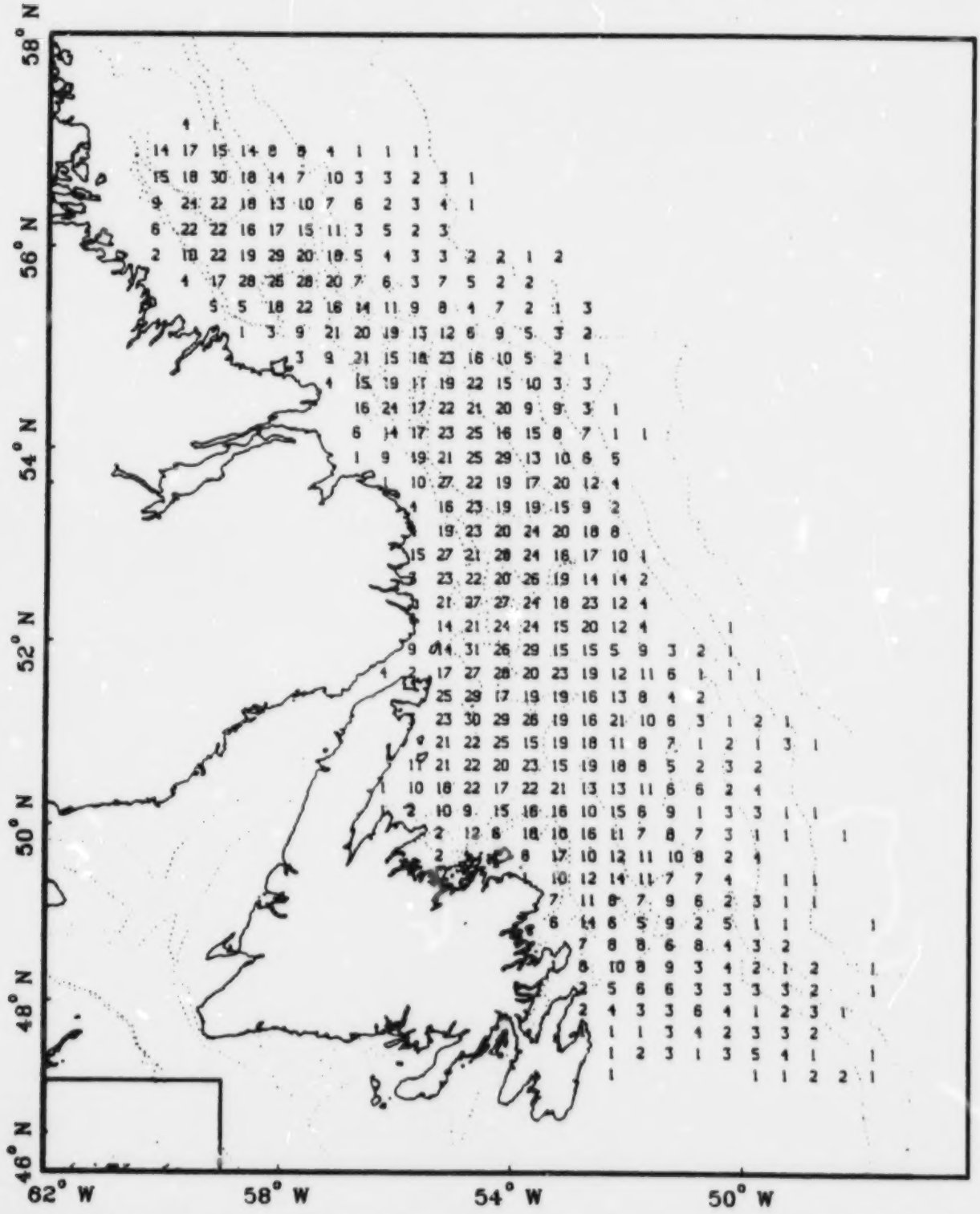


Figure 3(a). Number of points used to compute the mean ice drift in Fig. 2 for satellite imagery.

# NUMBER OF POINTS (BEACONS)

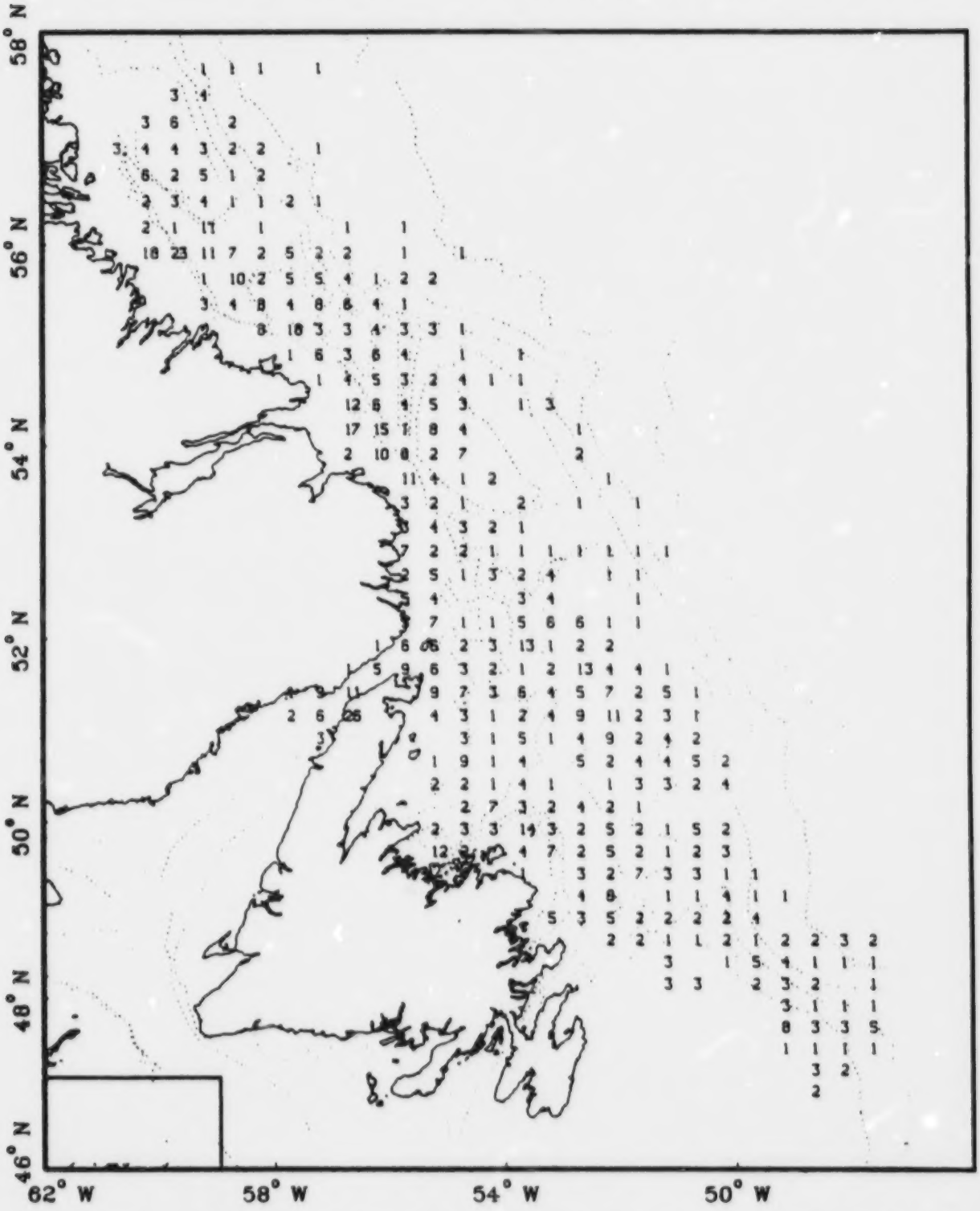


Figure 3(b). Number of points used to compute the mean ice drift in Fig. 2 for ice beacons.

# MEAN OF WIND (IMAGERY)

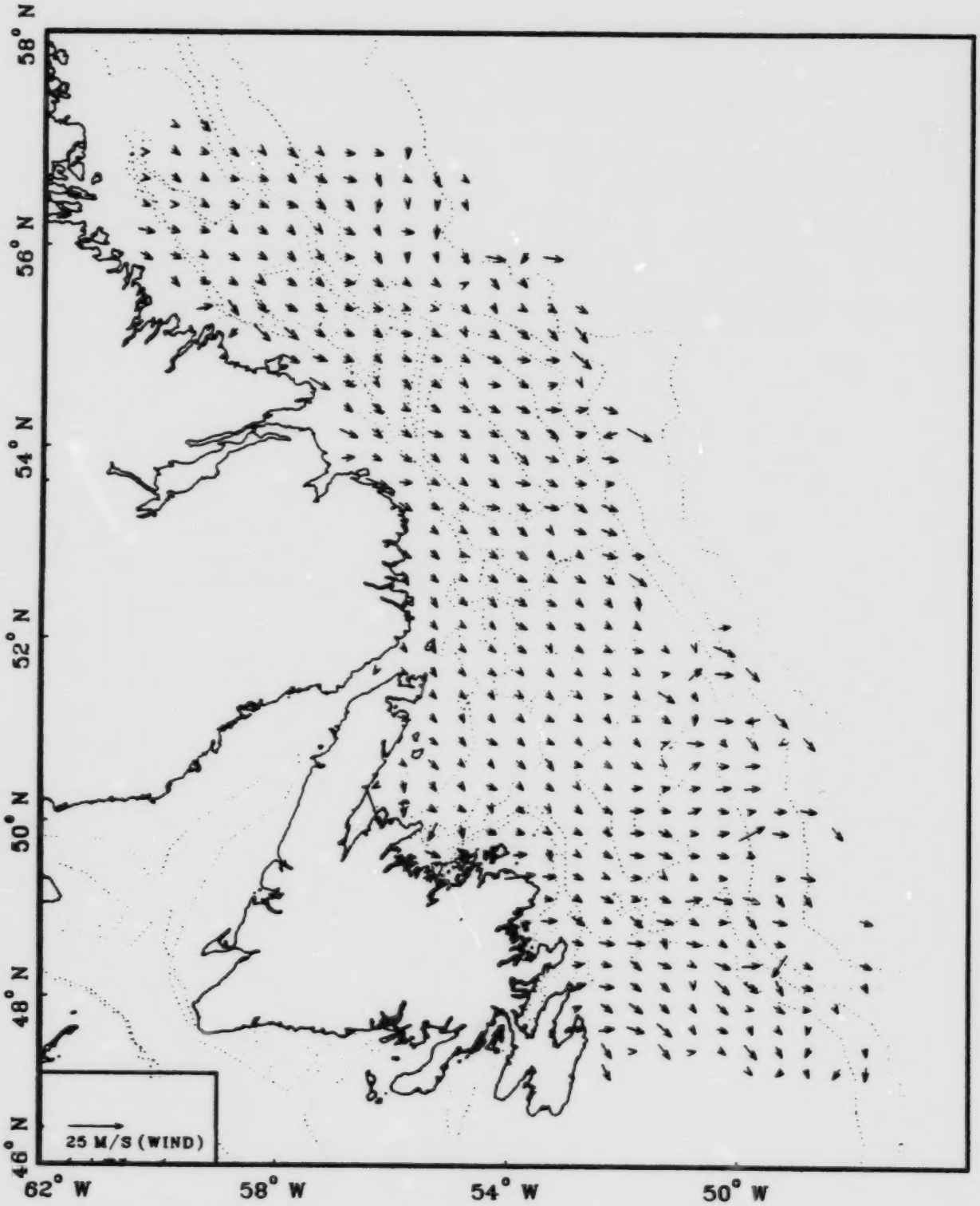


Figure 4(a). Mean geostrophic wind associated with mean ice drift in Fig. 2 for satellite imagery.

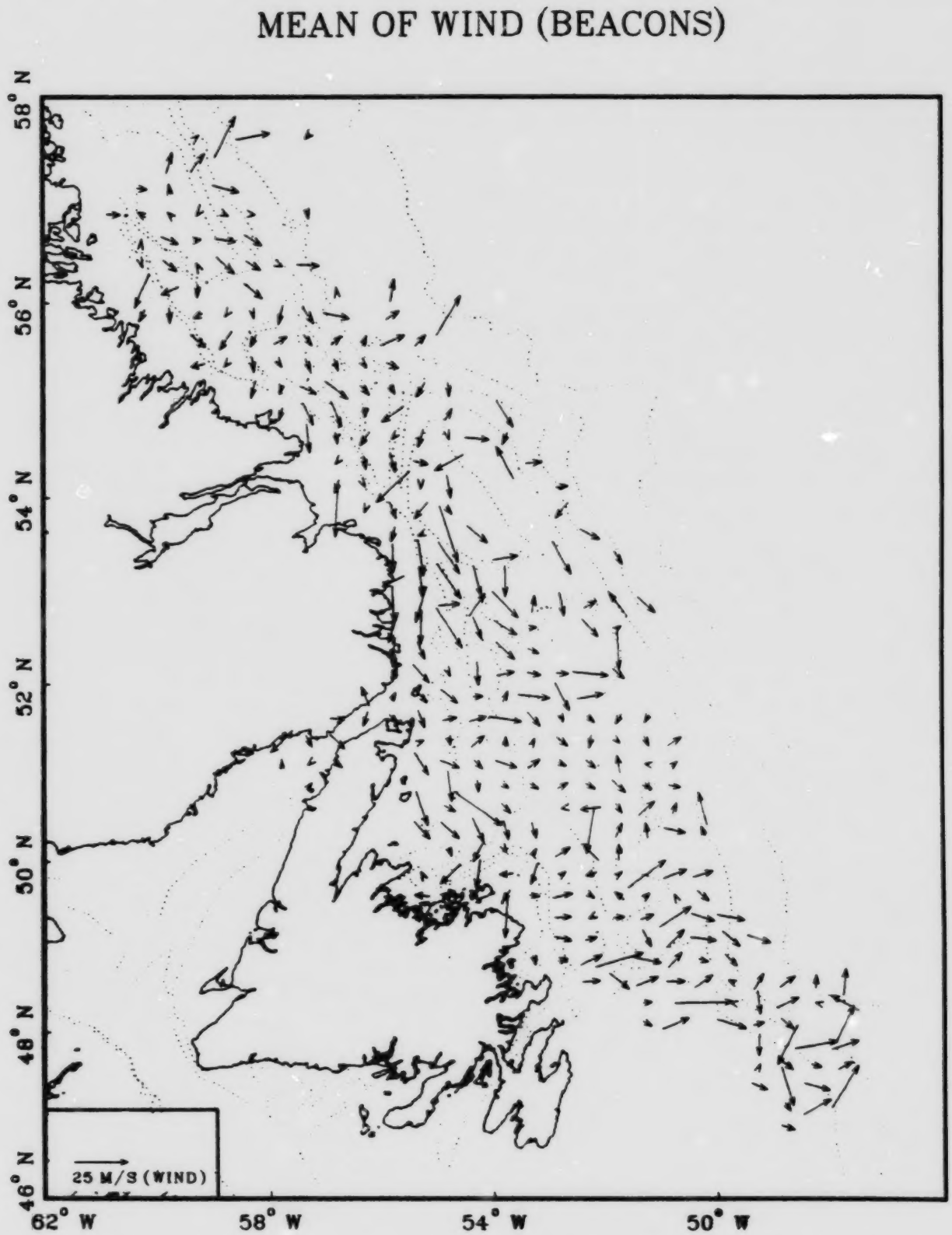


Figure 4(b). Mean geostrophic wind associated with mean ice drift in Fig. 2 for ice beacons.

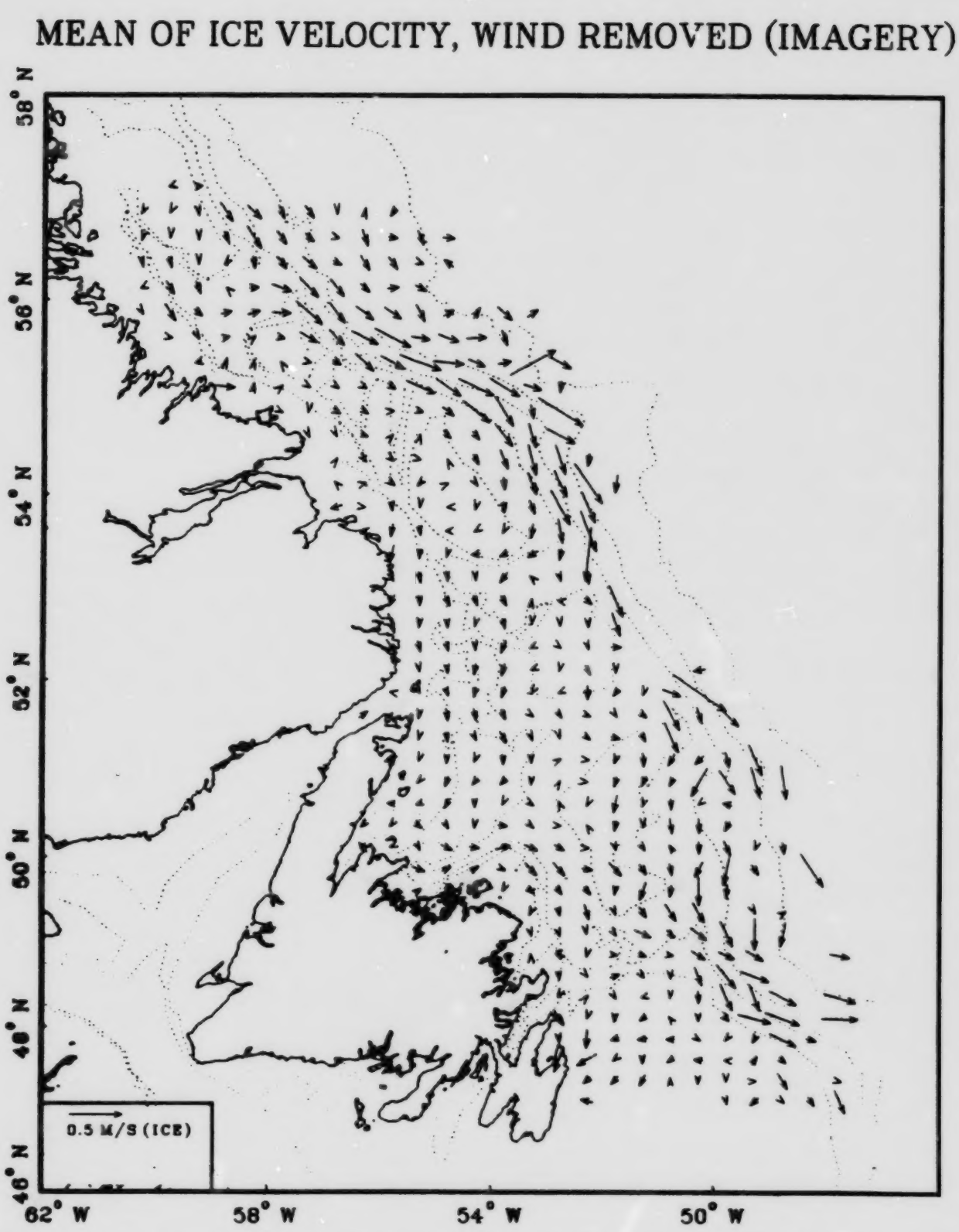


Figure 5(a). Mean ice drift minus wind effect (1.7% of mean geostrophic wind, 6.8° to the right of the wind) for imagery.

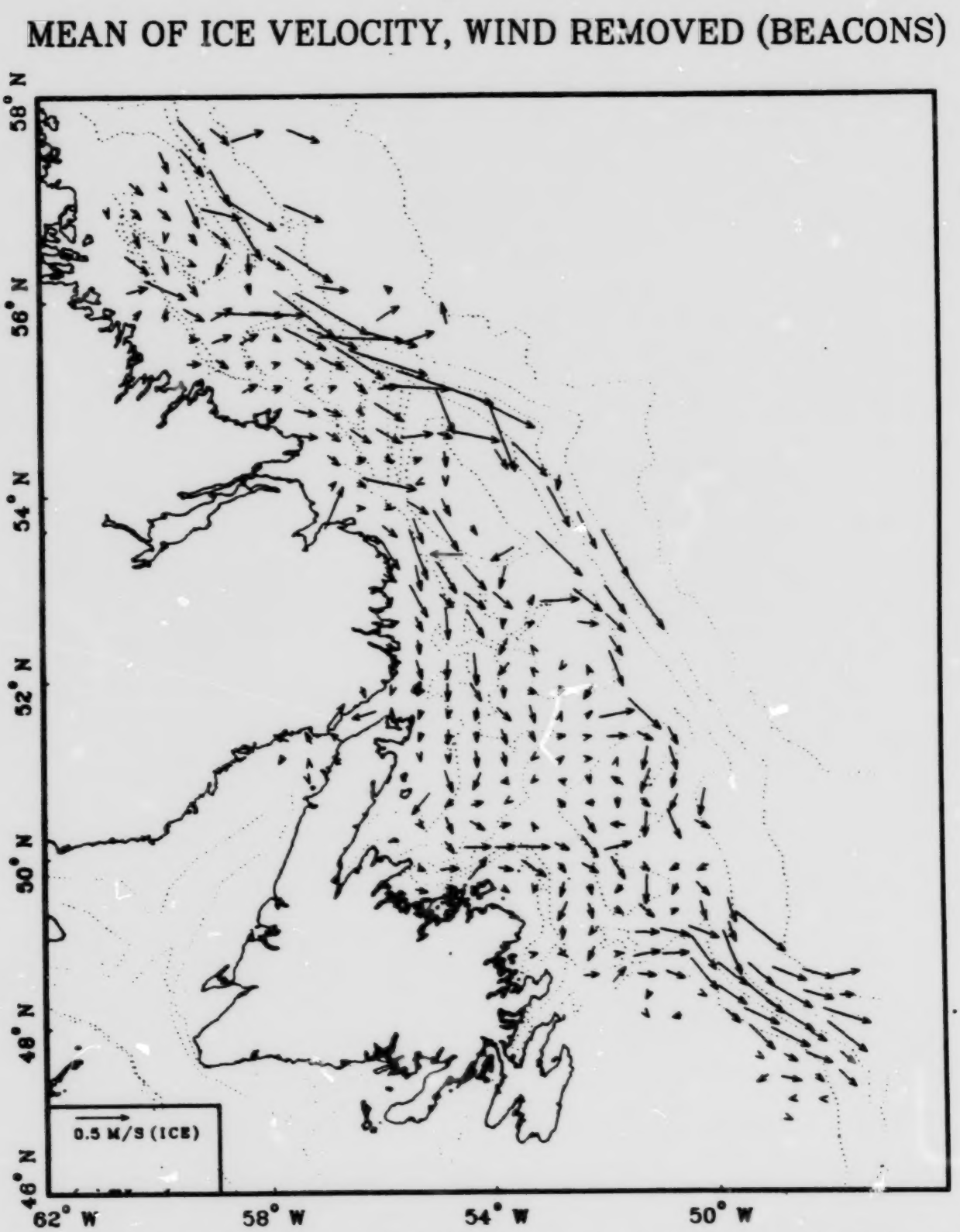


Figure 5(b). Mean ice drift minus wind effect (1.7% of mean geostrophic wind, 6.8° to the right of the wind) for ice beacons.

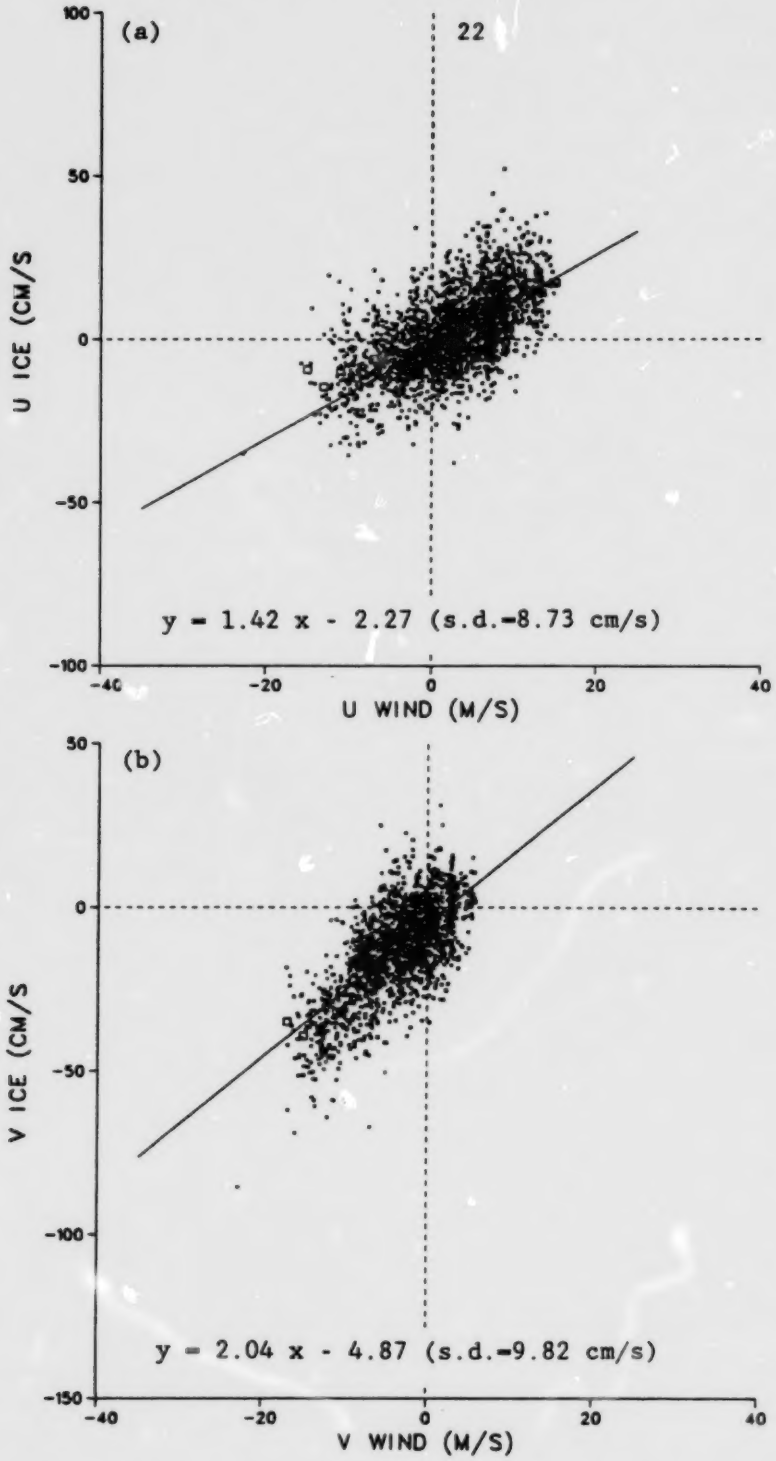


Figure 6. (a) U (cross-shore) component and (b) v (longshore) component of ice velocity derived from satellite imagery, vs. u and v components of geostrophic wind, for offshore wind cases south of 54.25°N. Positive u is toward 70°T and positive v is toward 340°T. In (a), onshore wind cases are plotted, but are not included in regression line. The squares represent mean ice velocities computed in bins of 2 m/s geostrophic winds.

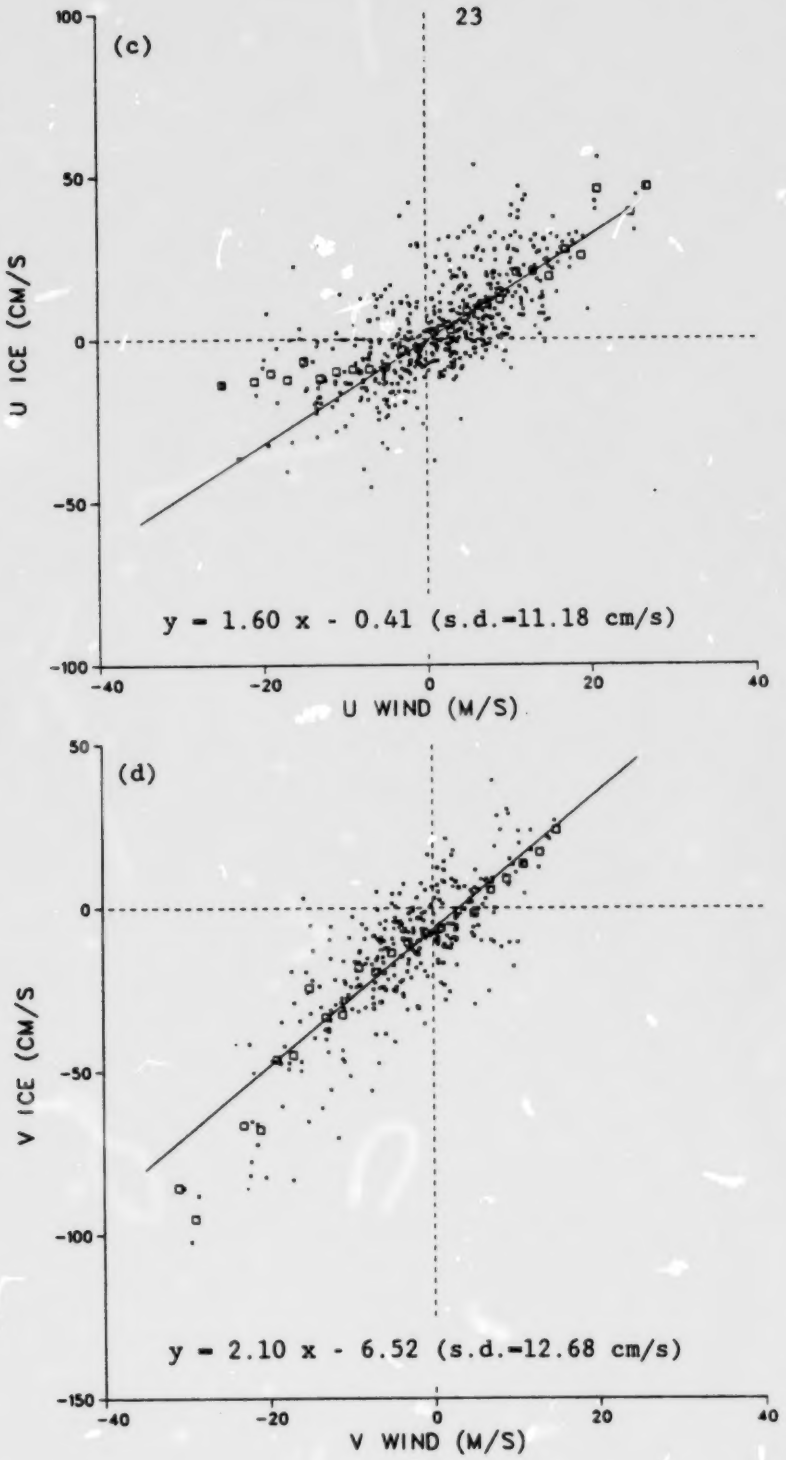


Figure 6. (c) U (cross-shore) component and (d) v (longshore) component of ice velocity derived from ice beacons, vs. u and v components of geostrophic wind, for offshore wind cases south of 54.25°N. Positive u is toward 70°T and positive v is toward 340°T. In (c), onshore wind cases are plotted, but are not included in regression line. The squares represent mean ice velocities computed in bins of 2 m/s geostrophic winds.

Appendix A. Ice velocity fields (1984-1987). The solid arrowheads denote the ice beacon velocities, while the open arrowheads denote the imagery-derived velocities. The geostrophic wind field for the same period is shown in the upper right hand corner, and covers the same area as the large map.

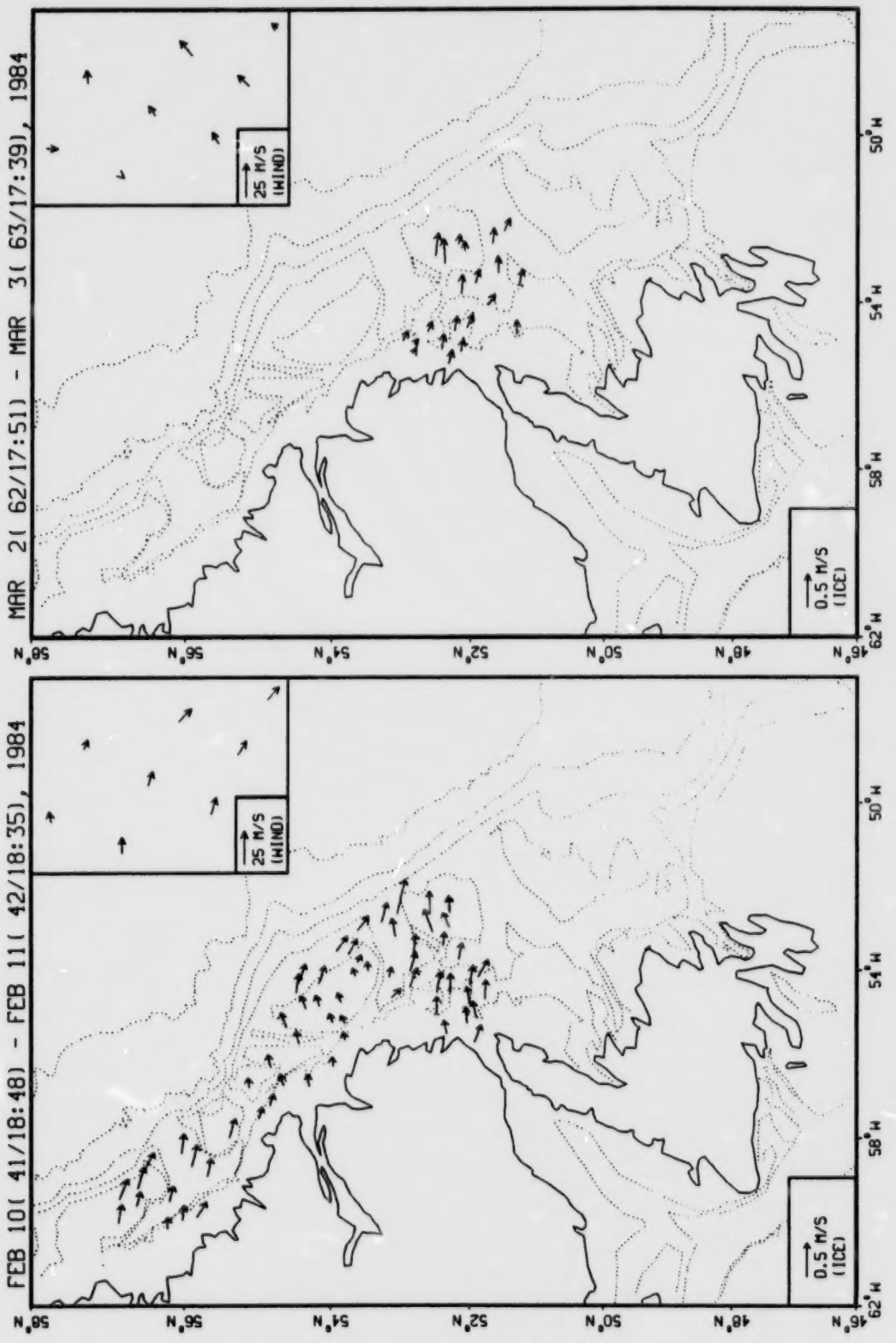
FEB 10( 41/18:48) - FEB 11( 42/18:35), 1984
MAR 2( 62/17:51) - MAR 3( 63/17:39), 1984
25 M/S (WIND)
0.5 M/S (ICE)
62°W
58°W
54°W
50°W
46°N
48°N
50°N
52°N
54°N
56°N
58°N

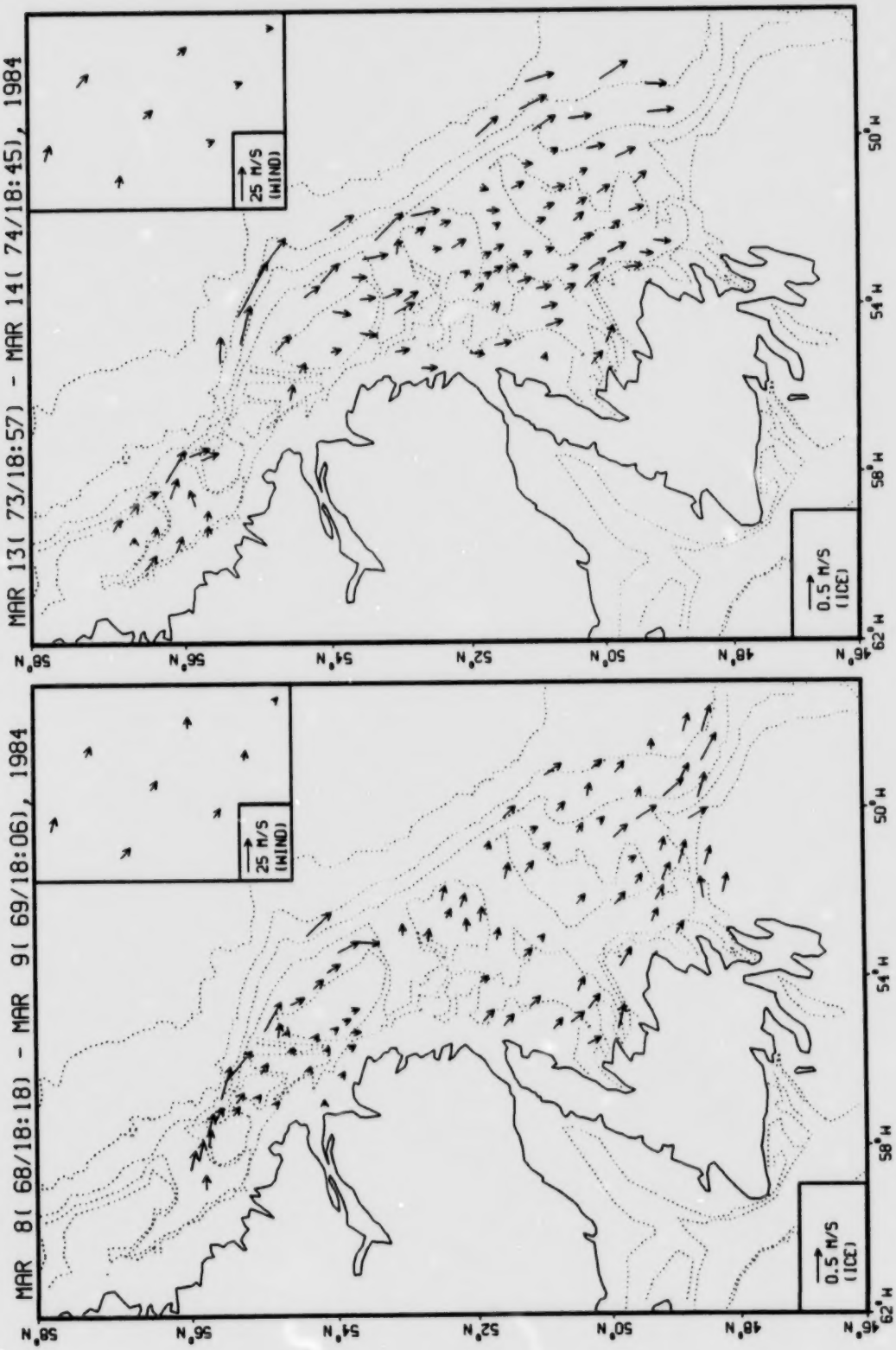
MAR 8( 68/18:18) - MAR 9( 69/18:06), 1984
25 M/S (WIND)
0.5 M/S (ICE)
MAR 13( 73/18:57) - MAR 14( 74/18:45), 1984
25 M/S (WIND)
0.5 M/S (ICE)
58°N
56°N
54°N
52°N
50°N
48°N
46°N
62°W
58°W
54°W
50°W

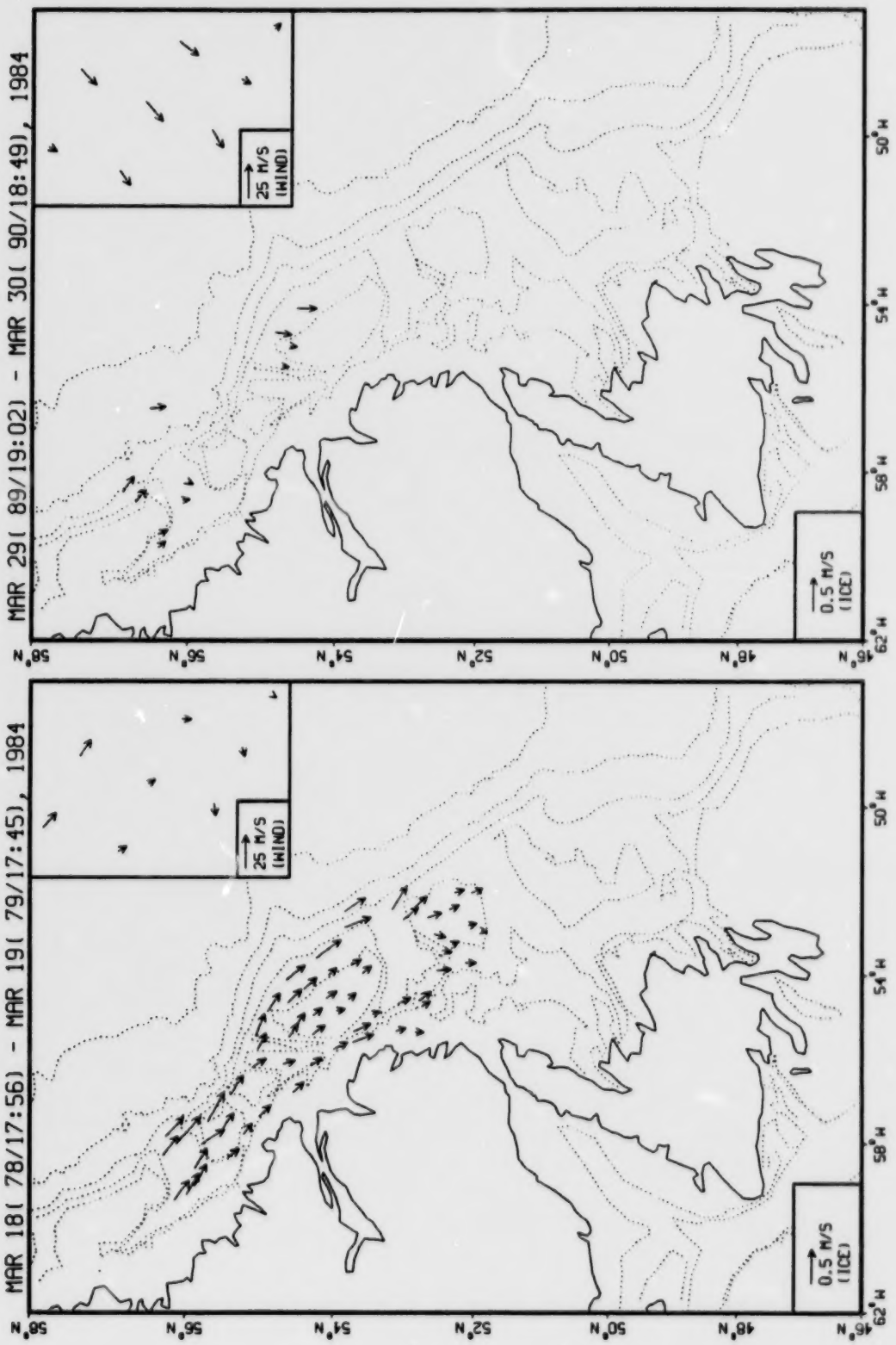
MAR 18( 78/17:56) - MAR 19( 79/17:45), 1984
25 M/S (WIND)
0.5 M/S (ICE)
MAR 29( 89/19:02) - MAR 30( 90/18:49), 1984
25 M/S (WIND)
0.5 M/S (ICE)
46°N
48°N
50°N
52°N
54°N
56°N
58°N
62°W
58°W
54°W
50°W

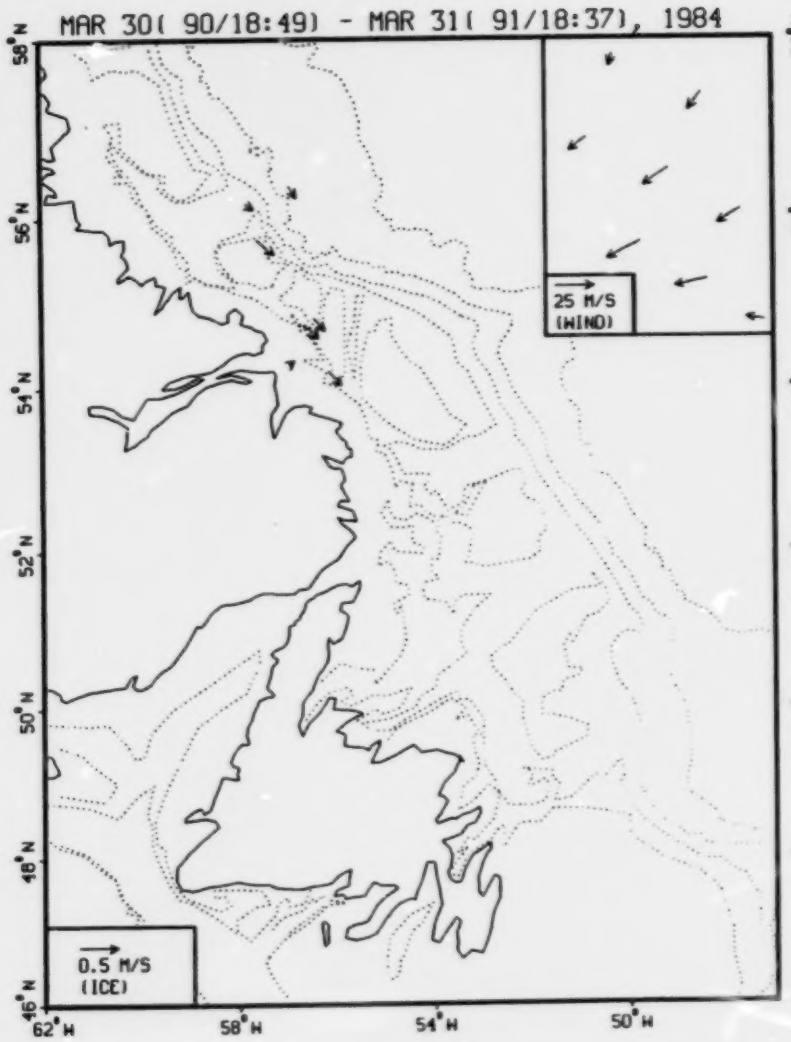
MAR 30( 90/18:49) - MAR 31( 91/18:37), 1984
25 M/S
(WIND)
0.5 M/S
(ICE)
58°N
56°N
54°N
52°N
50°N
48°N
46°N
62°W
58°W
54°W
50°W

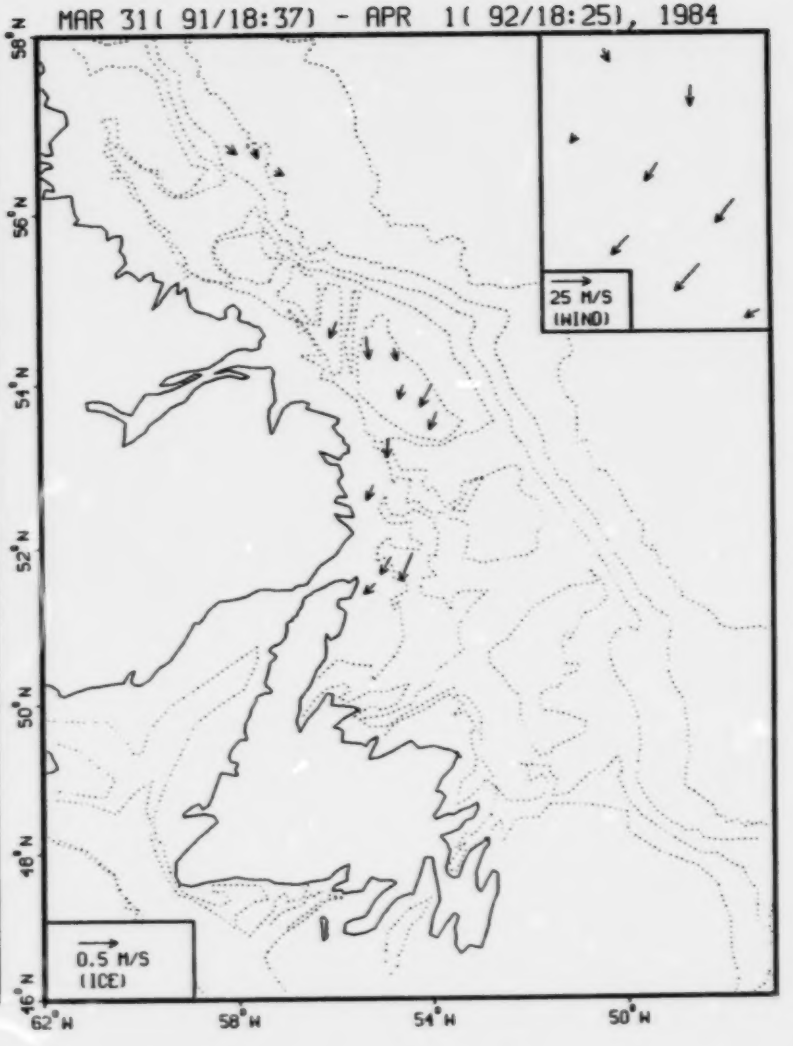
MAR 31( 91/18:37) - APR 1( 92/18:25), 1984
25 M/S
(WIND)
0.5 M/S
(ICE)
58°N
56°N
54°N
52°N
50°N
48°N
46°N
62°W
58°W
54°W
50°W

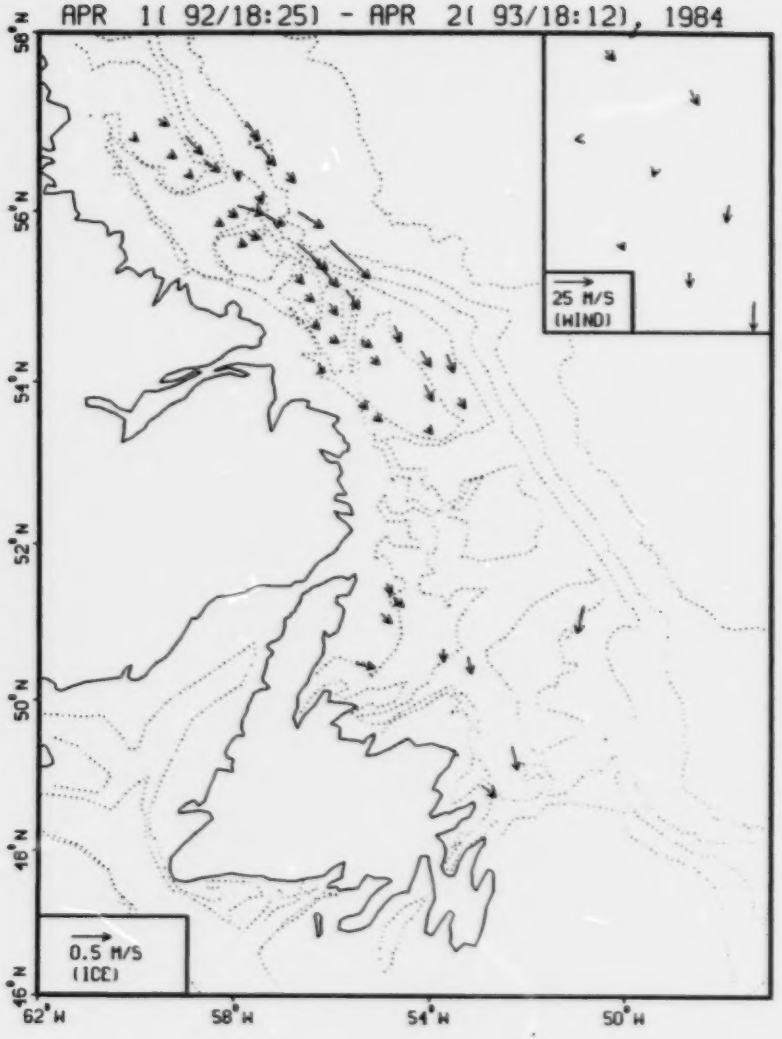
APR 1( 92/18:25) - APR 2( 93/18:12), 1984
25 M/S
(WIND)
0.5 M/S
(ICE)
58°N
56°N
54°N
52°N
50°N
48°N
46°N
62°W
58°W
54°W
50°W

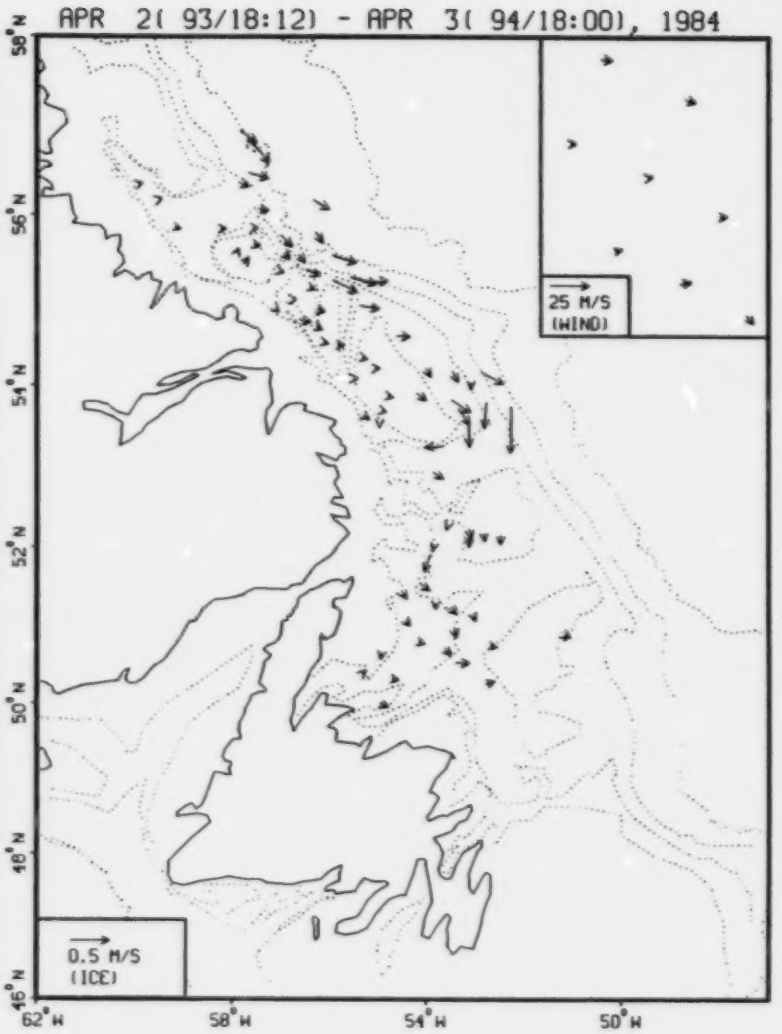
APR 2( 93/18:12) - APR 3( 94/18:00), 1984
25 M/S
(WIND)
0.5 M/S
(ICE)
58°N
56°N
54°N
52°N
50°N
48°N
46°N
62°W
58°W
54°W
50°W

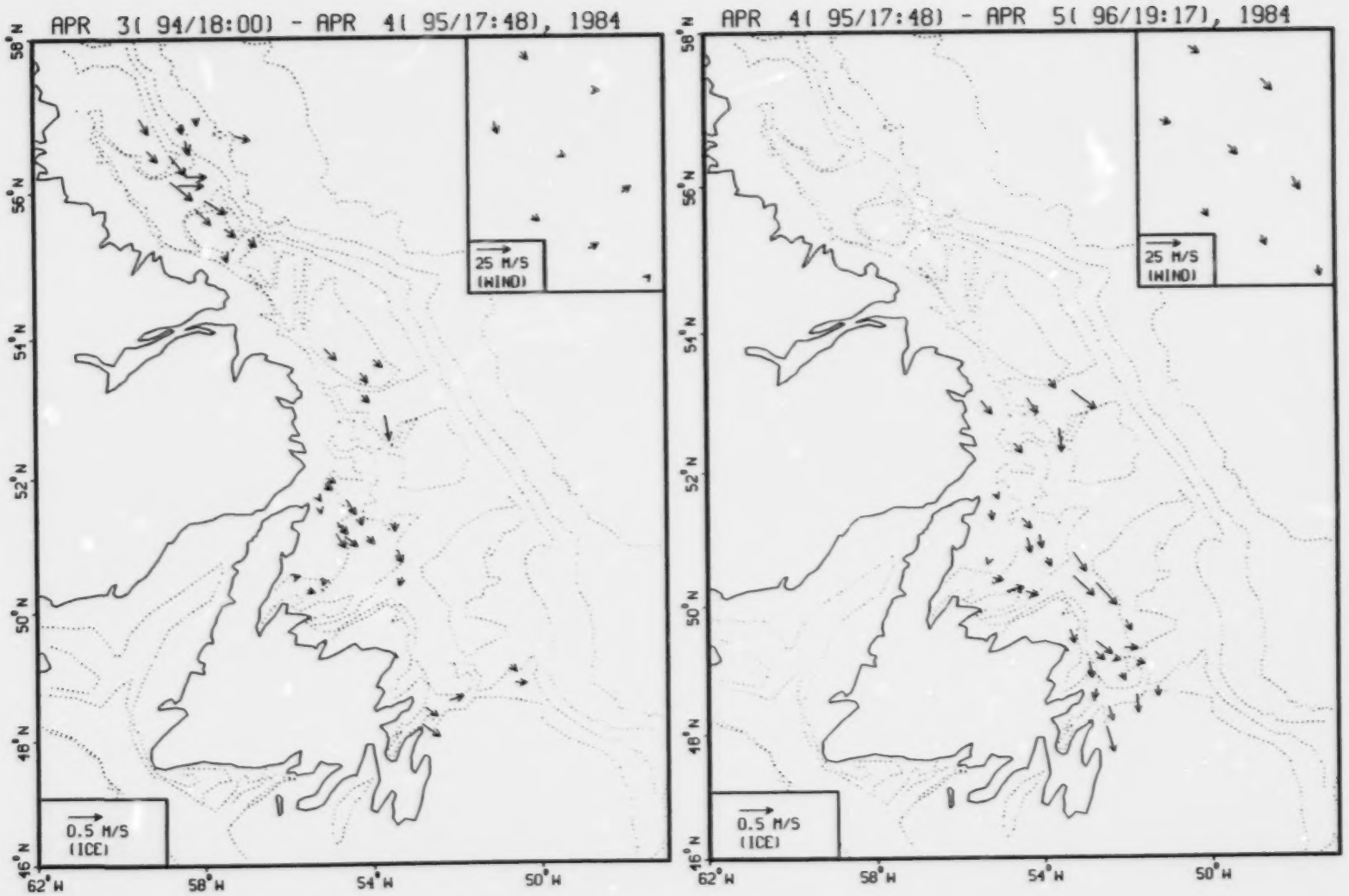
APR 3( 94/18:00) - APR 4( 95/17:48), 1984
APR 4( 95/17:48) - APR 5( 96/19:17), 1984
25 M/S (WIND)
0.5 M/S (ICE)
58°N
56°N
54°N
52°N
50°N
48°N
46°N
62°W
58°W
54°W
50°W

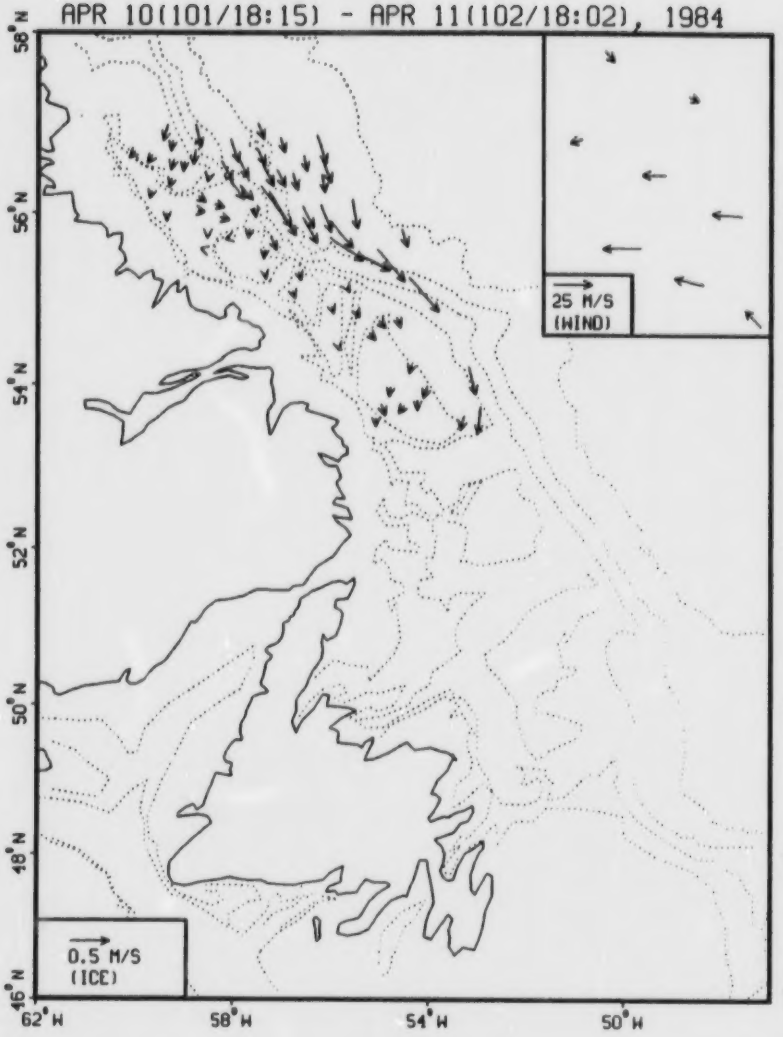
APR 10(101/18:15) - APR 11(102/18:02), 1984
25 M/S
(WIND)
0.5 M/S
(ICE)
58°N
56°N
54°N
52°N
50°N
48°N
46°N
62°W
58°W
54°W
50°W

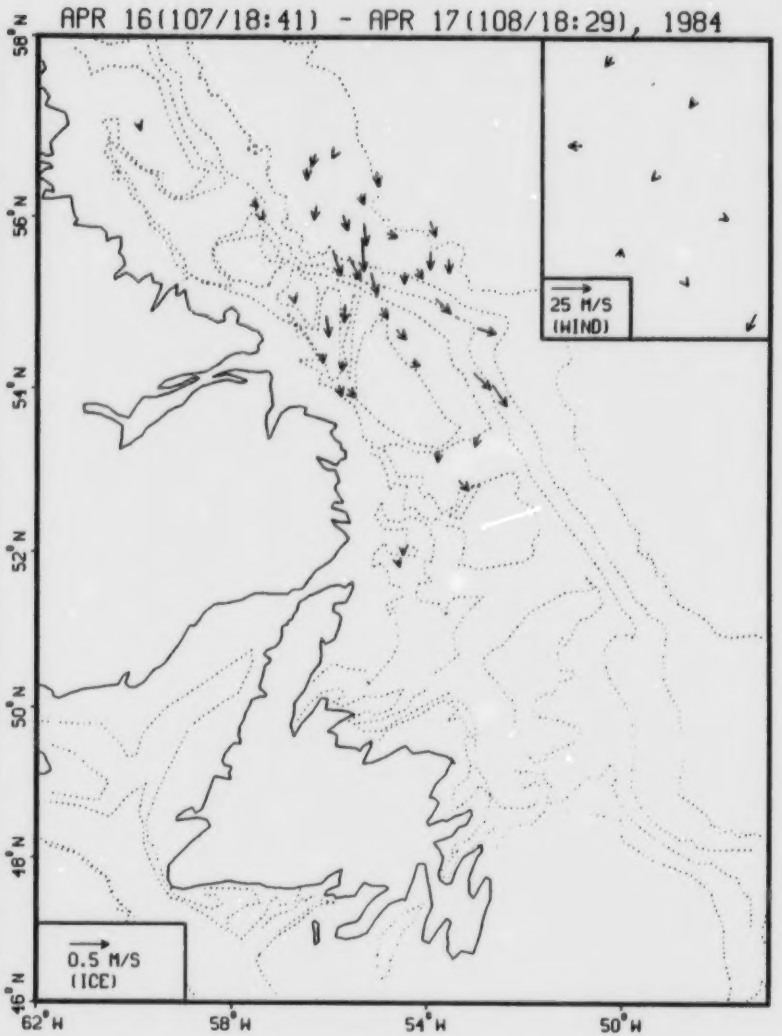
APR 16(107/18:41) - APR 17(108/18:29), 1984
25 M/S
(WIND)
0.5 M/S
(ICE)
58°N
56°N
54°N
52°N
50°N
48°N
46°N
62°W
58°W
54°W
50°W

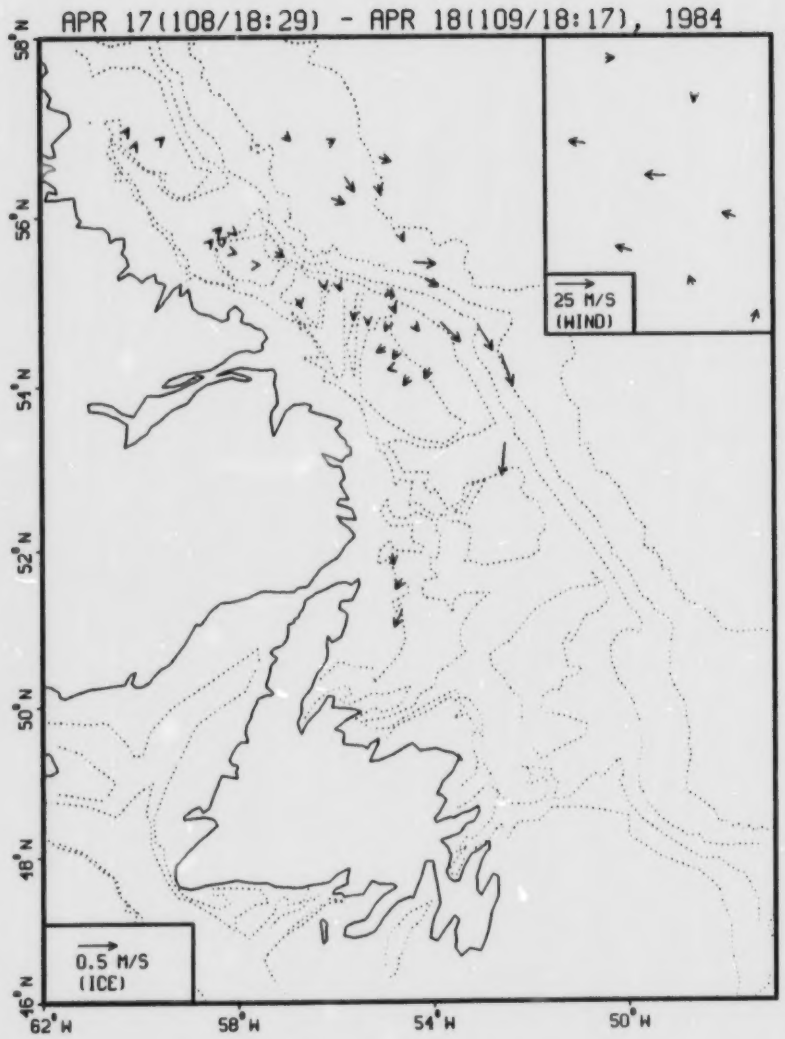
APR 17(108/18:29) - APR 18(109/18:17), 1984
25 M/S
(WIND)
0.5 M/S
(ICE)
58°N
56°N
54°N
52°N
50°N
48°N
46°N
62°W
58°W
54°W
50°W

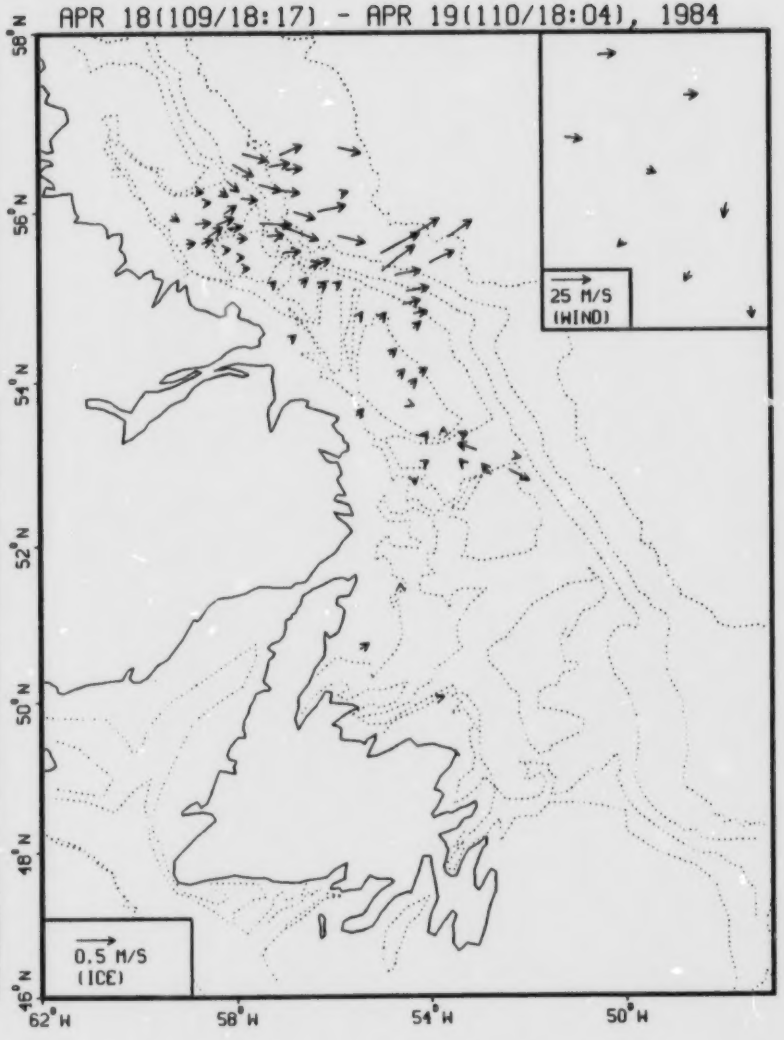
APR 18(109/18:17) - APR 19(110/18:04), 1984
25 M/S
(WIND)
0.5 M/S
(ICE)
58°N
56°N
54°N
52°N
50°N
48°N
46°N
62°W
58°W
54°W
50°W

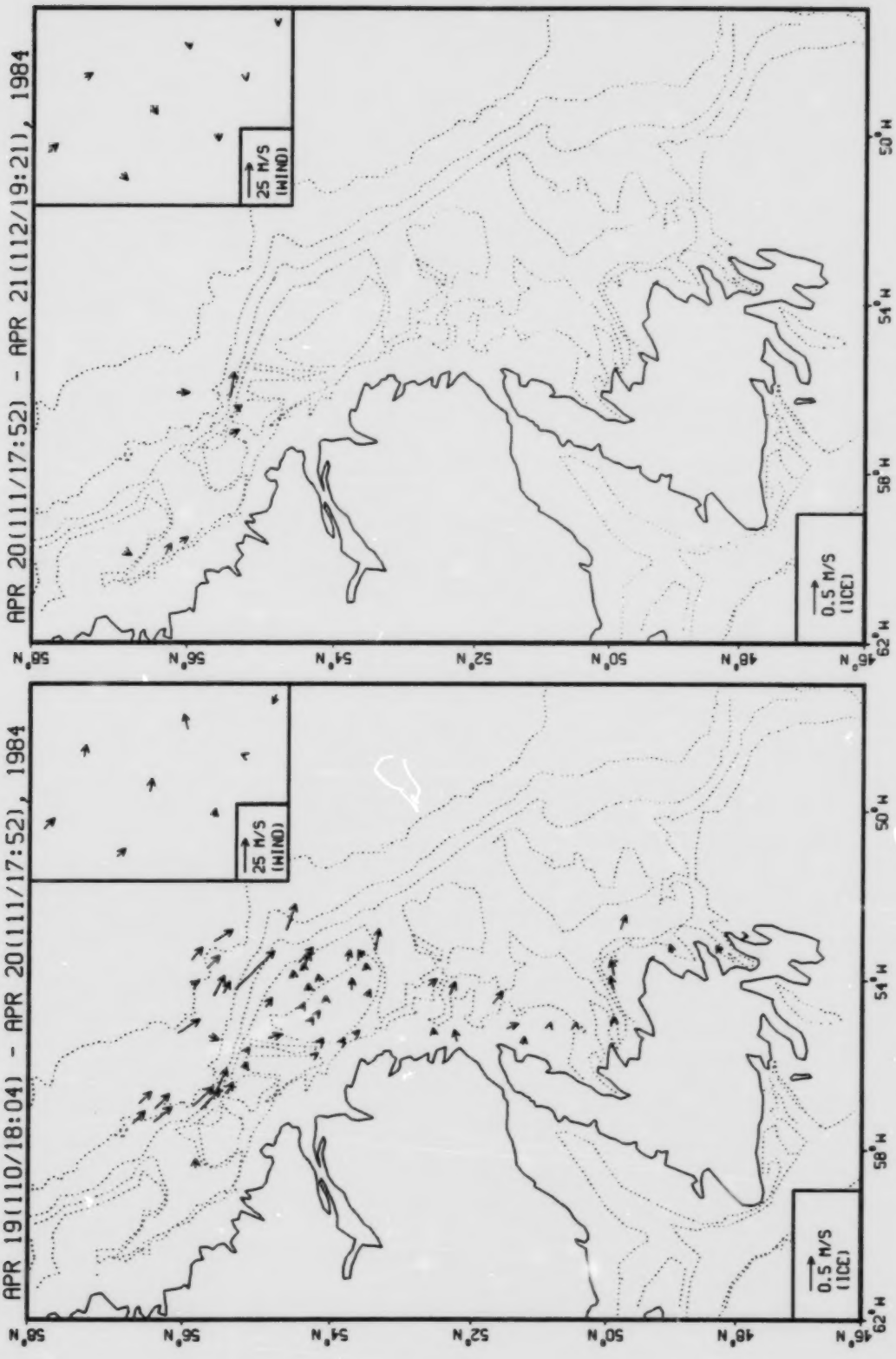
APR 19(110/18:04) - APR 20(111/17:52), 1984
25 M/S (WIND)
0.5 M/S (ICE)
APR 20(111/17:52) - APR 21(112/19:21), 1984
25 M/S (WIND)
0.5 M/S (ICE)
58°N
56°N
54°N
52°N
50°N
48°N
46°N
62°W
58°W
54°W
50°W

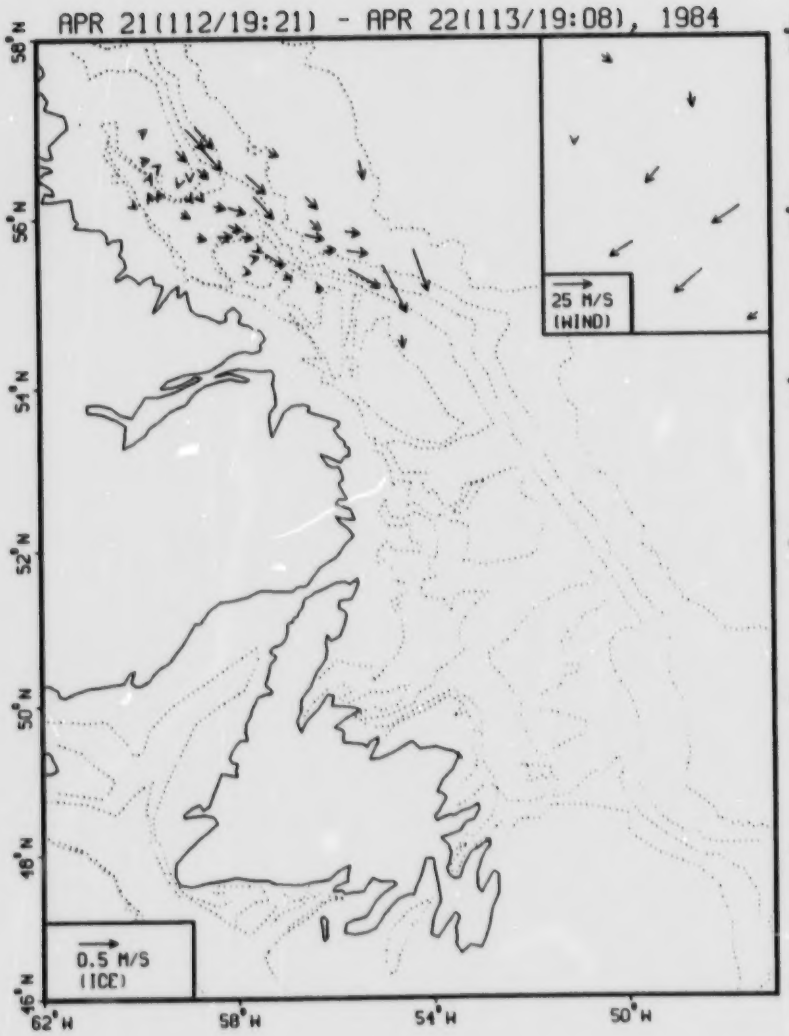
APR 21(112/19:21) - APR 22(113/19:08), 1984
25 M/S
(WIND)
0.5 M/S
(ICE)
58°N
56°N
54°N
52°N
50°N
48°N
46°N
62°W
58°W
54°W
50°W

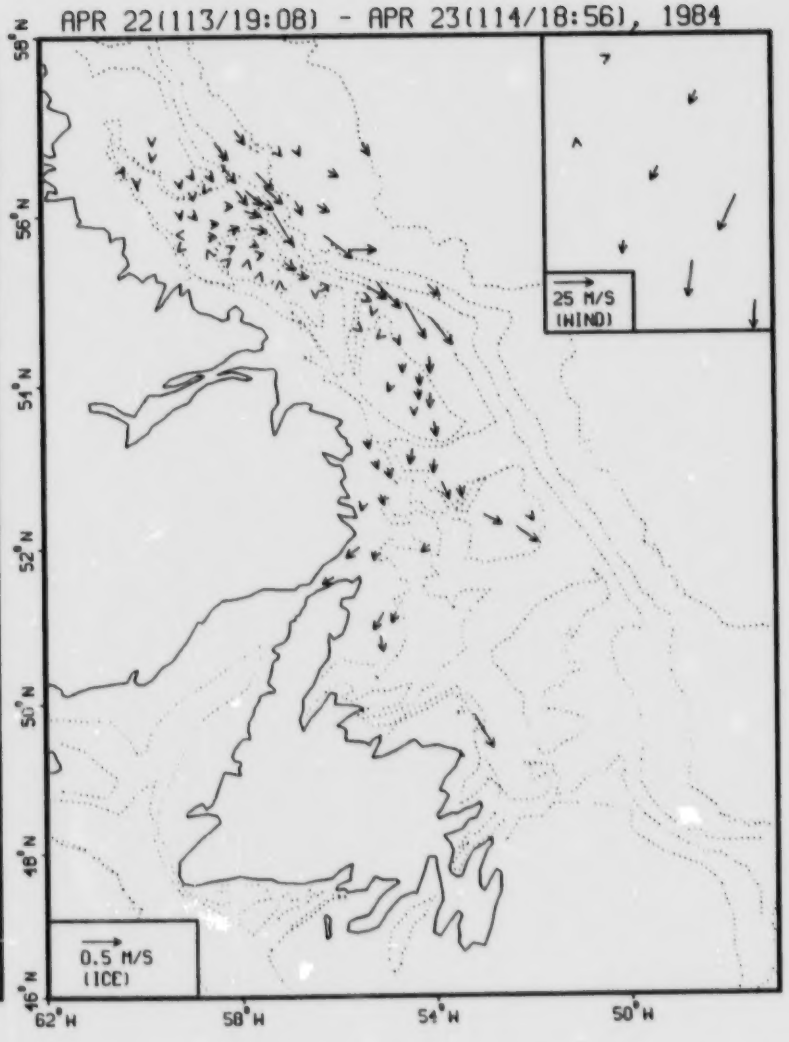
APR 22(113/19:08) - APR 23(114/18:56), 1984
25 M/S
(WIND)
0.5 M/S
(ICE)
58°N
56°N
54°N
52°N
50°N
48°N
46°N
62°W
58°W
54°W
50°W

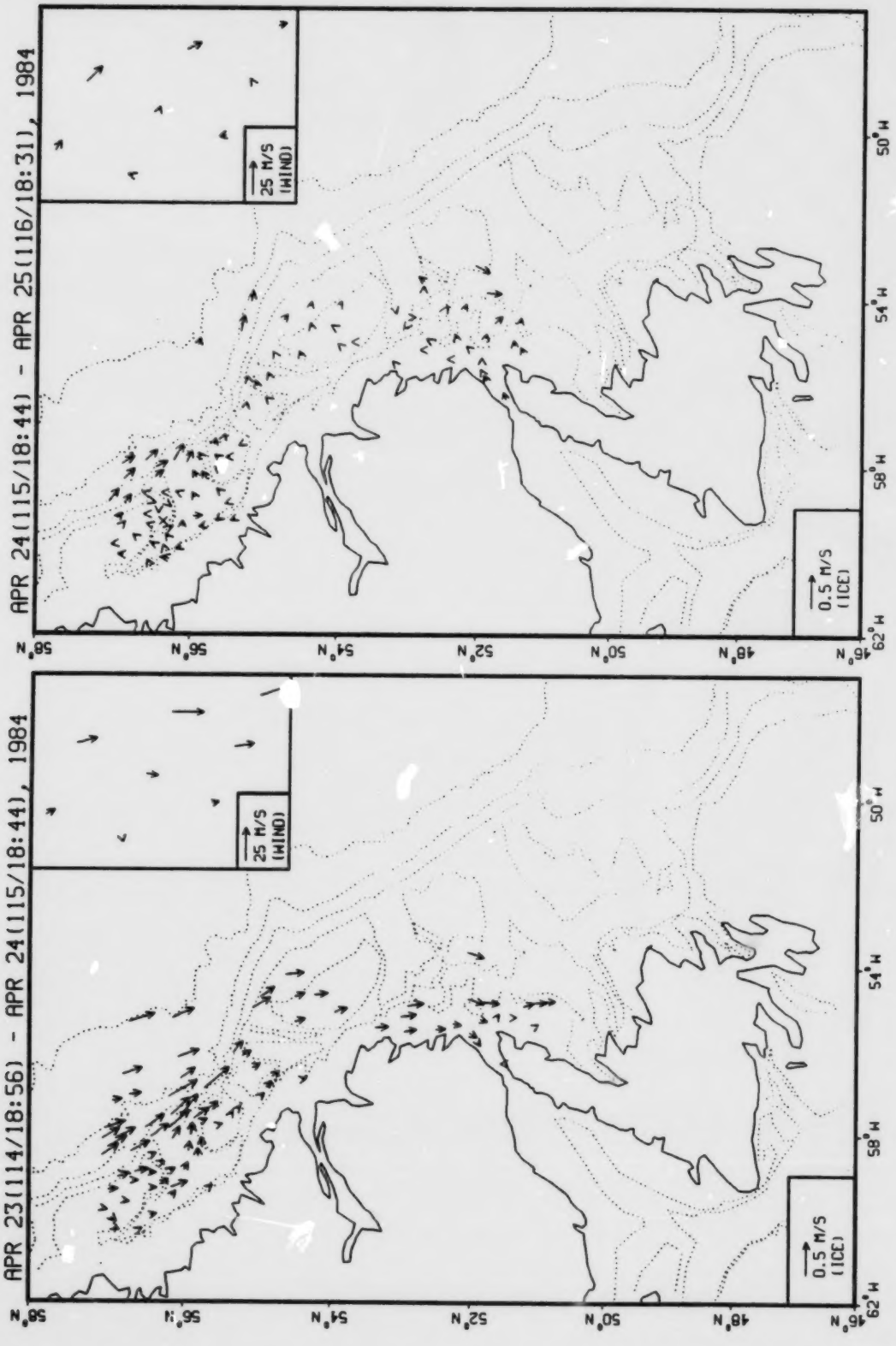
APR 24(115/18:44) - APR 25(116/18:31), 1984
25 M/S (WIND)
0.5 M/S (ICE)
APR 23(114/18:56) - APR 24(115/18:44), 1984
25 M/S (WIND)
0.5 M/S (ICE)
58°N
56°N
54°N
52°N
50°N
48°N
46°N
62°W
58°W
54°W
50°W

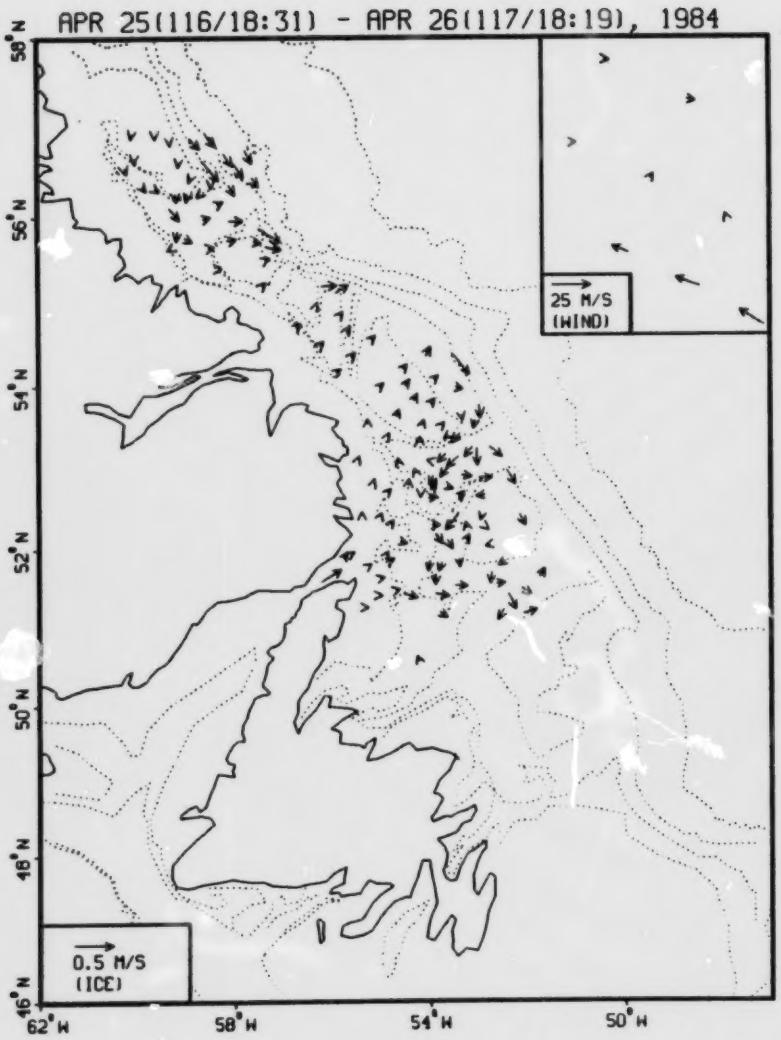
APR 25(116/18:31) - APR 26(117/18:19), 1984
25 M/S
(WIND)
0.5 M/S
(ICE)
58°N
56°N
54°N
52°N
50°N
48°N
46°N
62°W
58°W
54°W
50°W

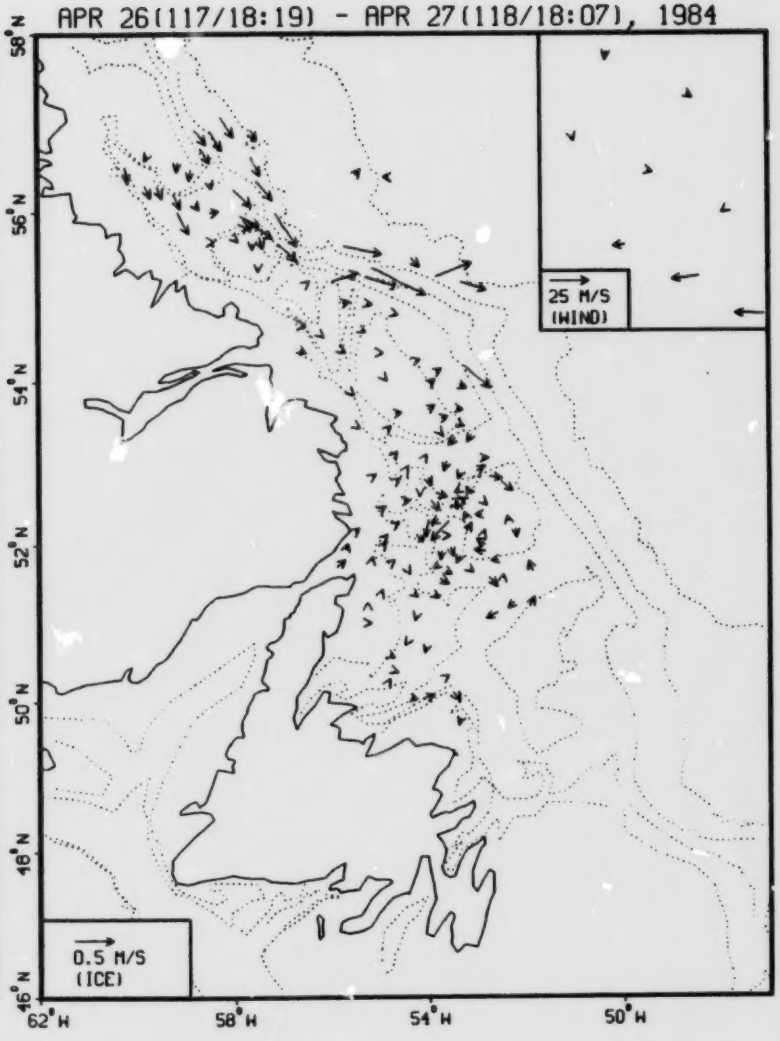
APR 26(117/18:19) - APR 27(118/18:07), 1984
25 M/S
(WIND)
0.5 M/S
(ICE)
58°N
56°N
54°N
52°N
50°N
48°N
46°N
62°W
58°W
54°W
50°W

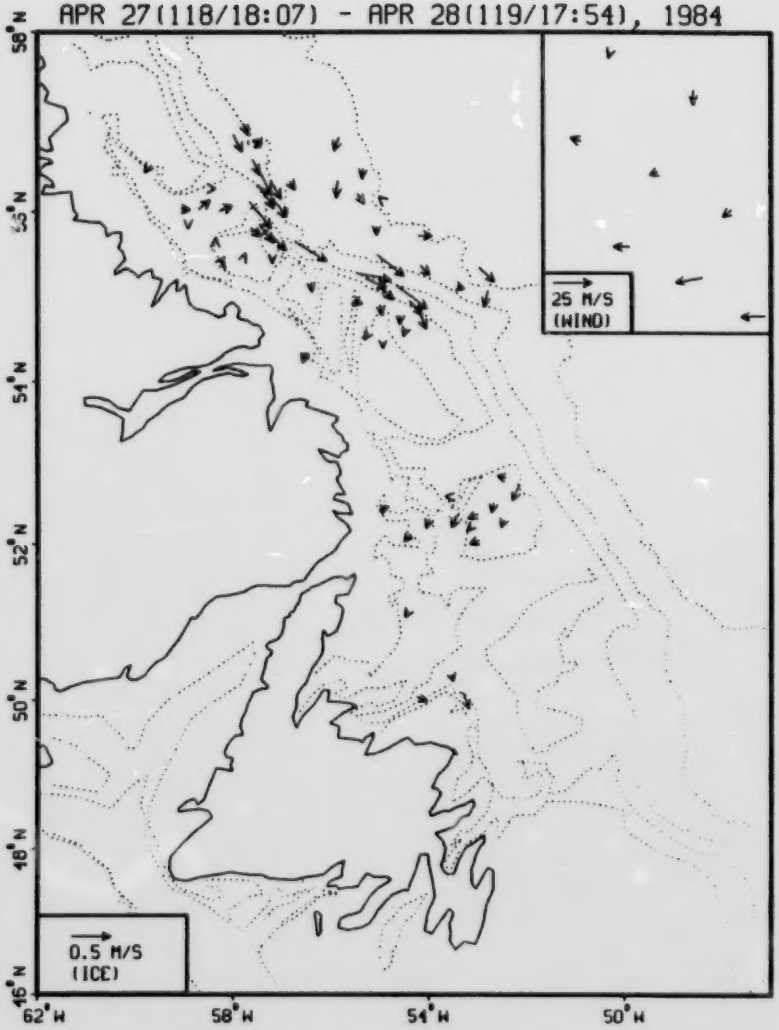
APR 27(118/18:07) - APR 28(119/17:54), 1984
25 M/S
(WIND)
0.5 M/S
(ICE)
58°N
56°N
54°N
52°N
50°N
48°N
46°N
62°W
58°W
54°W
50°W

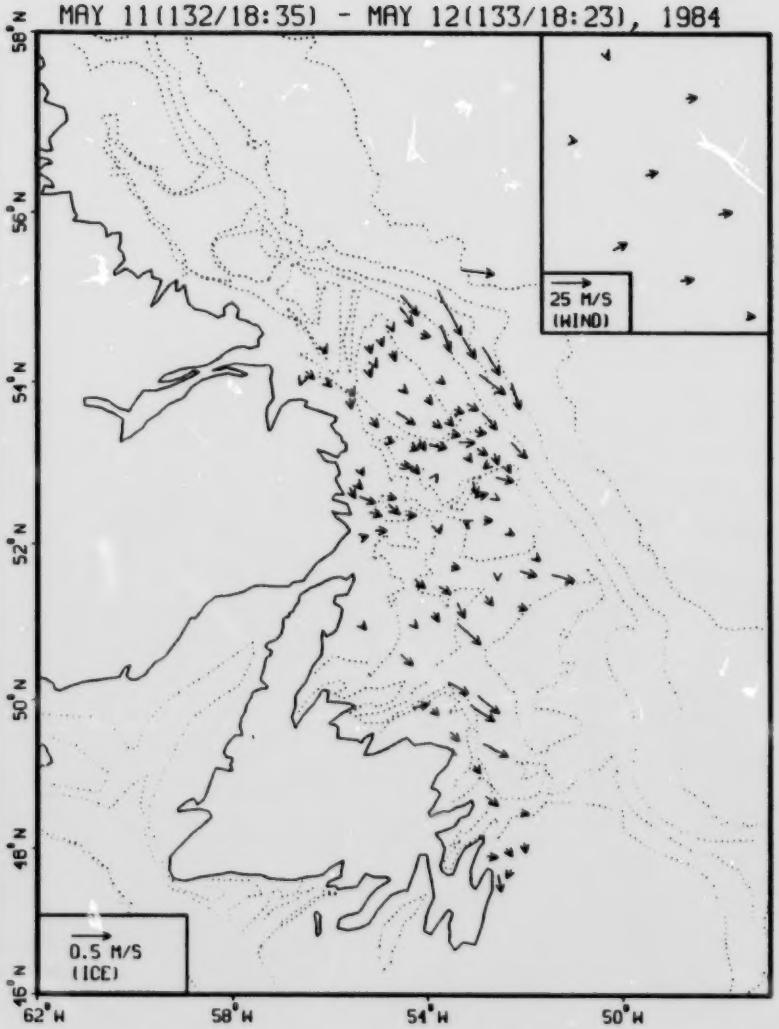
MAY 11(132/18:35) - MAY 12(133/18:23), 1984
25 M/S
(WIND)
0.5 M/S
(ICE)
58°N
56°N
54°N
52°N
50°N
48°N
46°N
62°W
58°W
54°W
50°W

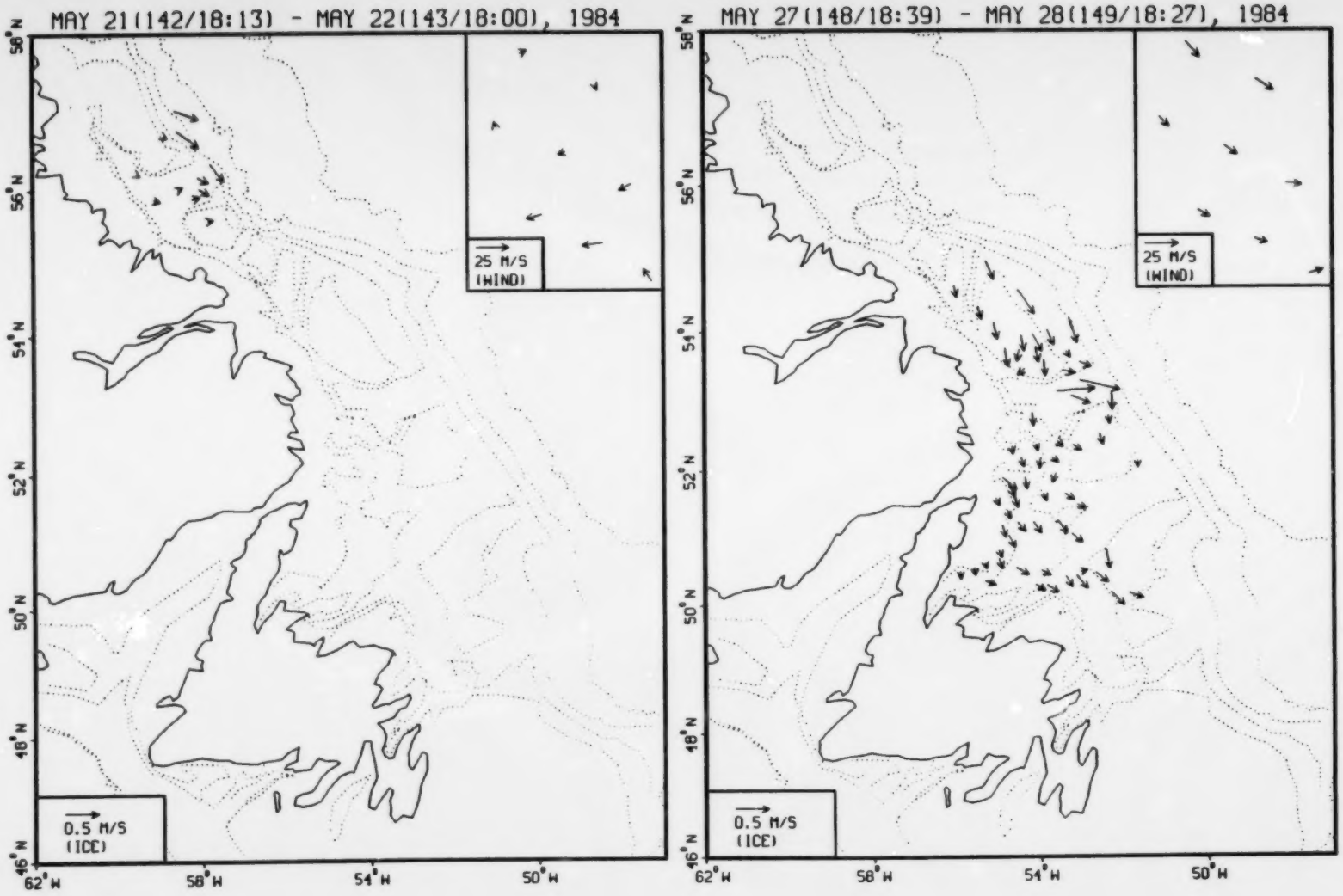
MAY 21(142/18:13) - MAY 22(143/18:00), 1984
MAY 27(148/18:39) - MAY 28(149/18:27), 1984
25 M/S
(WIND)
0.5 M/S
(ICE)
58°N
56°N
54°N
52°N
50°N
48°N
46°N
62°W
58°W
54°W
50°W

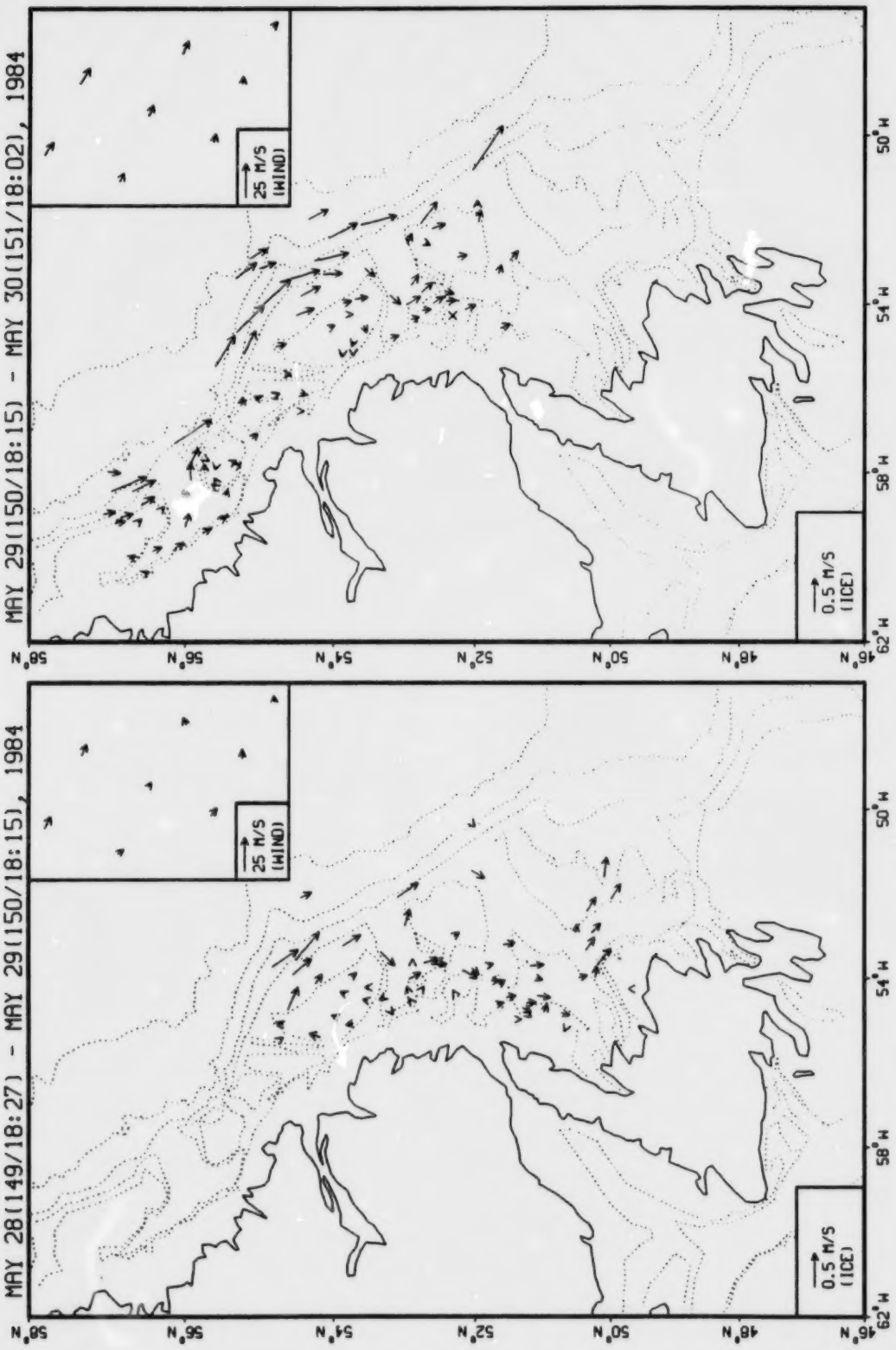
MAY 28(149/18:27) - MAY 29(150/18:15), 1984
25 M/S (WIND)
0.5 M/S (ICE)
MAY 29(150/18:15) - MAY 30(151/18:02), 1984
25 M/S (WIND)
0.5 M/S (ICE)
58°N
56°N
54°N
52°N
50°N
48°N
46°N
62°W
58°W
54°W
50°W

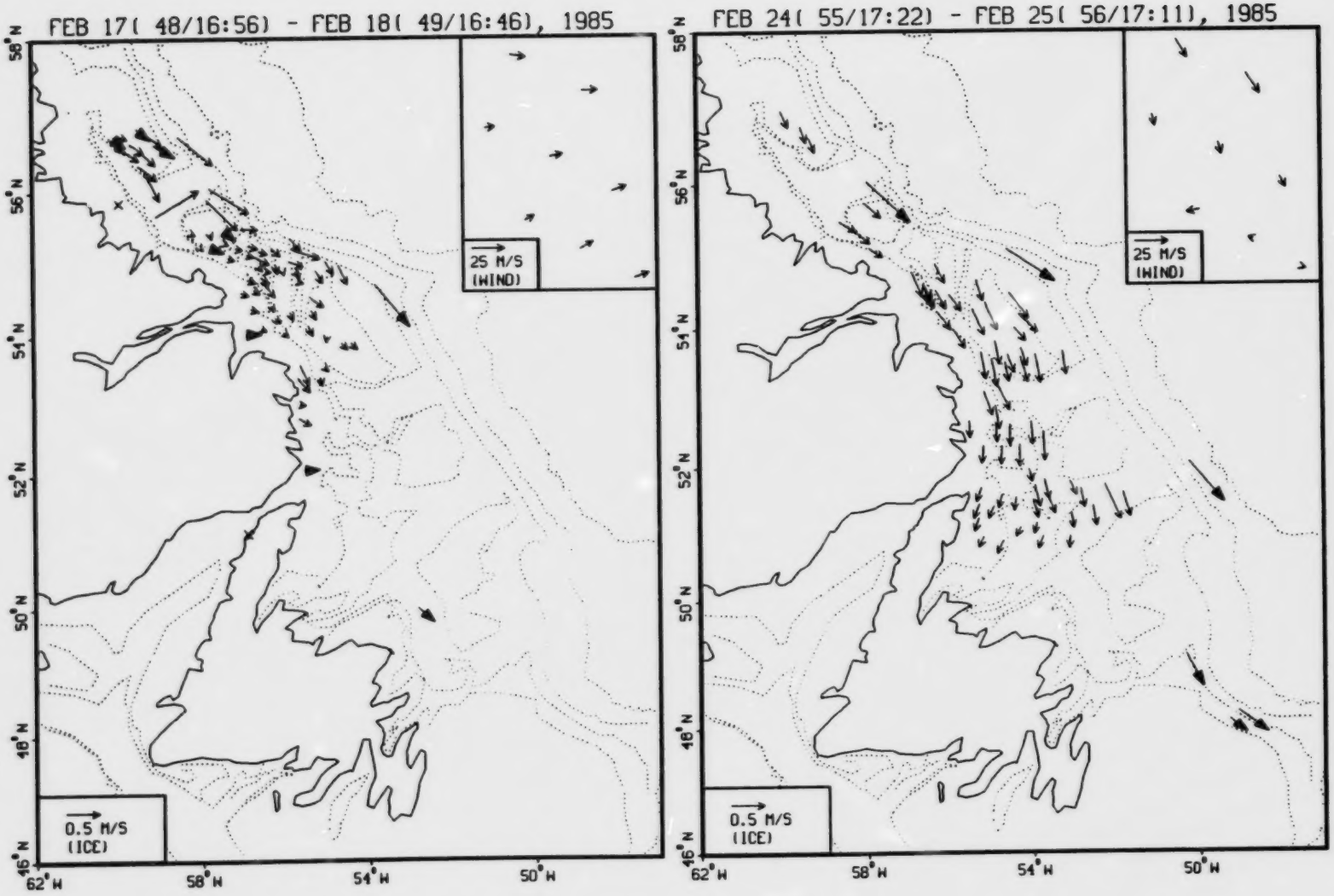
FEB 17( 48/16:56) - FEB 18( 49/16:46), 1985
25 M/S
(WIND)
0.5 M/S
(ICE)
58°N
56°N
54°N
52°N
50°N
48°N
46°N
62°W
58°W
54°W
50°W
FEB 24( 55/17:22) - FEB 25( 56/17:11), 1985
25 M/S
(WIND)
0.5 M/S
(ICE)
58°N
56°N
54°N
52°N
50°N
48°N
46°N
62°W
58°W
54°W
50°W

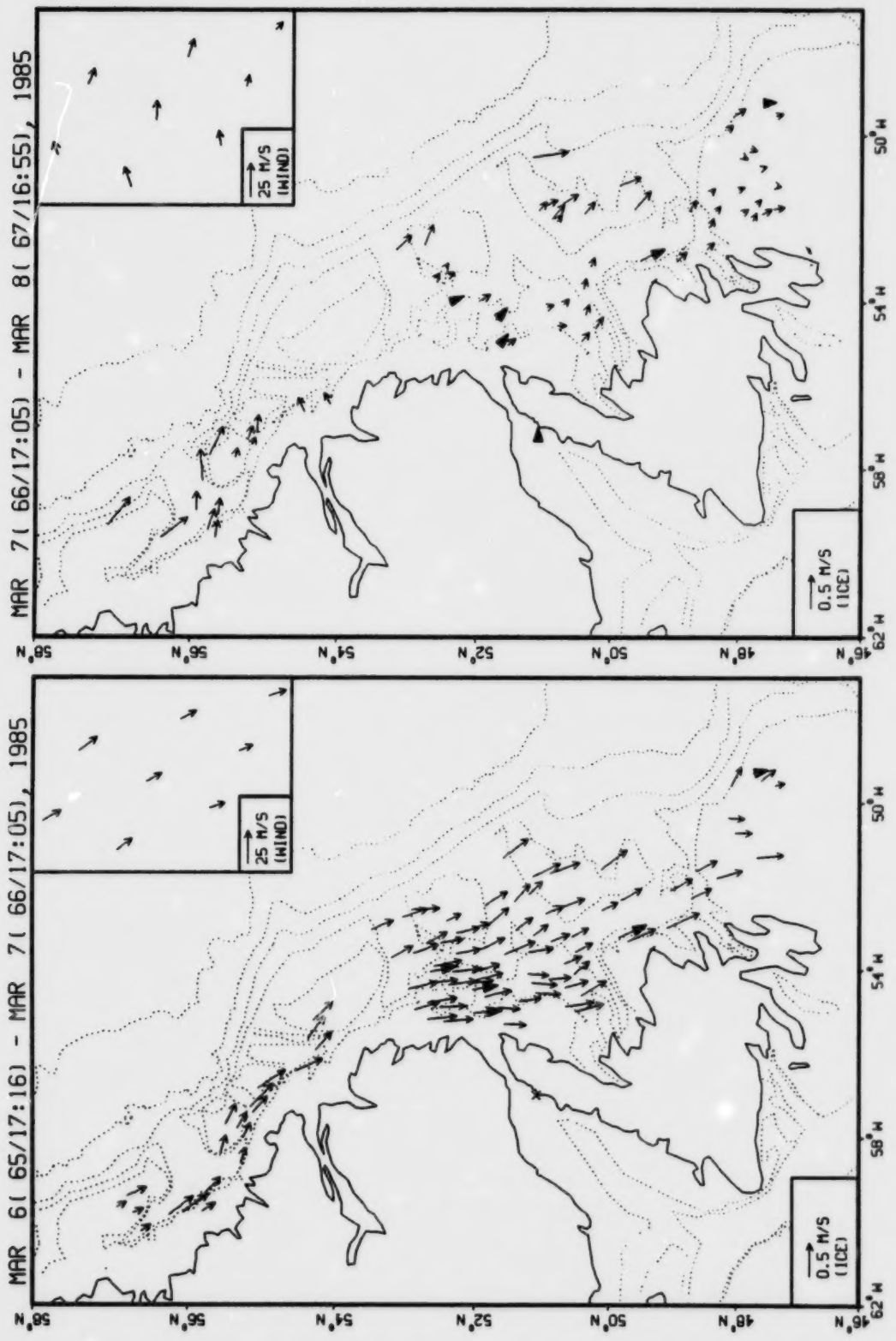
MAR 6( 65/17:16) - MAR 7( 66/17:05), 1985
25 M/S (WIND)
0.5 M/S (ICE)
MAR 7( 66/17:05) - MAR 8( 67/16:55), 1985
25 M/S (WIND)
0.5 M/S (ICE)
58°N
56°N
54°N
52°N
50°N
48°N
46°N
62°W
58°W
54°W
50°W

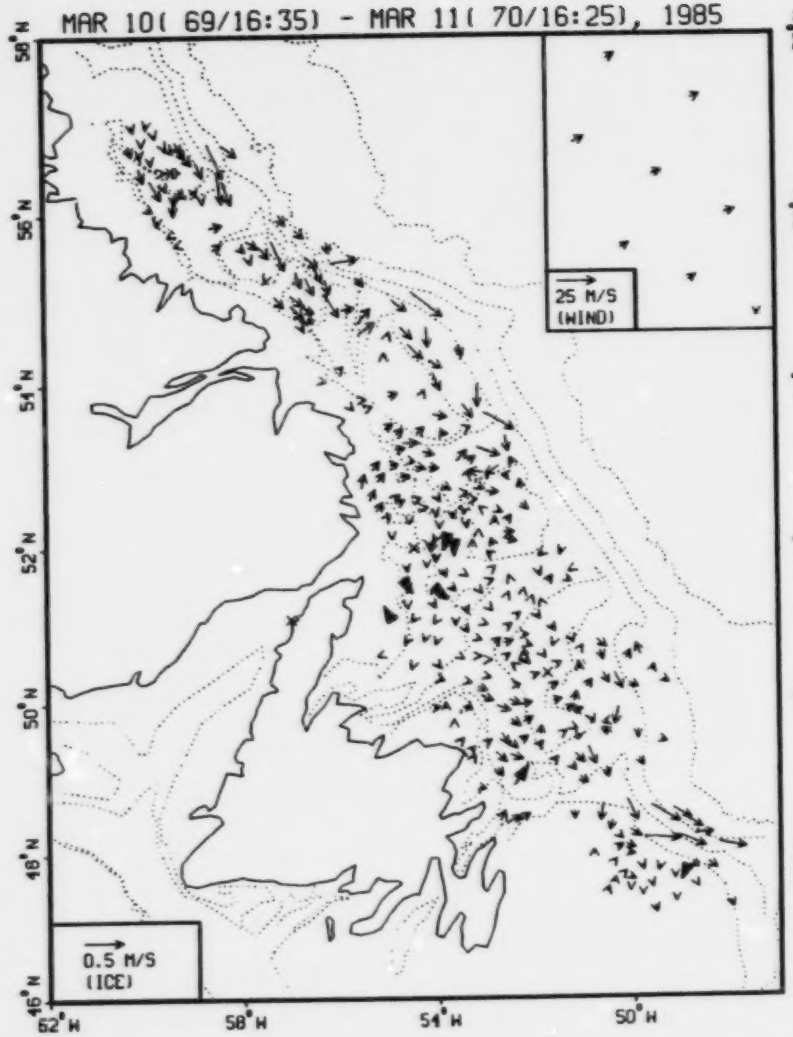
MAR 10( 69/16:35) - MAR 11( 70/16:25), 1985
25 M/S
(WIND)
0.5 M/S
(ICE)
58°N
56°N
54°N
52°N
50°N
48°N
46°N
62°W
58°W
54°W
50°W

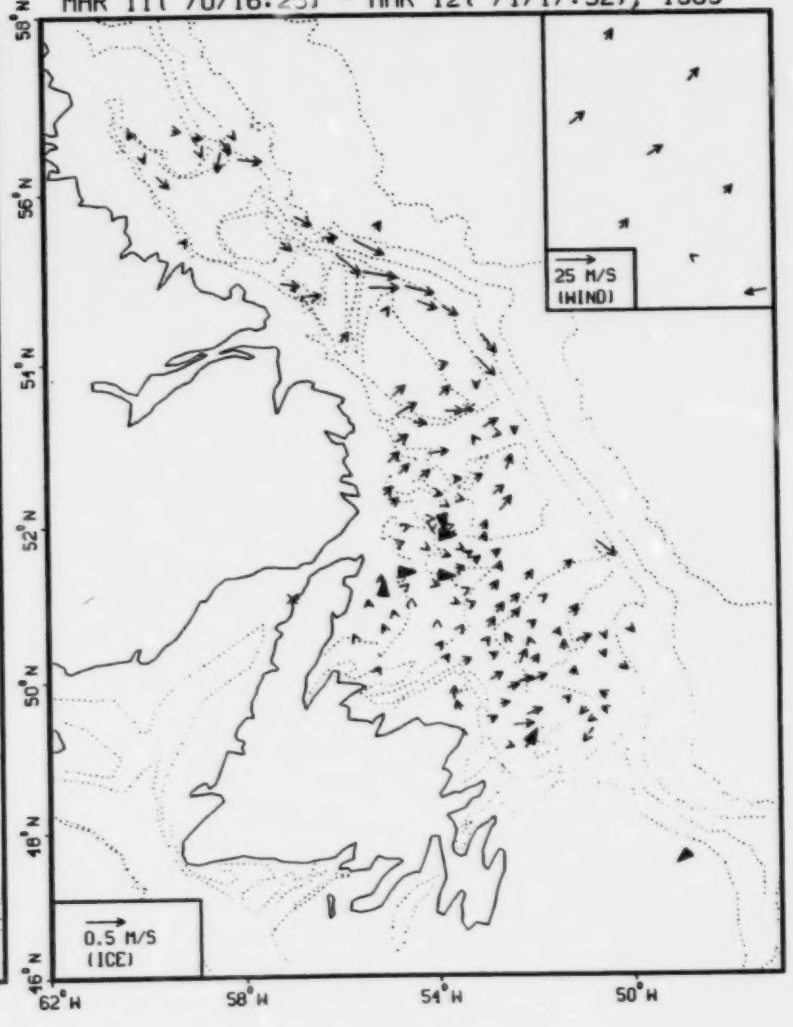
MAR 11( 70/16:25) - MAR 12( 71/17:52), 1985
25 M/S
(WIND)
0.5 M/S
(ICE)
58°N
56°N
54°N
52°N
50°N
48°N
46°N
62°W
58°W
54°W
50°W

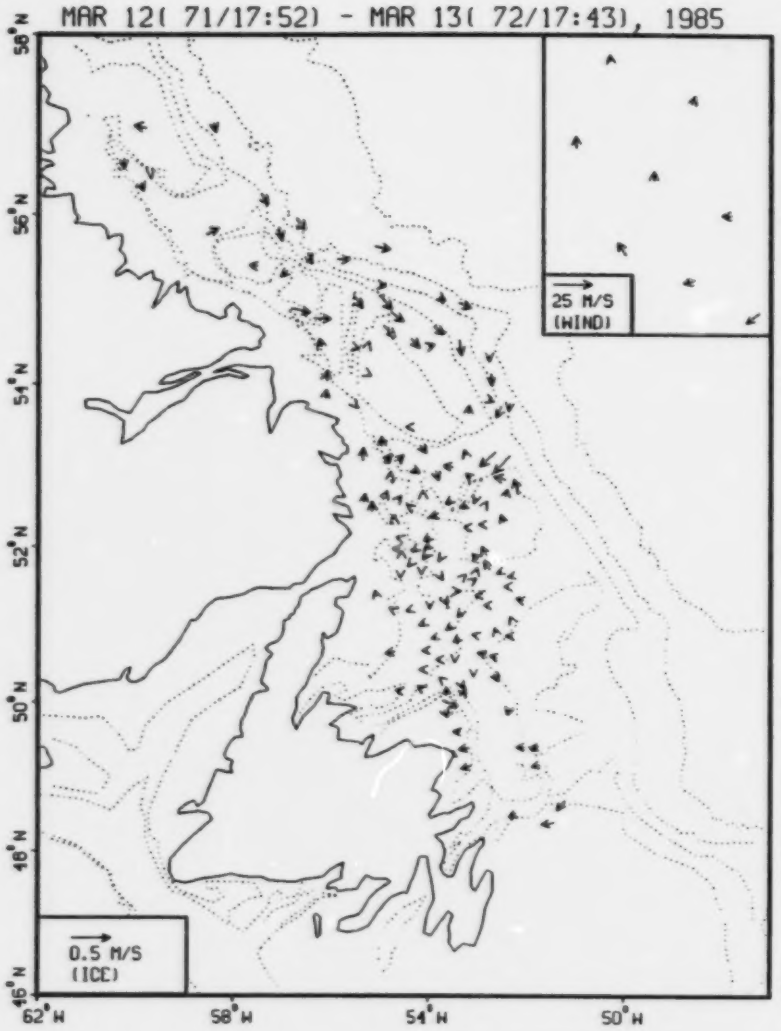
MAR 12( 71/17:52) - MAR 13( 72/17:43), 1985
25 M/S
(WIND)
0.5 M/S
(ICE)
58°N
56°N
54°N
52°N
50°N
48°N
46°N
62°W
58°W
54°W
50°W

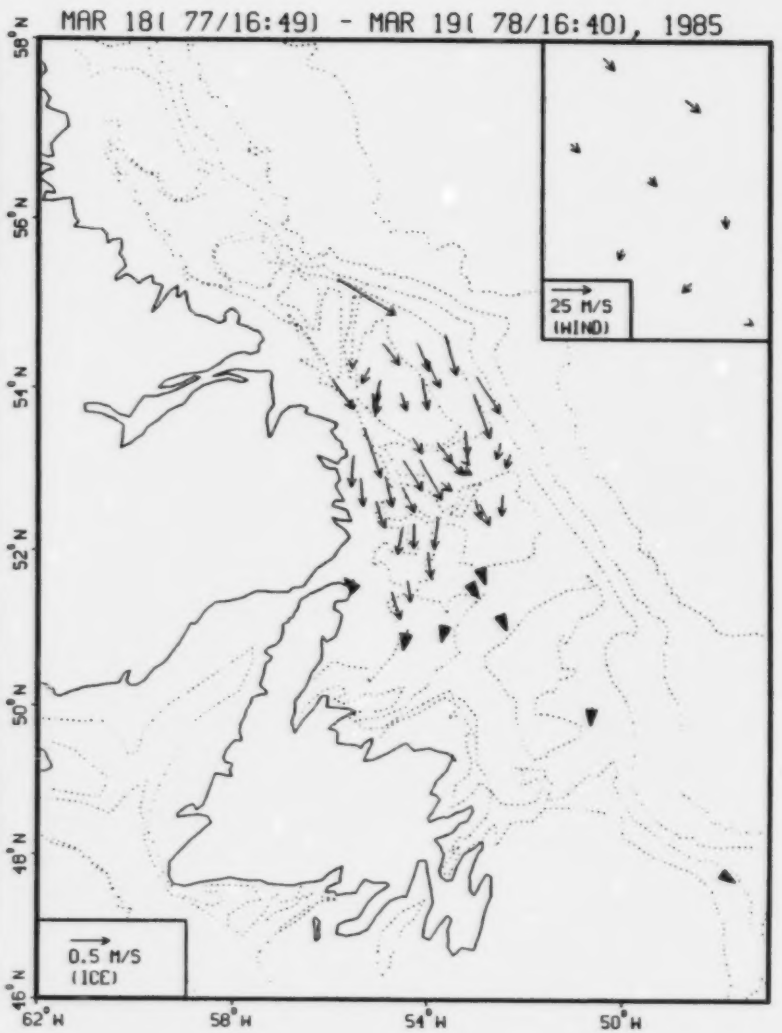
MAR 18( 77/16:49) - MAR 19( 78/16:40), 1985
25 M/S
(WIND)
0.5 M/S
(ICE)
58°N
56°N
54°N
52°N
50°N
48°N
46°N
62°W
58°W
54°W
50°W

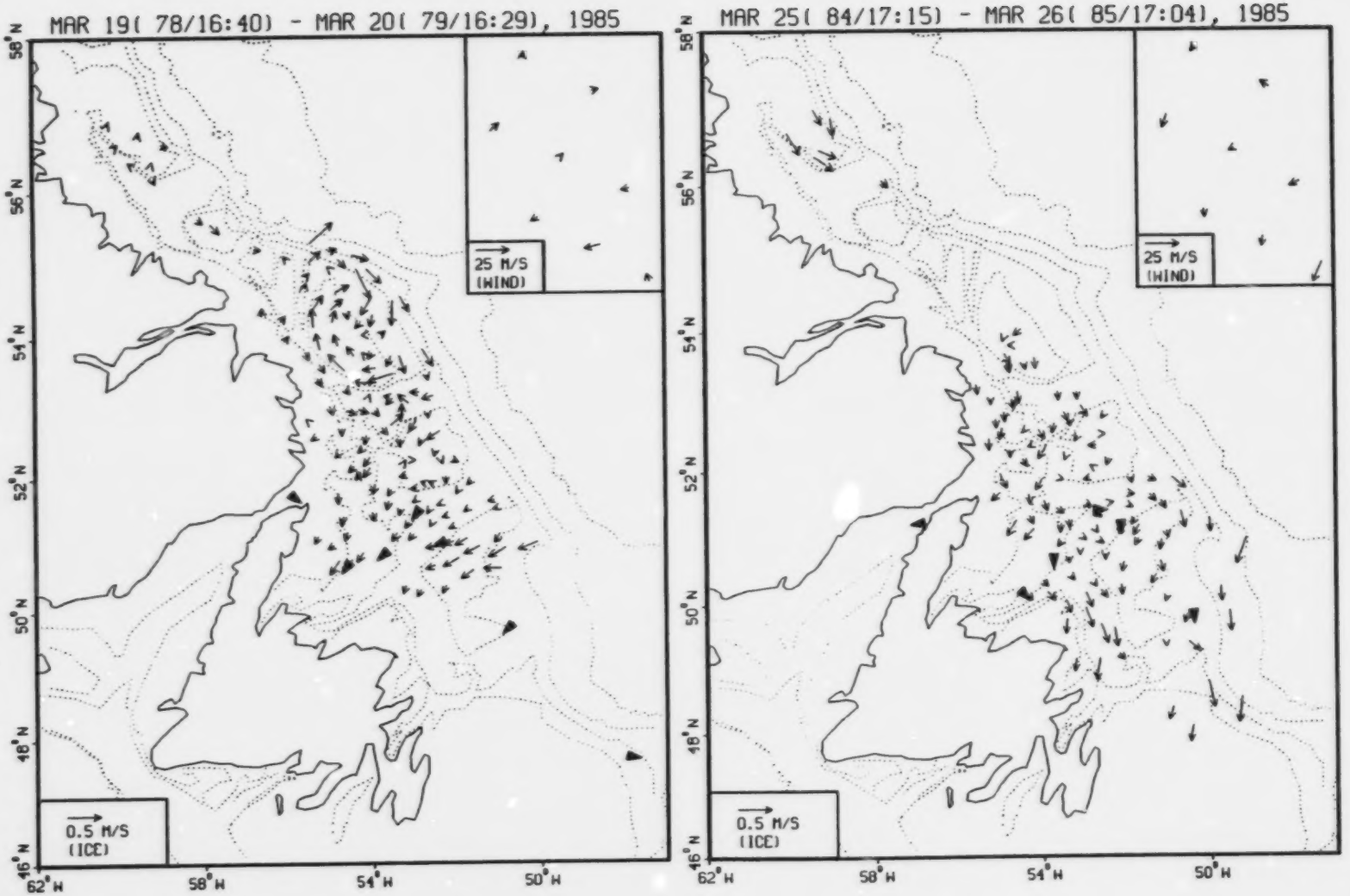
MAR 19( 78/16:40) - MAR 20( 79/16:29), 1985
25 M/S (WIND)
0.5 M/S (ICE)
MAR 25( 84/17:15) - MAR 26( 85/17:04), 1985
25 M/S (WIND)
0.5 M/S (ICE)
58°N
56°N
54°N
52°N
50°N
48°N
46°N
62°W
58°W
54°W
50°W

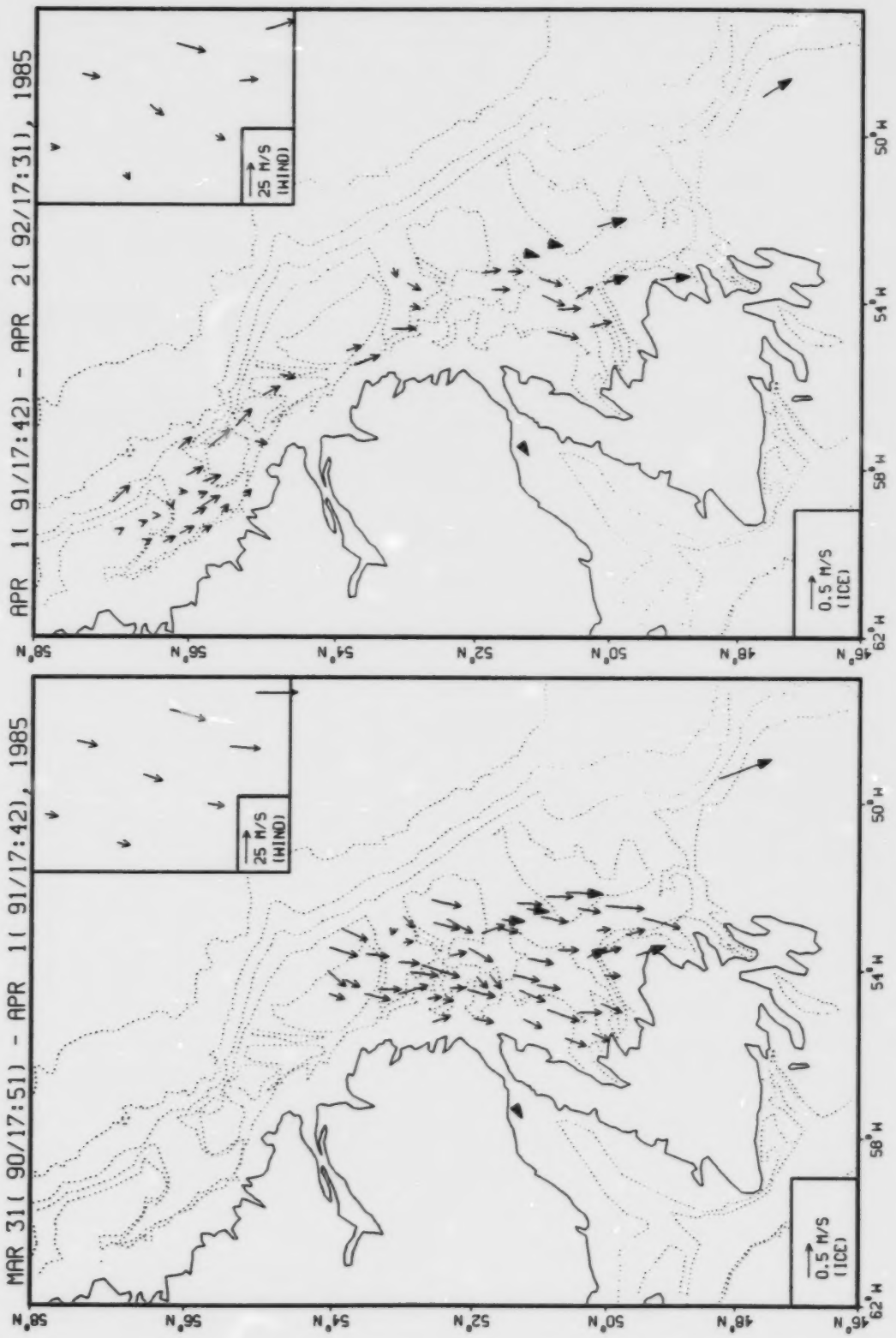
MAR 31( 90/17:51) - APR 1( 91/17:42), 1985
APR 1( 91/17:42) - APR 2( 92/17:31), 1985
25 M/S (WIND)
0.5 M/S (ICE)
62°W
58°W
54°W
50°W
46°N
48°N
50°N
52°N
54°N
56°N
58°N

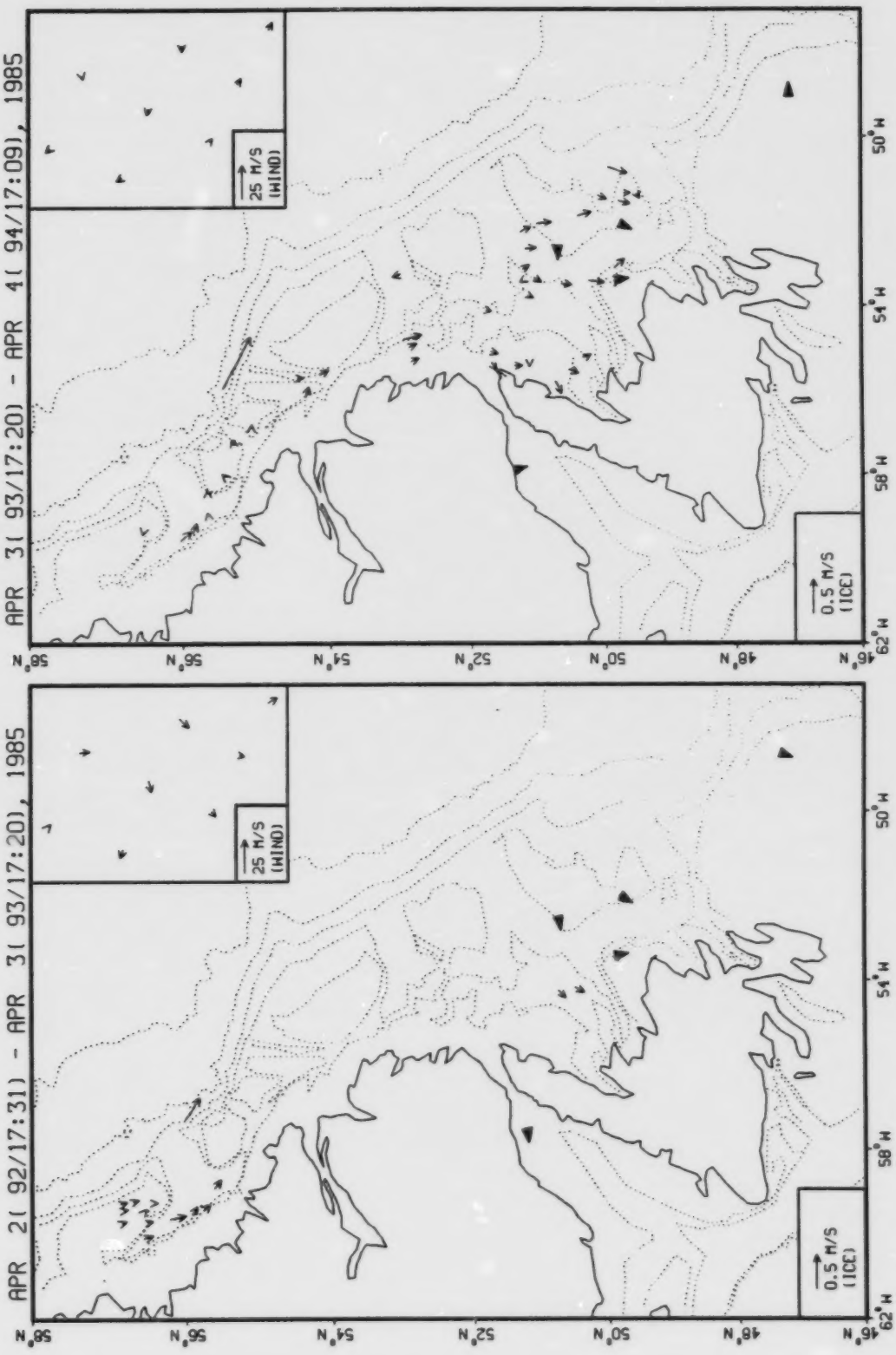
APR 2( 92/17:31) - APR 3( 93/17:20), 1985
APR 3( 93/17:20) - APR 4( 94/17:09), 1985
25 M/S (WIND)
0.5 M/S (ICE)
58°N
56°N
54°N
52°N
50°N
48°N
46°N
62°W
58°W
54°W
50°W

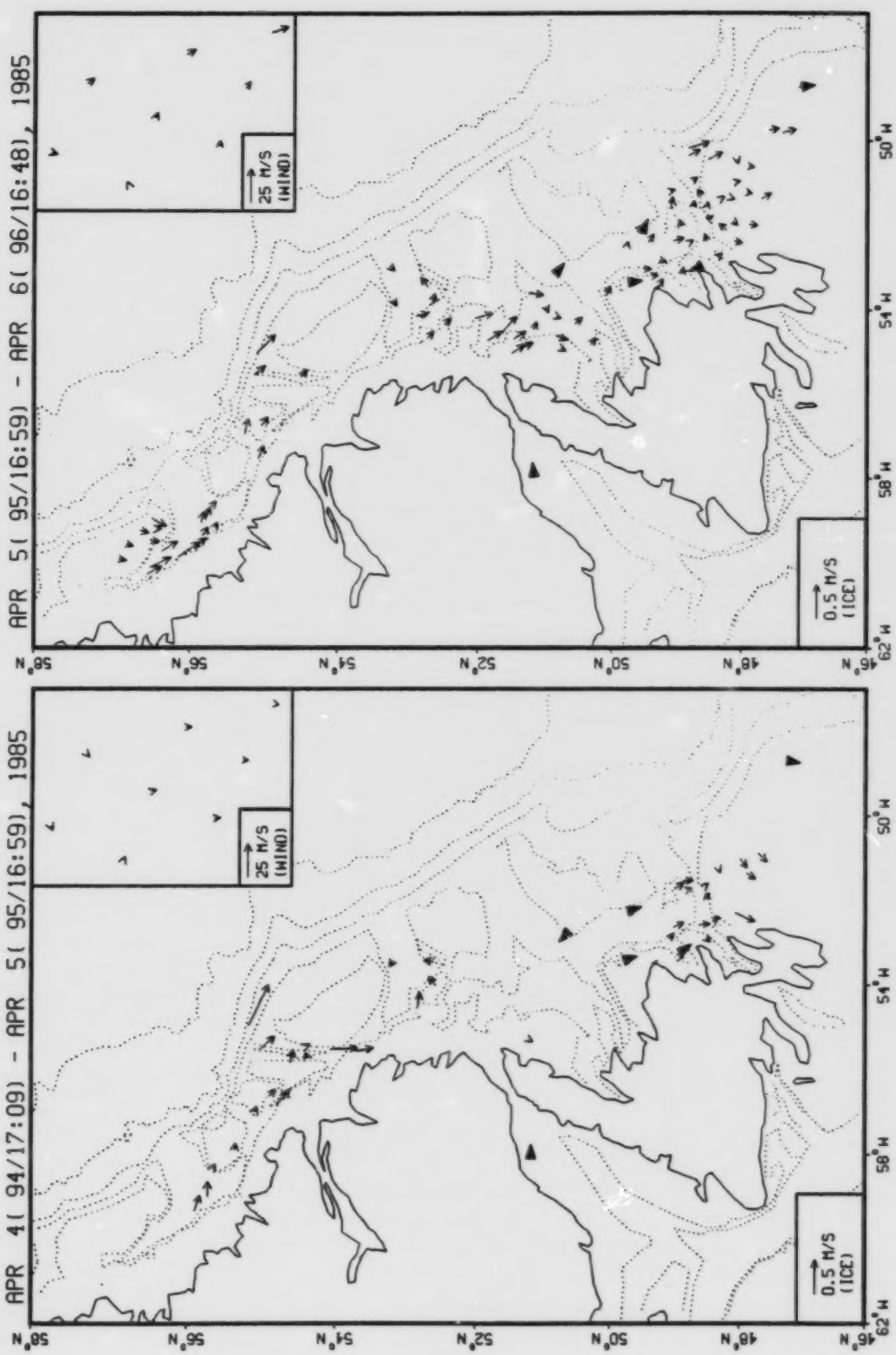
APR 4( 94/17:09) - APR 5( 95/16:59), 1985
APR 5( 95/16:59) - APR 6( 96/16:48), 1985
25 M/S (WIND)
0.5 M/S (ICE)
58°N
56°N
54°N
52°N
50°N
48°N
46°N
62°W
58°W
54°W
50°W

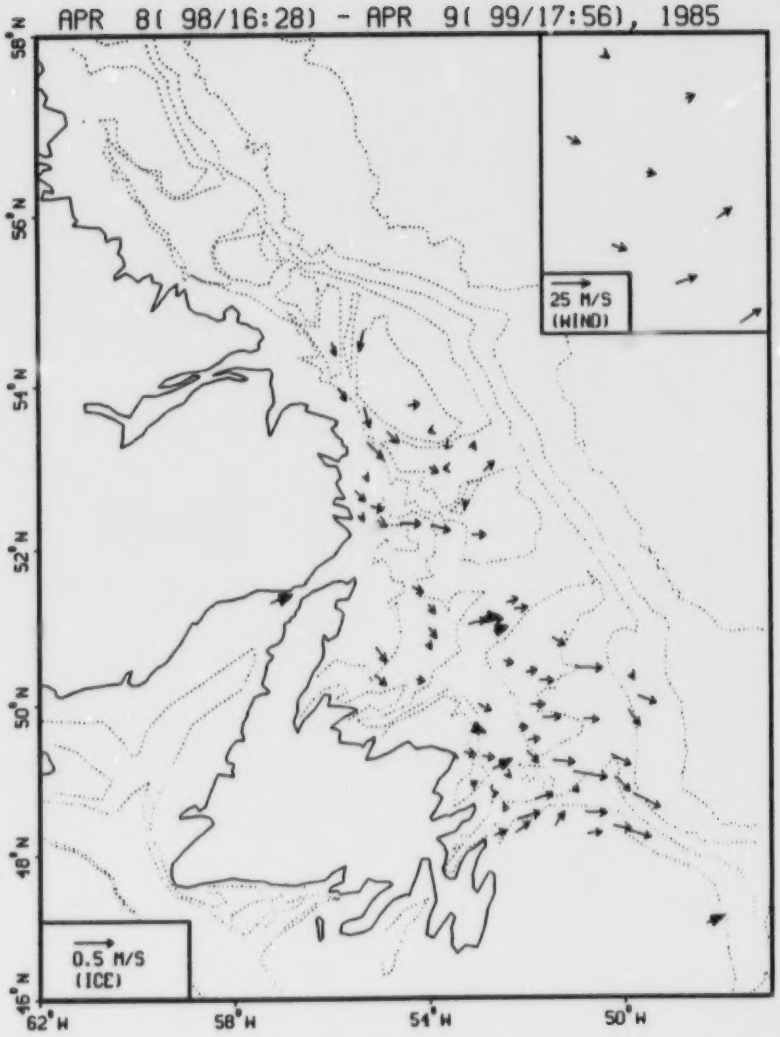
APR 8( 98/16:28) - APR 9( 99/17:56), 1985
25 M/S
(WIND)
0.5 M/S
(ICE)
58°N
56°N
54°N
52°N
50°N
48°N
46°N
62°W
58°W
54°W
50°W

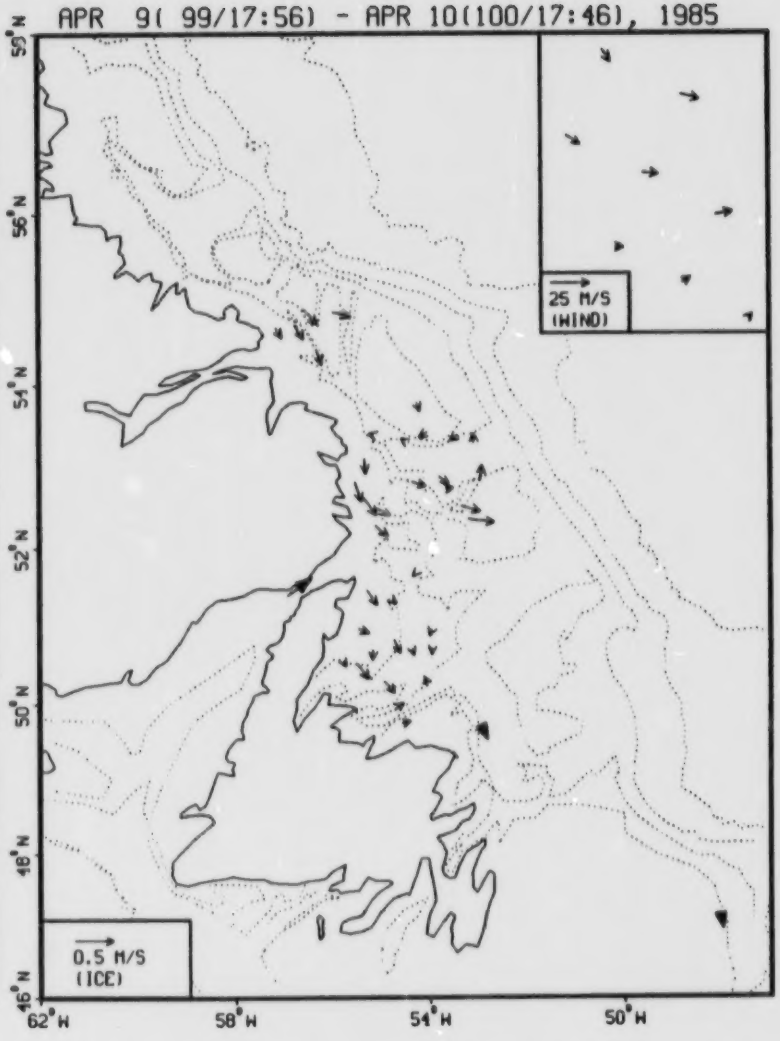
APR 9( 99/17:56) - APR 10(100/17:46), 1985
25 M/S
(WIND)
0.5 M/S
(ICE)
58°N
56°N
54°N
52°N
50°N
48°N
46°N
62°W
58°W
54°W
50°W

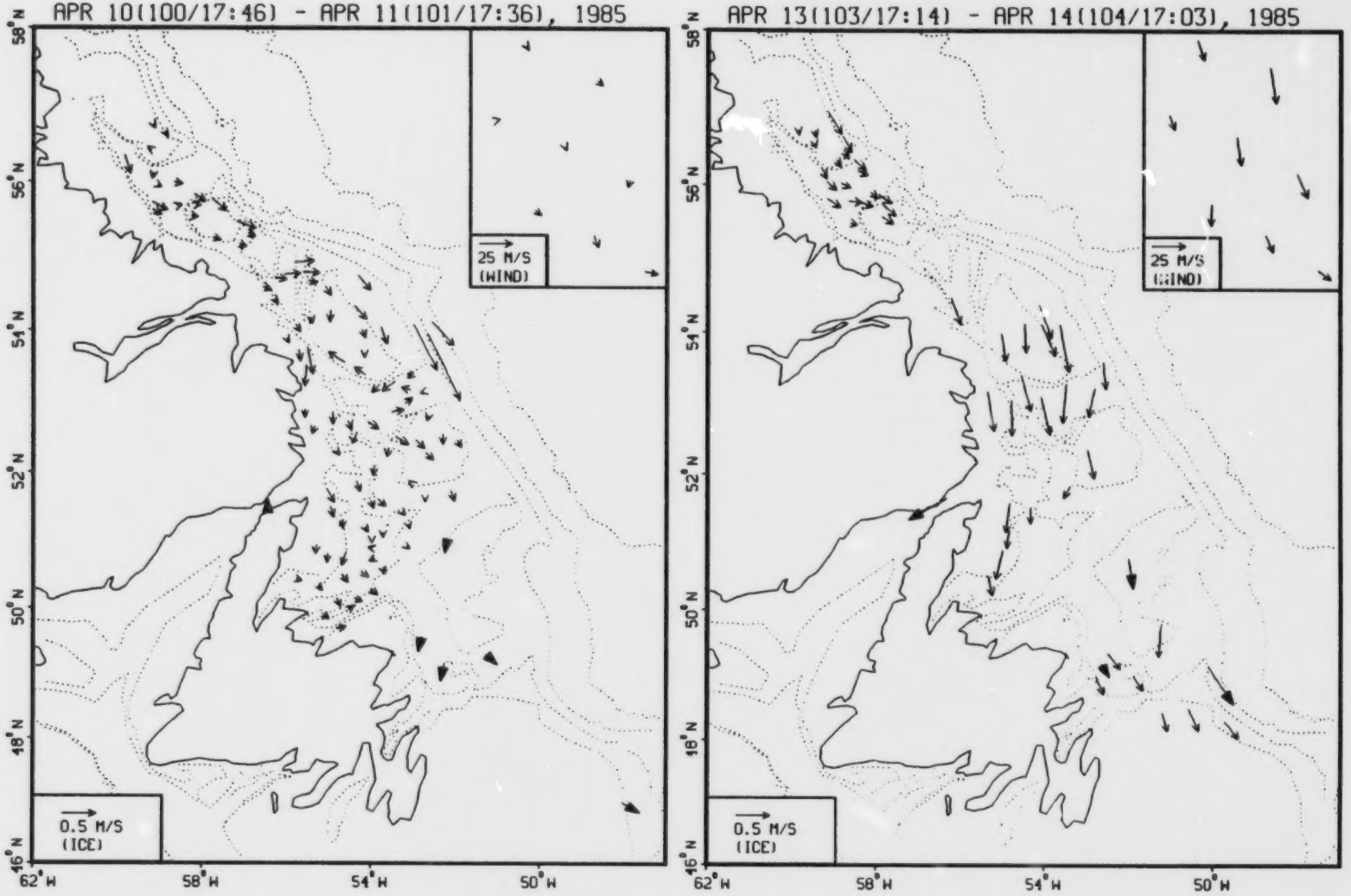
APR 10(100/17:46) - APR 11(101/17:36), 1985
25 M/S
(WIND)
0.5 M/S
(ICE)
APR 13(103/17:14) - APR 14(104/17:03), 1985
25 M/S
(WIND)
0.5 M/S
(ICE)
58°N
56°N
54°N
52°N
50°N
18°N
16°N
62°W
58°W
54°W
50°W

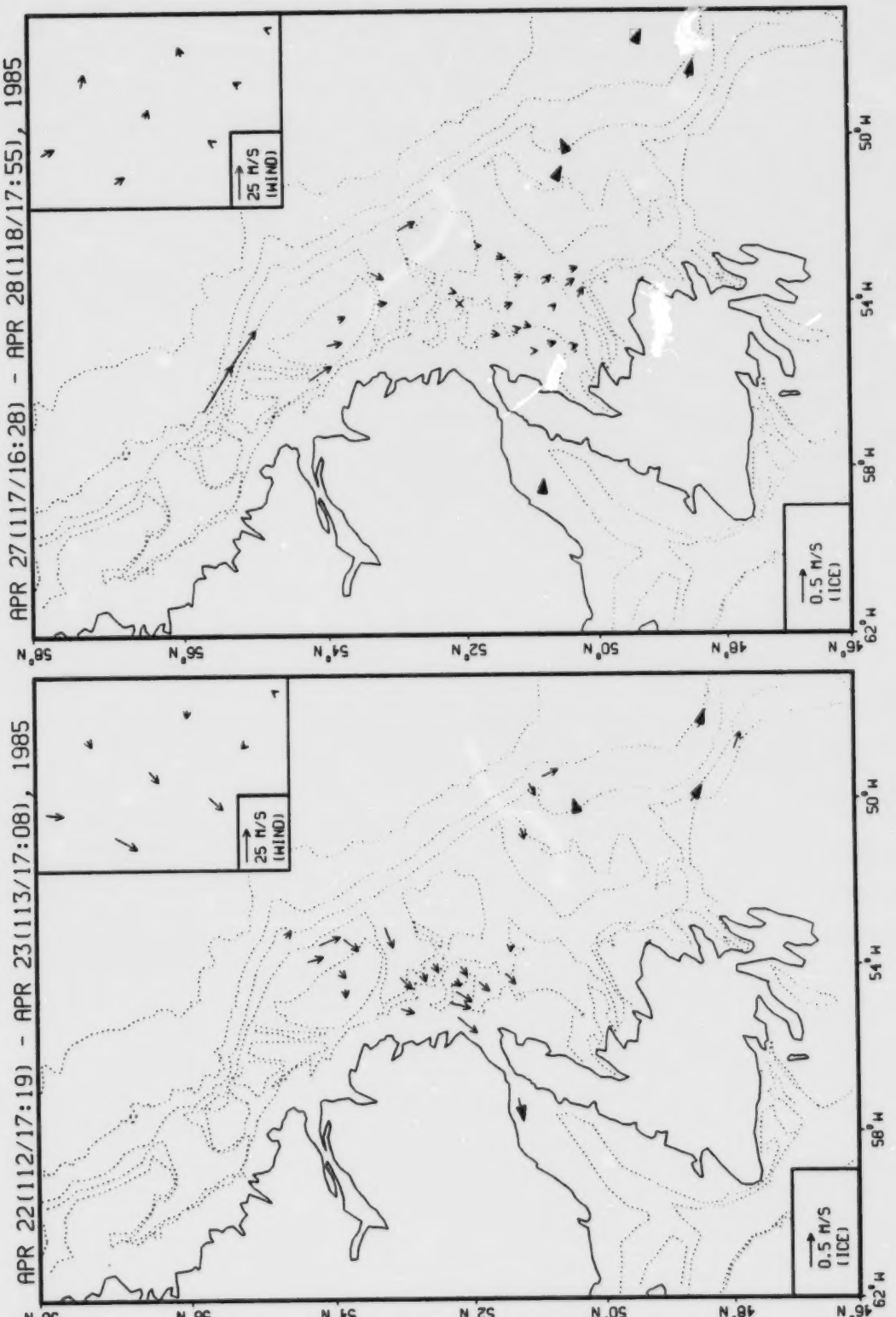
APR 27(117/16:28) - APR 28(118/17:55), 1985
APR 22(112/17:19) - APR 23(113/17:08), 1985
25 M/S (WIND)
0.5 M/S (ICE)
62°W
58°W
54°W
50°W
46°N
48°N
50°N
52°N
54°N
56°N
58°N

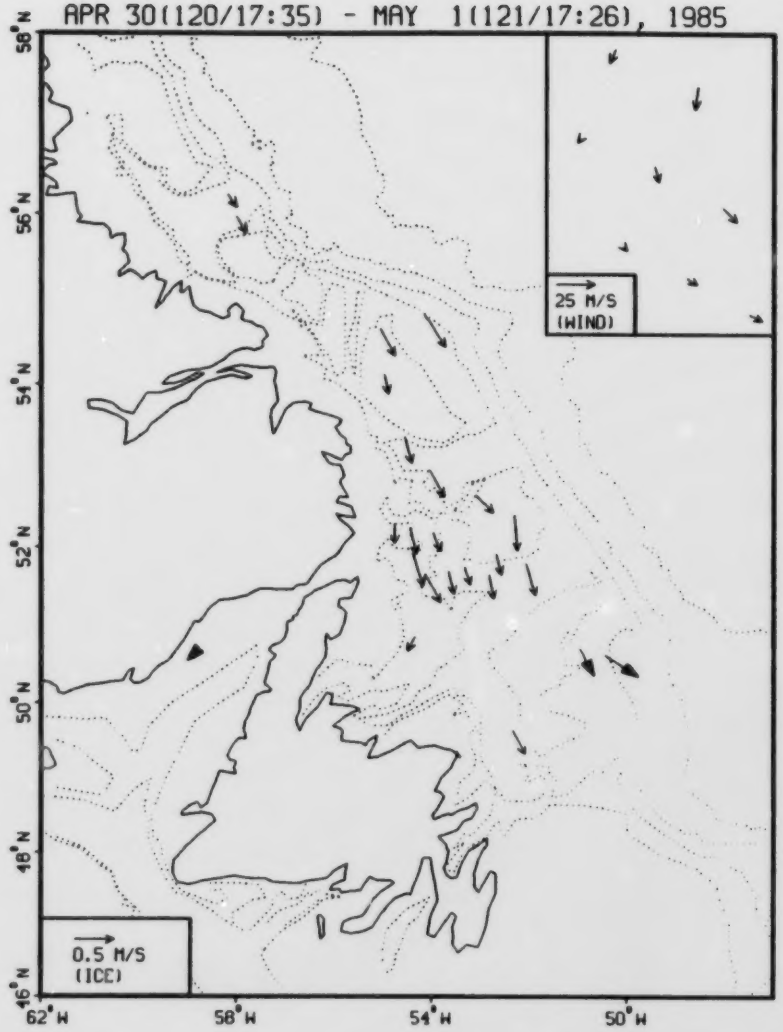
APR 30(120/17:35) - MAY 1(121/17:26), 1985
25 M/S
(WIND)
0.5 M/S
(ICE)
58°N
56°N
54°N
52°N
50°N
48°N
46°N
62°W
58°W
54°W
50°W

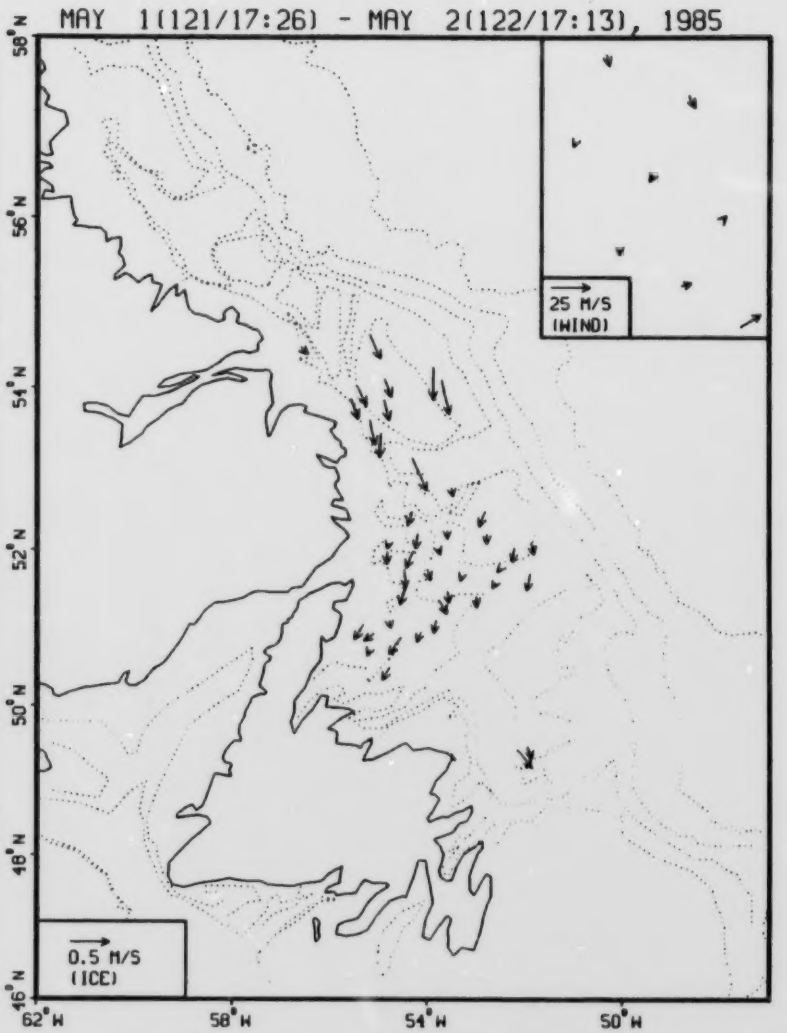
MAY 1(121/17:26) - MAY 2(122/17:13), 1985
25 M/S
(WIND)
0.5 M/S
(ICE)
58°N
56°N
54°N
52°N
50°N
48°N
46°N
62°W
58°W
54°W
50°W

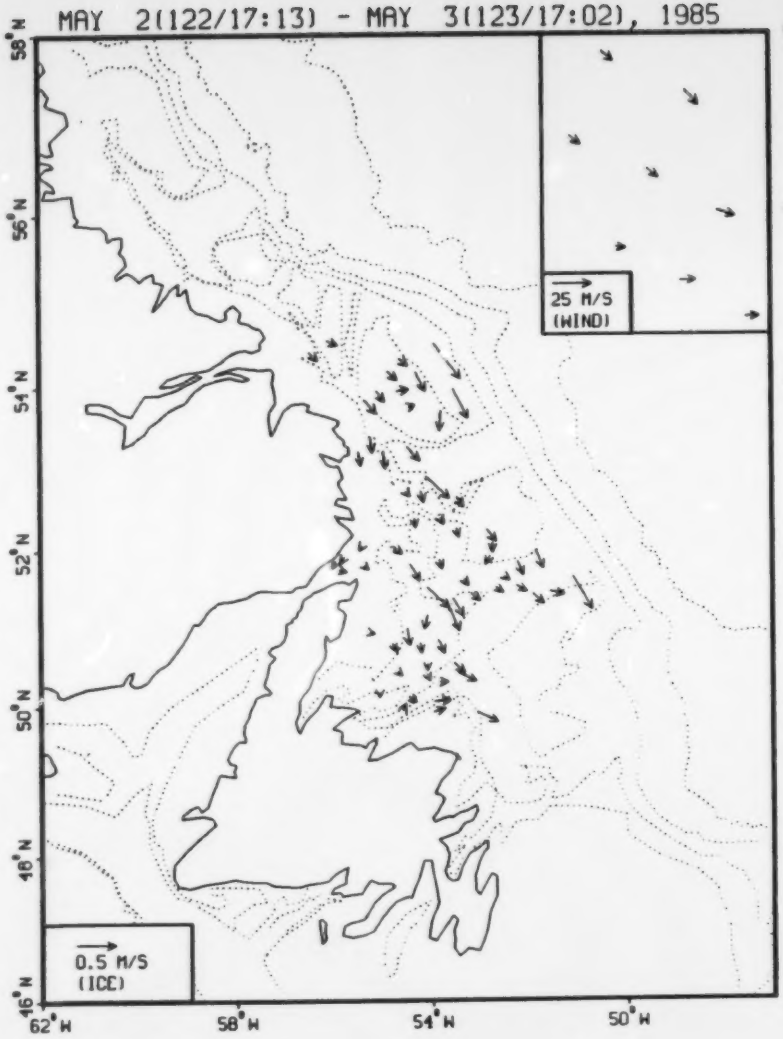
MAY 2(122/17:13) - MAY 3(123/17:02), 1985
25 M/S
(WIND)
0.5 M/S
(ICE)
58°N
56°N
54°N
52°N
50°N
48°N
46°N
62°W
58°W
54°W
50°W

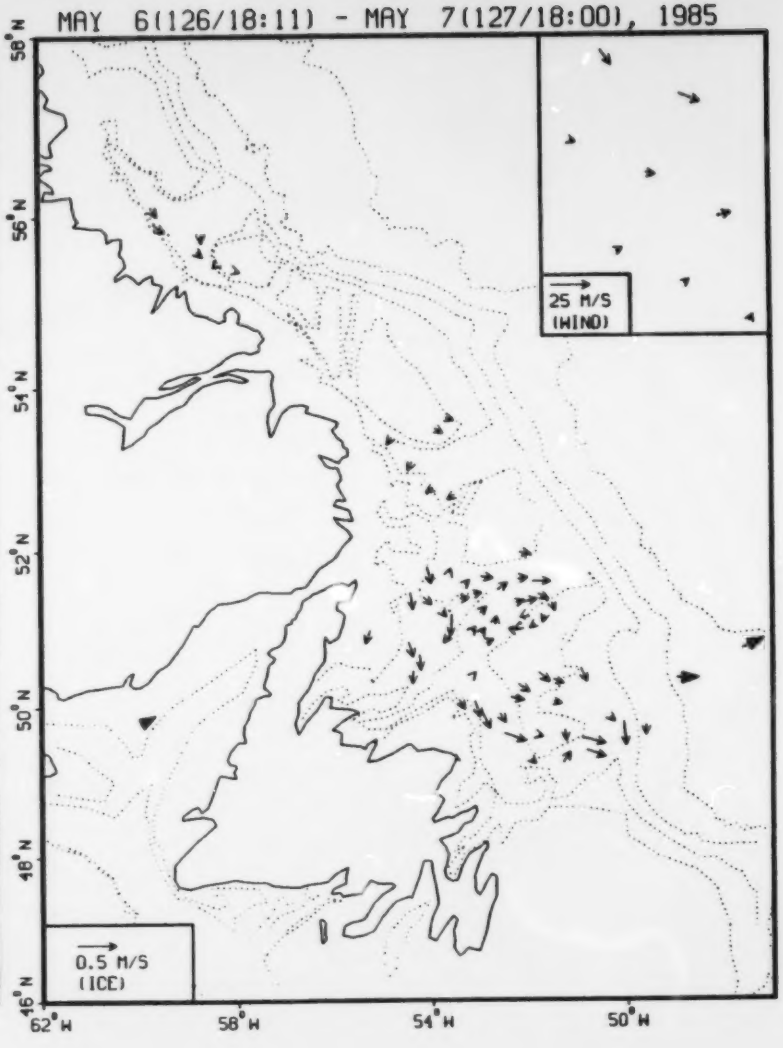
MAY 6(126/18:11) - MAY 7(127/18:00), 1985
25 M/S
(WIND)
0.5 M/S
(ICE)
58°N
56°N
54°N
52°N
50°N
48°N
46°N
62°W
58°W
54°W
50°W

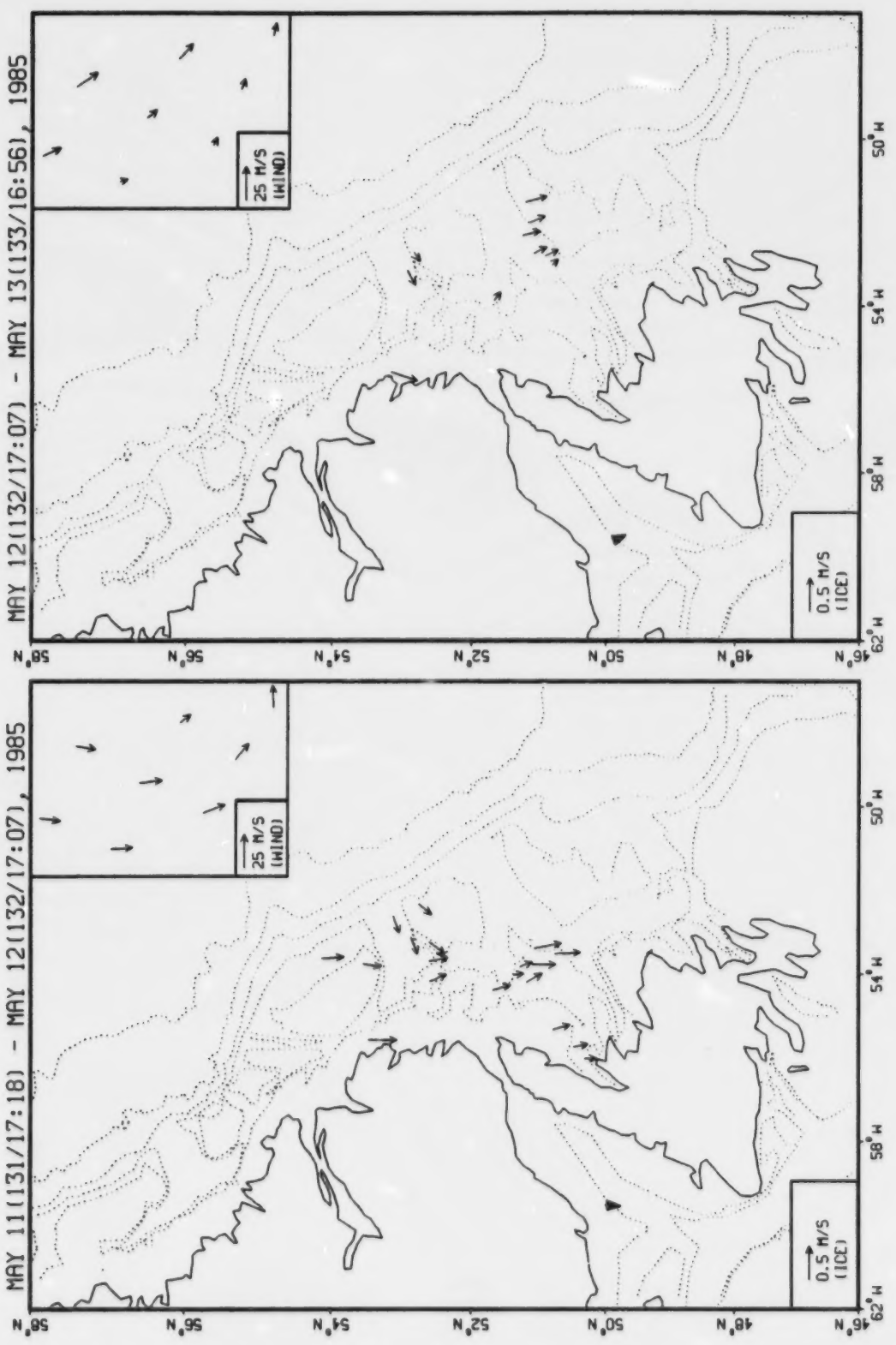
MAY 11(131/17:18) - MAY 12(132/17:07), 1985
25 M/S (WIND)
0.5 M/S (ICE)
MAY 12(132/17:07) - MAY 13(133/16:56), 1985
25 M/S (WIND)
0.5 M/S (ICE)
58°N
56°N
54°N
52°N
50°N
48°N
46°N
62°W
58°W
54°W
50°W

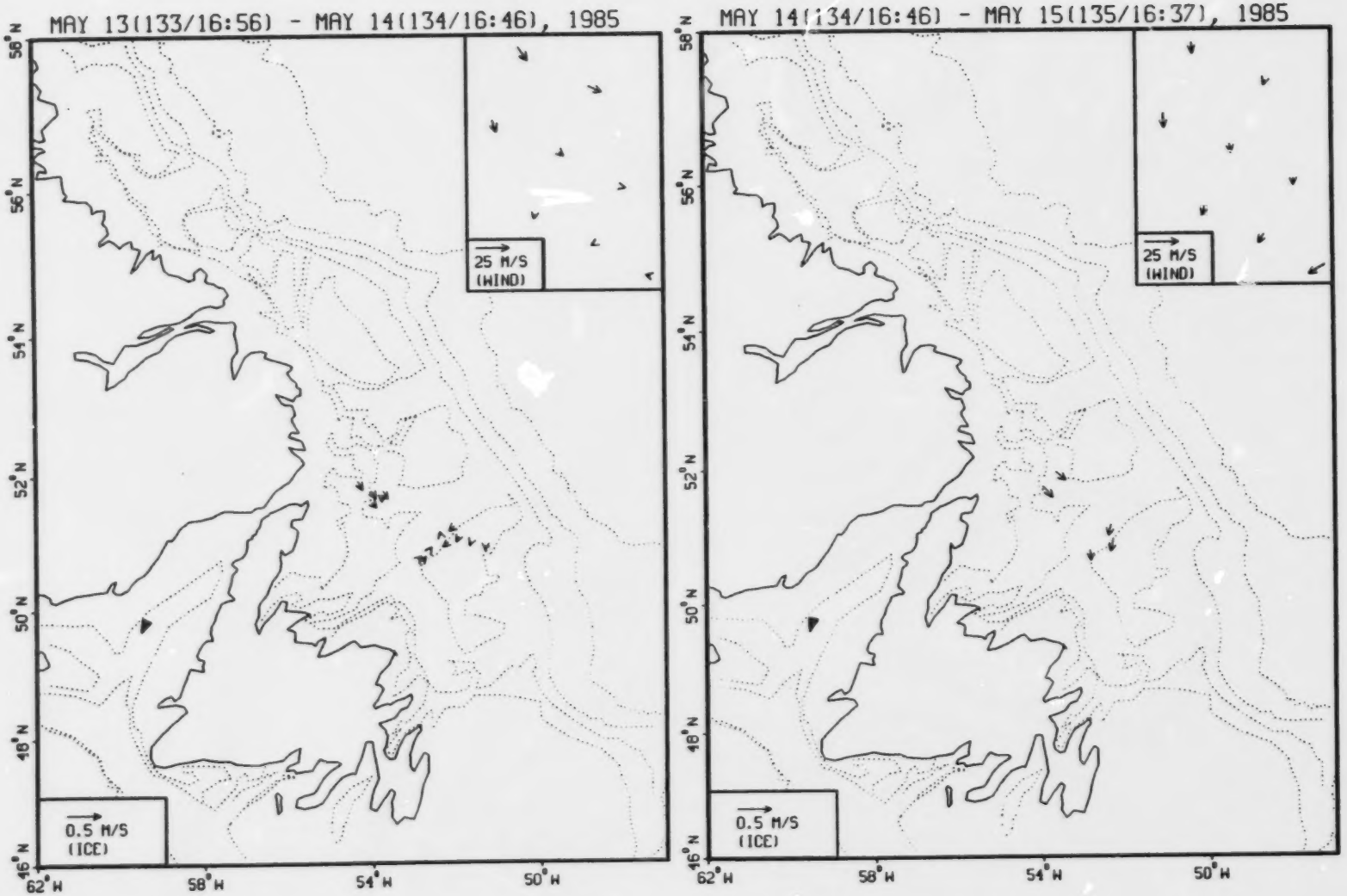
MAY 13(133/16:56) - MAY 14(134/16:46), 1985
MAY 14(134/16:46) - MAY 15(135/16:37), 1985
25 M/S
(WIND)
0.5 M/S
(ICE)
58°N
56°N
54°N
52°N
50°N
48°N
46°N
62°W
58°W
54°W
50°W

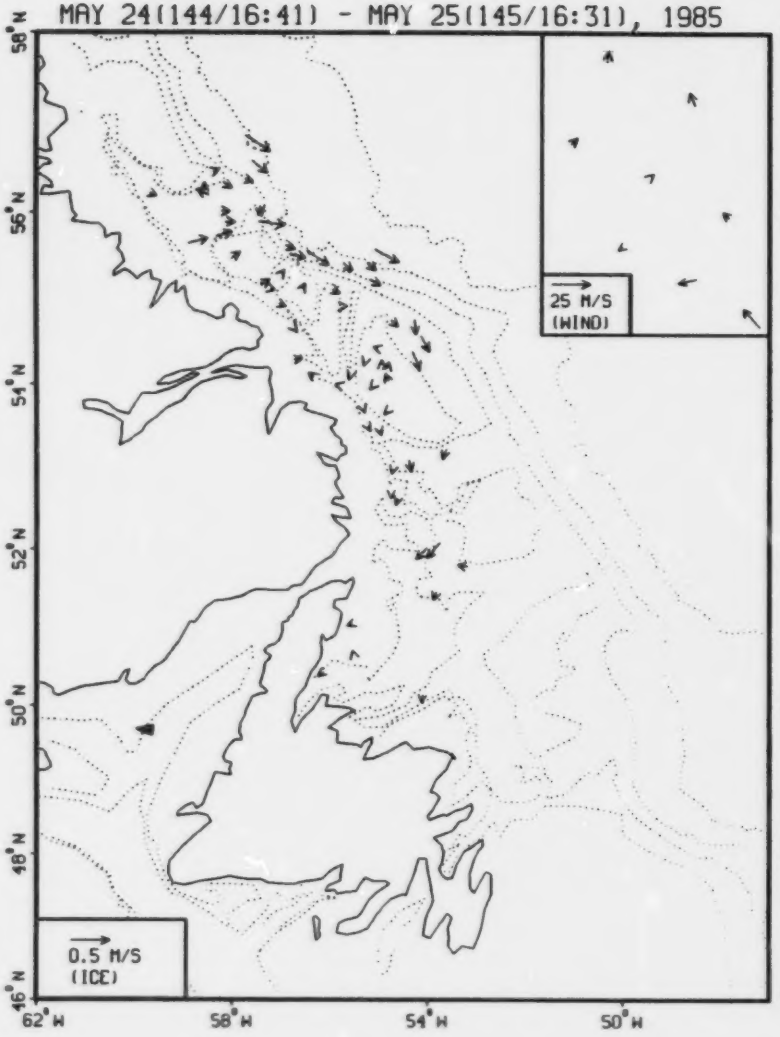
MAY 24(144/16:41) - MAY 25(145/16:31), 1985
58°N
56°N
54°N
52°N
50°N
48°N
46°N
62°W
58°W
54°W
50°W
25 M/S
(WIND)
0.5 M/S
(ICE)

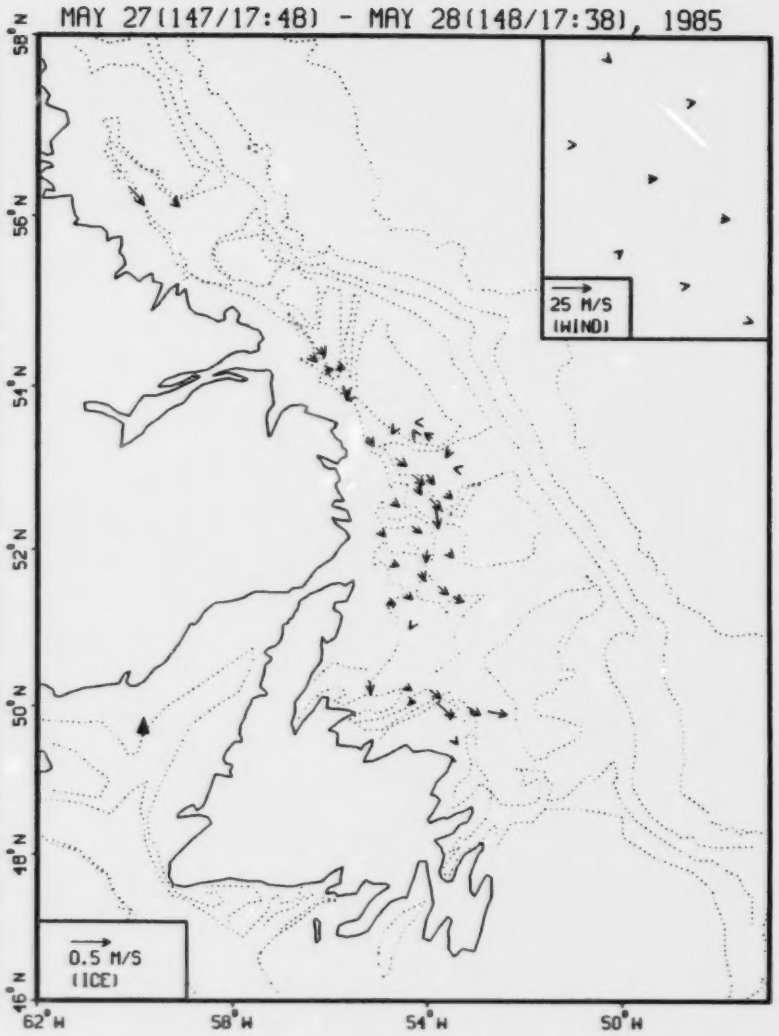
MAY 27(147/17:48) - MAY 28(148/17:38), 1985
58°N
56°N
54°N
52°N
50°N
48°N
46°N
62°W
58°W
54°W
50°W
25 M/S
(WIND)
0.5 M/S
(ICE)

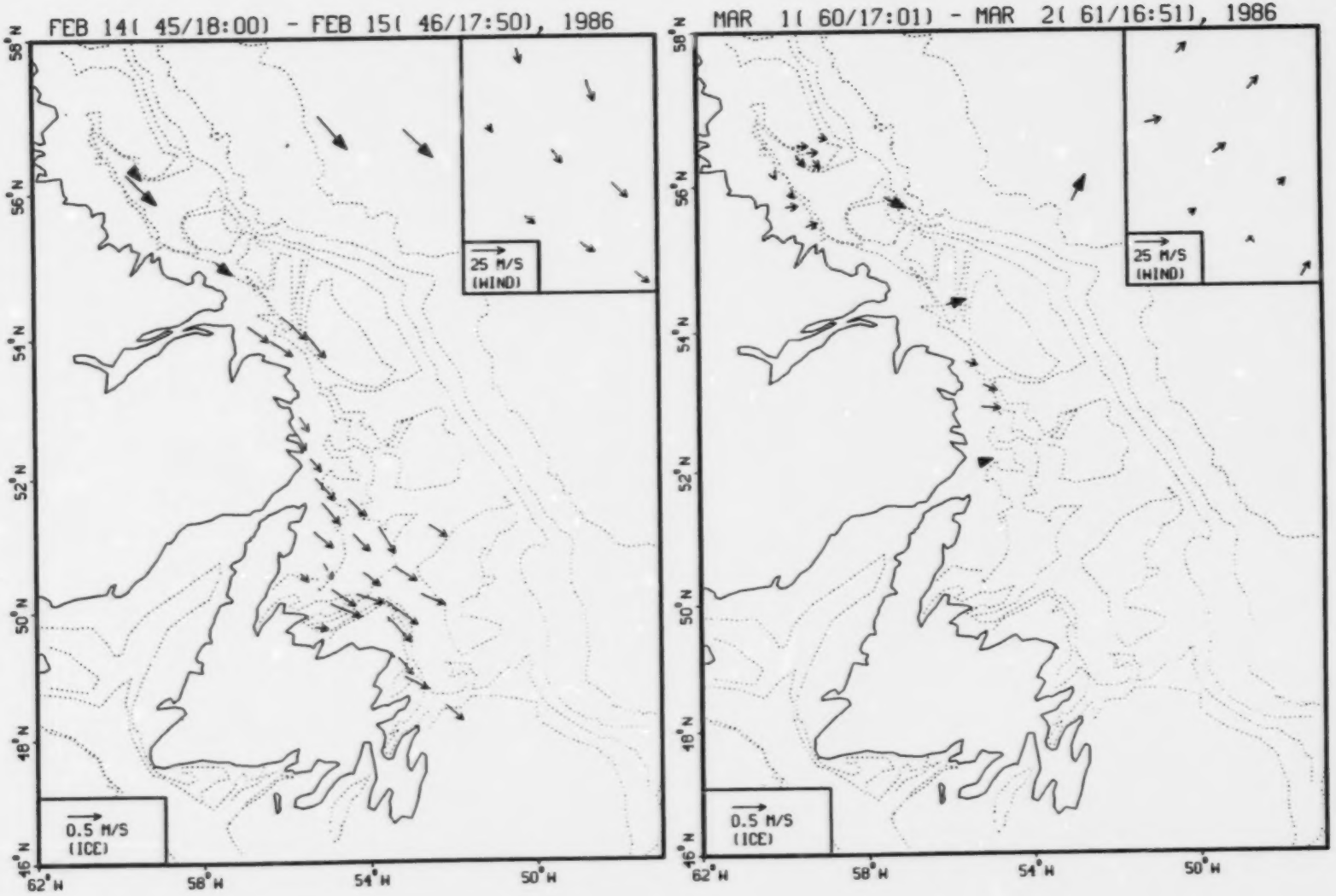
FEB 14( 45/18:00) - FEB 15( 46/17:50), 1986
MAR 1( 60/17:01) - MAR 2( 61/16:51), 1986
25 M/S
(WIND)
0.5 M/S
(ICE)
58°N
56°N
54°N
52°N
50°N
48°N
46°N
62°W
58°W
54°W
50°W

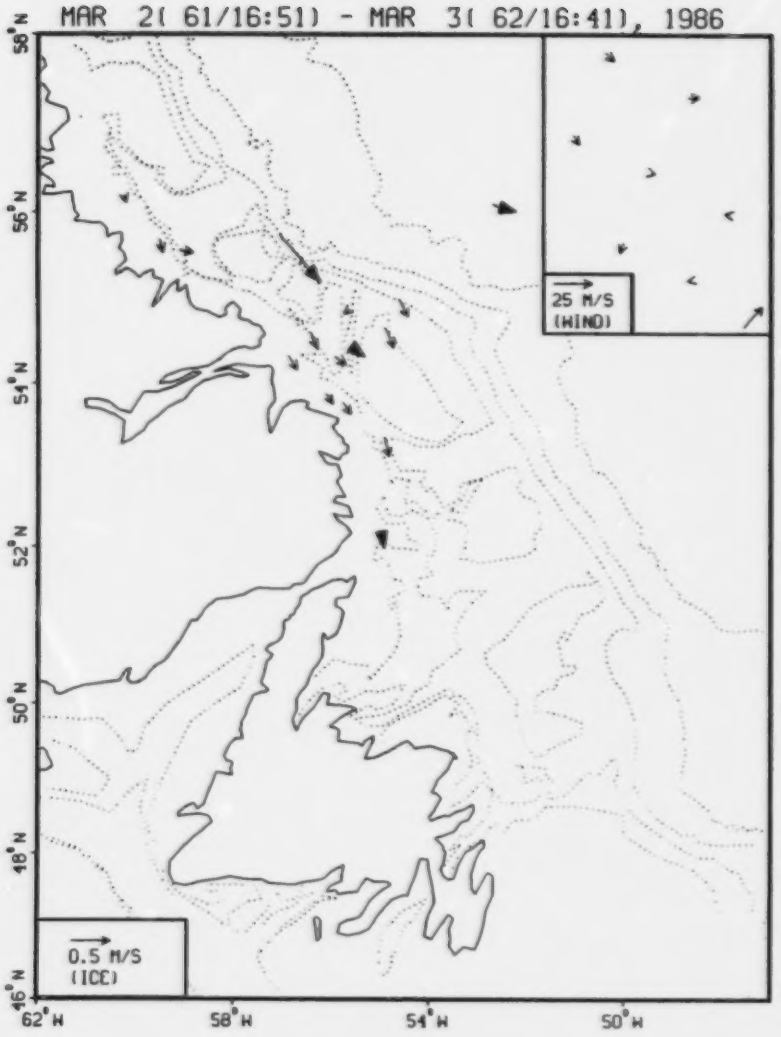
MAR 2( 61/16:51) - MAR 3( 62/16:41), 1986
25 M/S
(WIND)
0.5 M/S
(ICE)
62°W
58°W
54°W
50°W
46°N
50°N
52°N
54°N
56°N
58°N

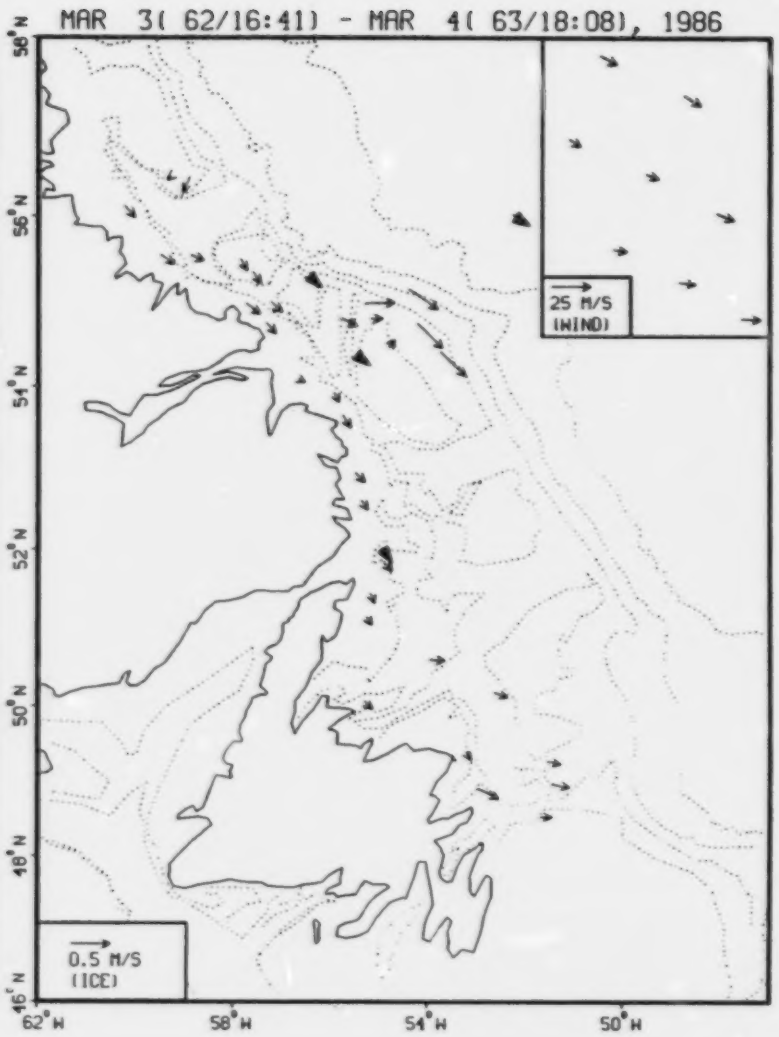
MAR 3( 62/16:41) - MAR 4( 63/18:08), 1986
25 M/S
(WIND)
0.5 M/S
(ICE)
62°W
58°W
54°W
50°W
46°N
50°N
52°N
54°N
56°N
58°N

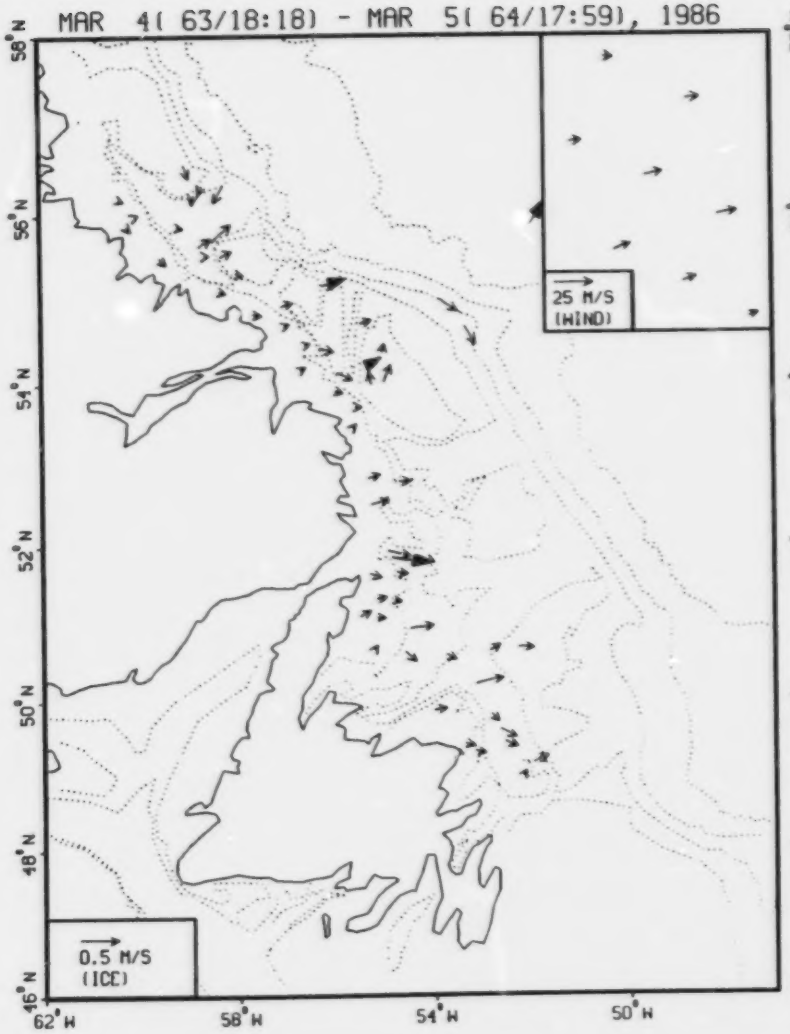
MAR 4( 63/18:18) - MAR 5( 64/17:59), 1986
25 M/S
(WIND)
0.5 M/S
(ICE)
58°N
56°N
54°N
52°N
50°N
48°N
46°N
62°W
58°W
54°W
50°W

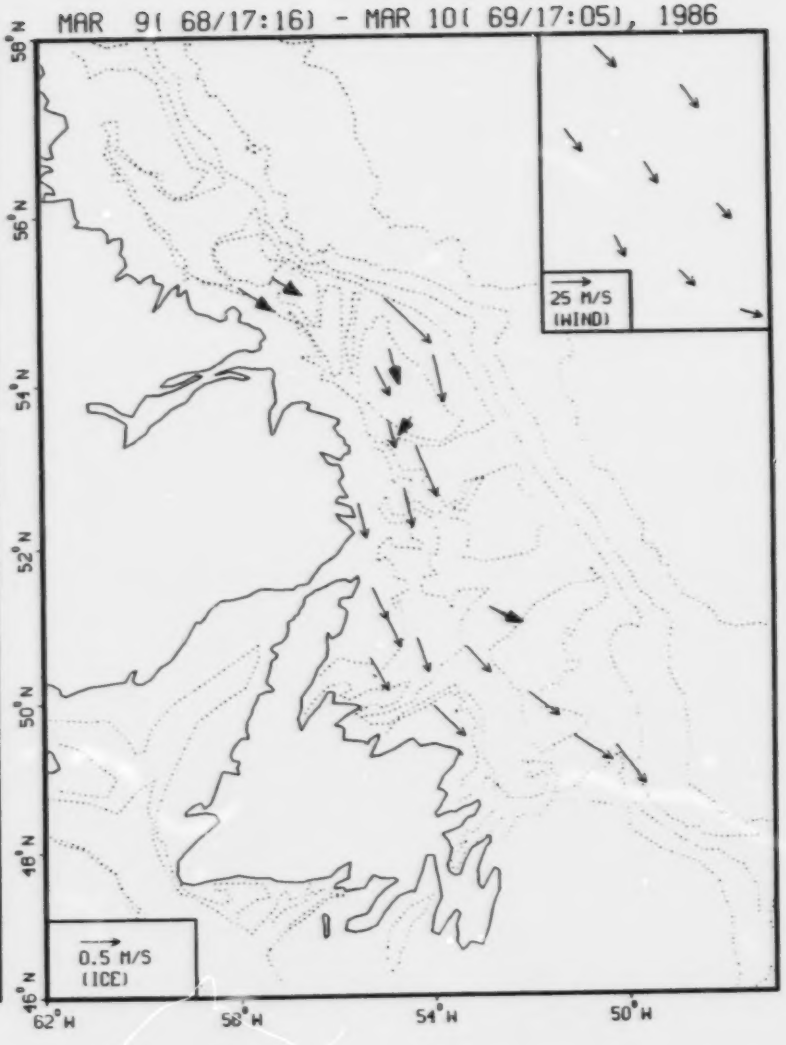
MAR 9( 68/17:16) - MAR 10( 69/17:05), 1986
25 M/S
(WIND)
0.5 M/S
(ICE)
58°N
56°N
54°N
52°N
50°N
48°N
46°N
62°W
58°W
54°W
50°W

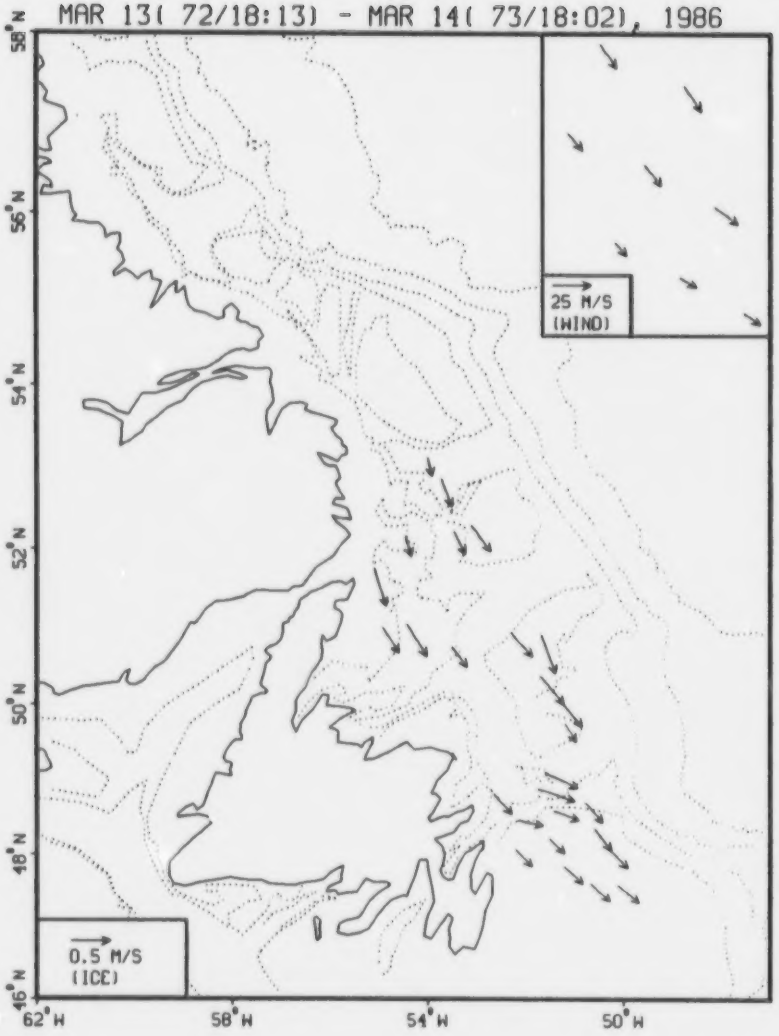
MAR 13( 72/18:13) - MAR 14( 73/18:02), 1986
25 M/S
(WIND)
0.5 M/S
(ICE)
58°N
56°N
54°N
52°N
50°N
48°N
46°N
62°W
58°W
54°W
50°W

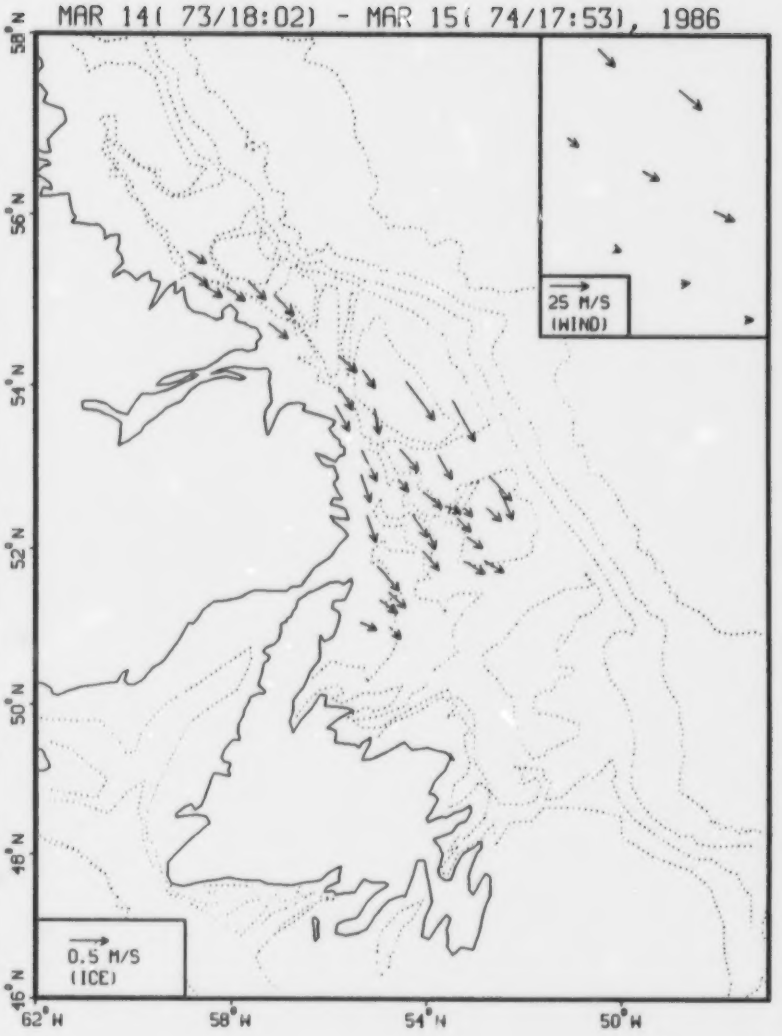
MAR 14( 73/18:02) - MAR 15( 74/17:53), 1986
25 M/S
(WIND)
0.5 M/S
(ICE)
58°N
56°N
54°N
52°N
50°N
48°N
46°N
62°W
58°W
54°W
50°W

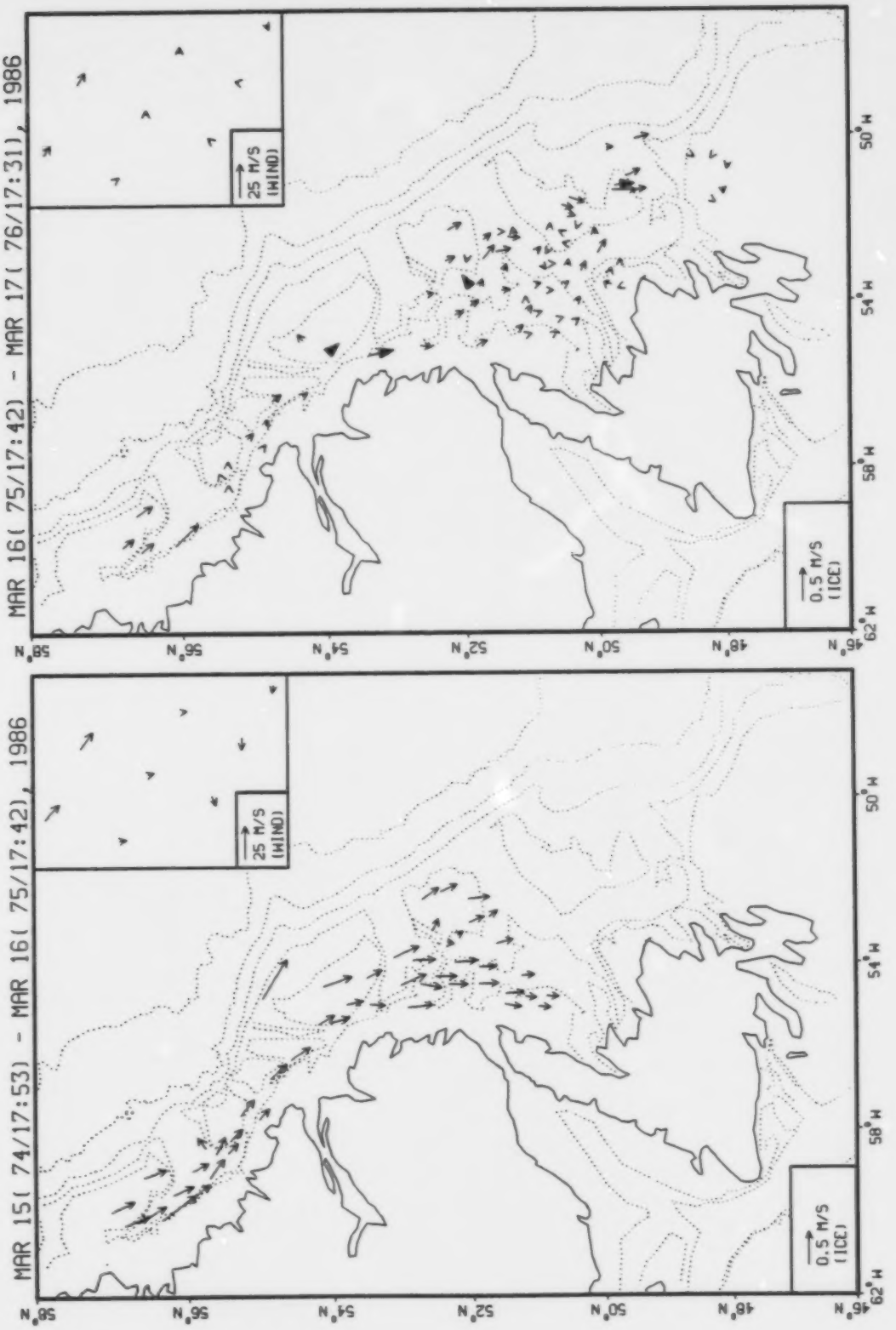
MAR 16( 75/17:42) - MAR 17( 76/17:31), 1986
MAR 15( 74/17:53) - MAR 16( 75/17:42), 1986
25 M/S (WIND)
0.5 M/S (ICE)
58°N
56°N
54°N
52°N
50°N
48°N
46°N
62°W
58°W
54°W
50°W

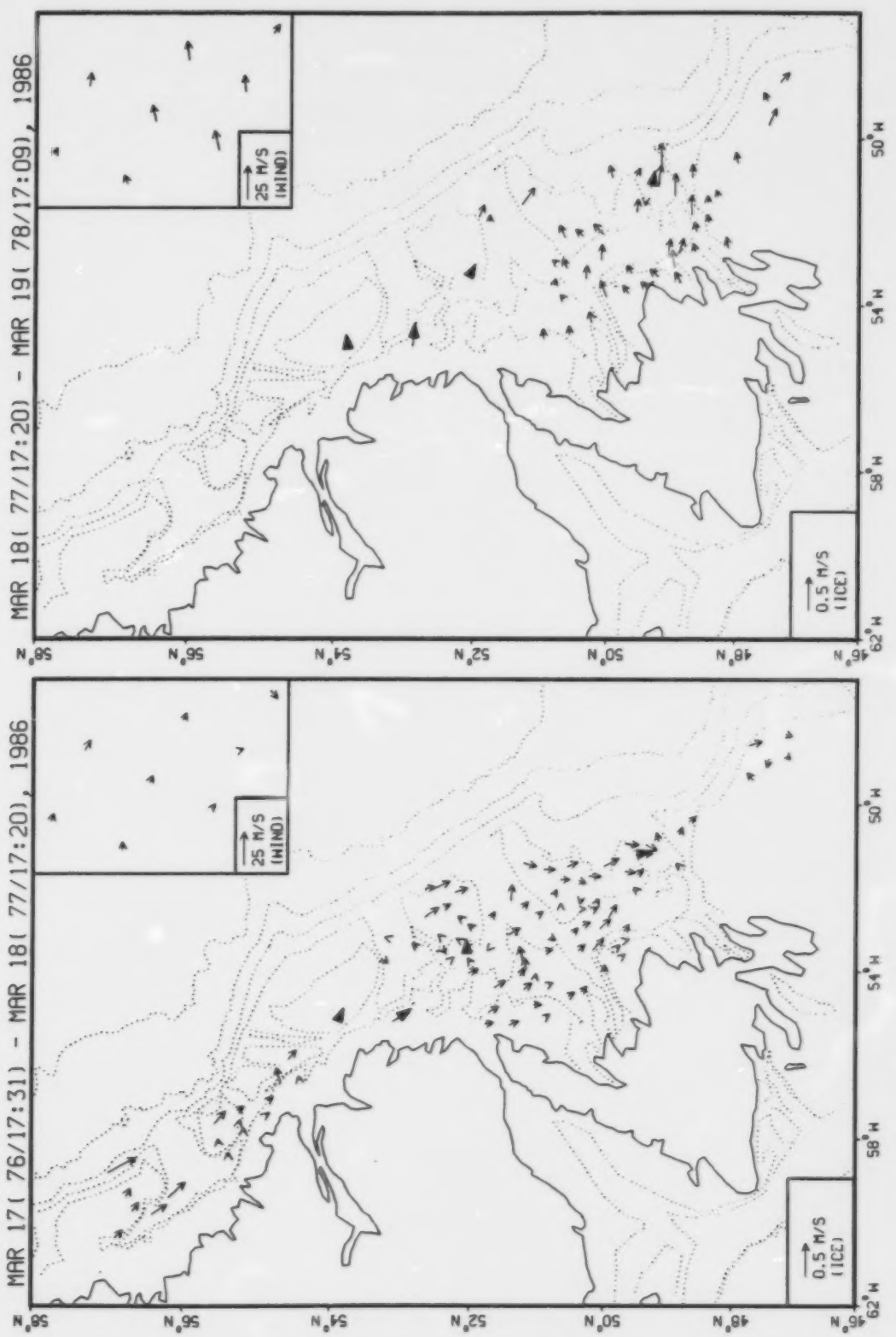
MAR 18( 77/17:20) - MAR 19( 78/17:09), 1986
25 M/S (WIND)
0.5 M/S (ICE)
MAR 17( 76/17:31) - MAR 18( 77/17:20), 1986
25 M/S (WIND)
0.5 M/S (ICE)
46°N
48°N
50°N
52°N
54°N
56°N
58°N
62°W
58°W
54°W
50°W

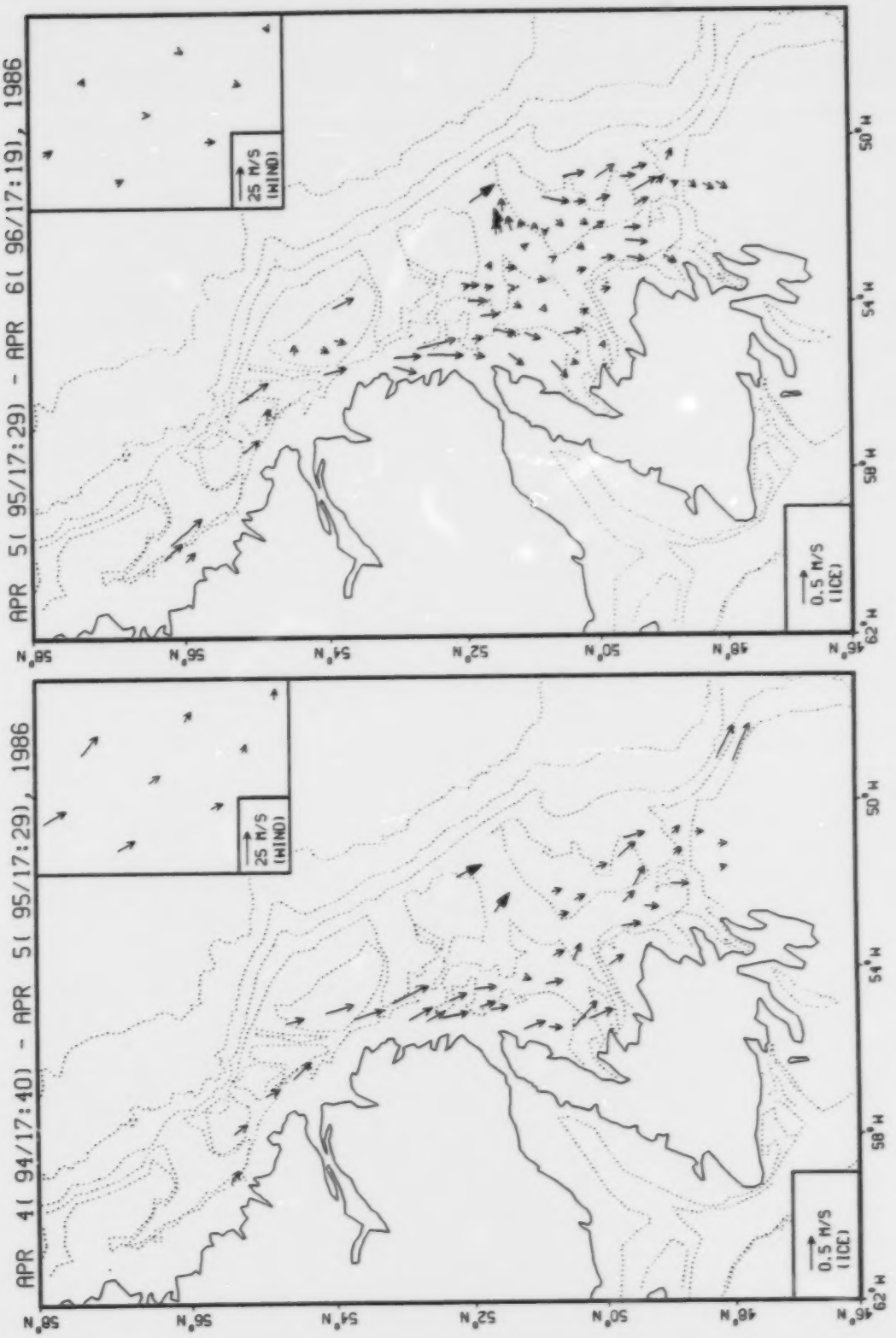
APR 4( 94/17:40) - APR 5( 95/17:29), 1986
25 M/S (WIND)
0.5 M/S (ICE)
APR 5( 95/17:29) - APR 6( 96/17:19), 1986
25 M/S (WIND)
0.5 M/S (ICE)
58°N
56°N
54°N
52°N
50°N
48°N
46°N
62°W
58°W
54°W
50°W

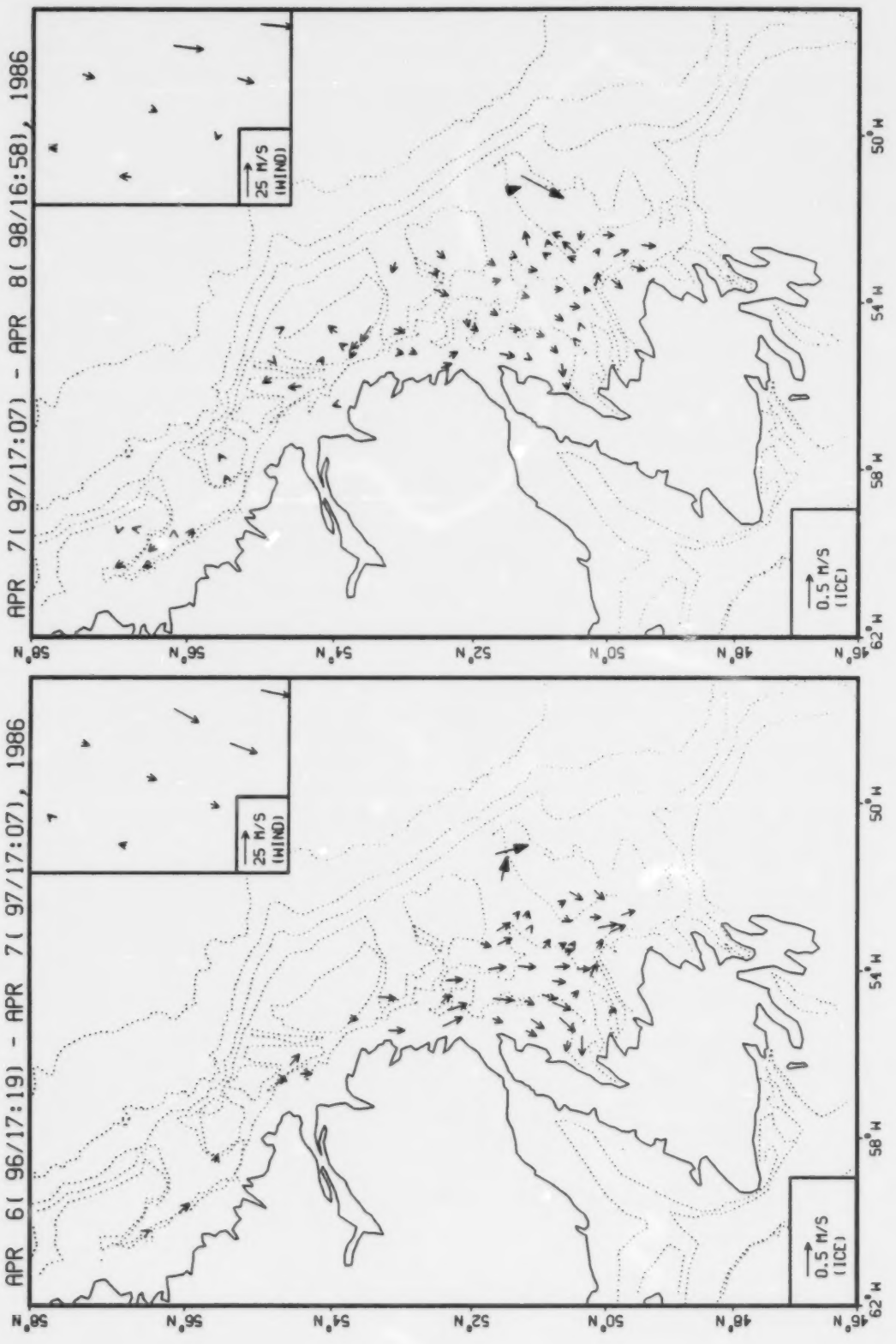
APR 6( 96/17:19) - APR 7( 97/17:07), 1986
APR 7( 97/17:07) - APR 8( 98/16:58), 1986
25 M/S (WIND)
0.5 M/S (ICE)
62°W
58°W
54°W
50°W
46°N
48°N
50°N
52°N
54°N
56°N
58°N

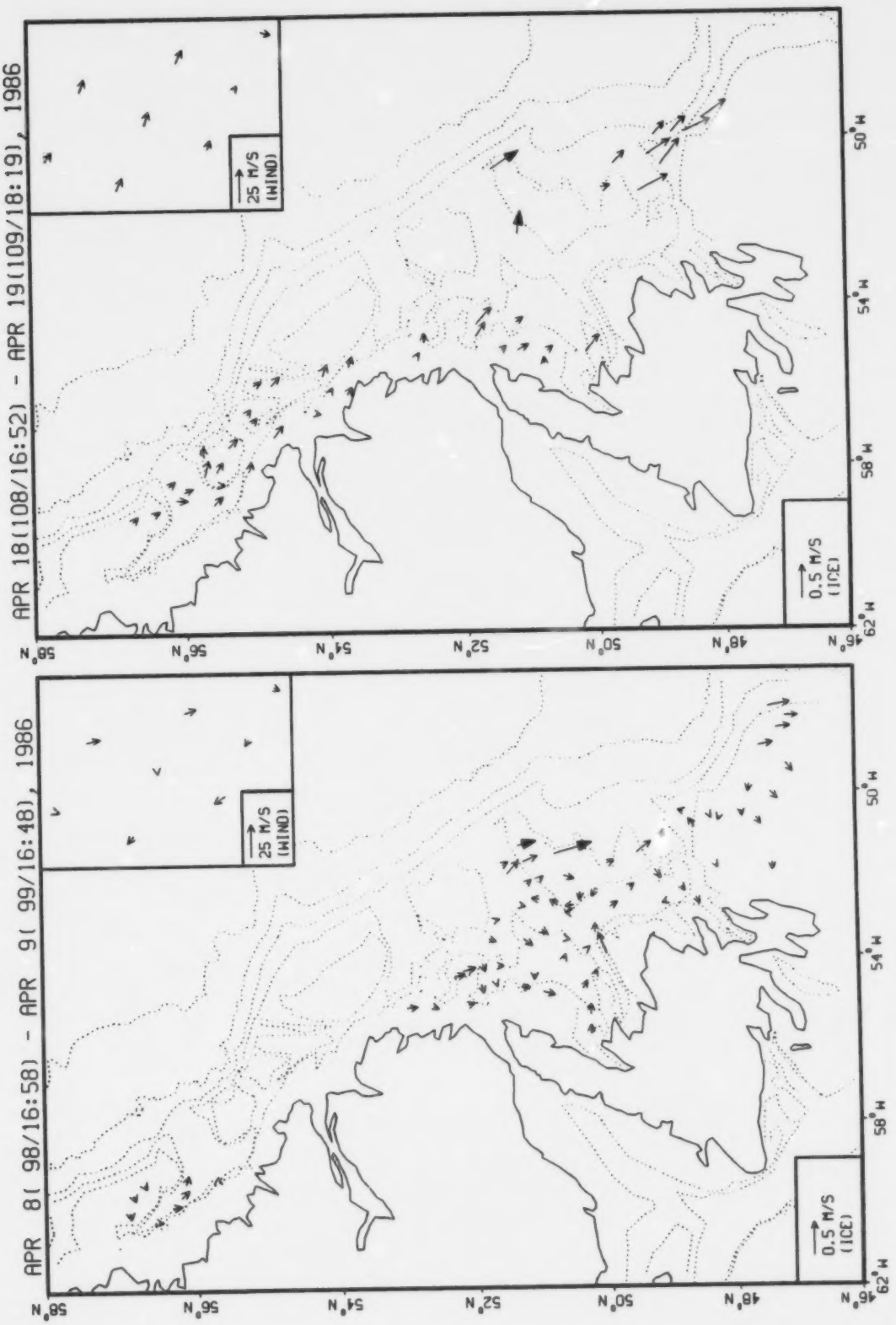
APR 18(108/16:52) - APR 19(109/18:19), 1986
25 M/S (WIND)
0.5 M/S (10I)
APR 8( 98/16:58) - APR 9( 99/16:48), 1986
25 M/S (WIND)
0.5 M/S (10I)
62°W
58°W
54°W
50°W
46°N
48°N
50°N
52°N
54°N
56°N
58°N

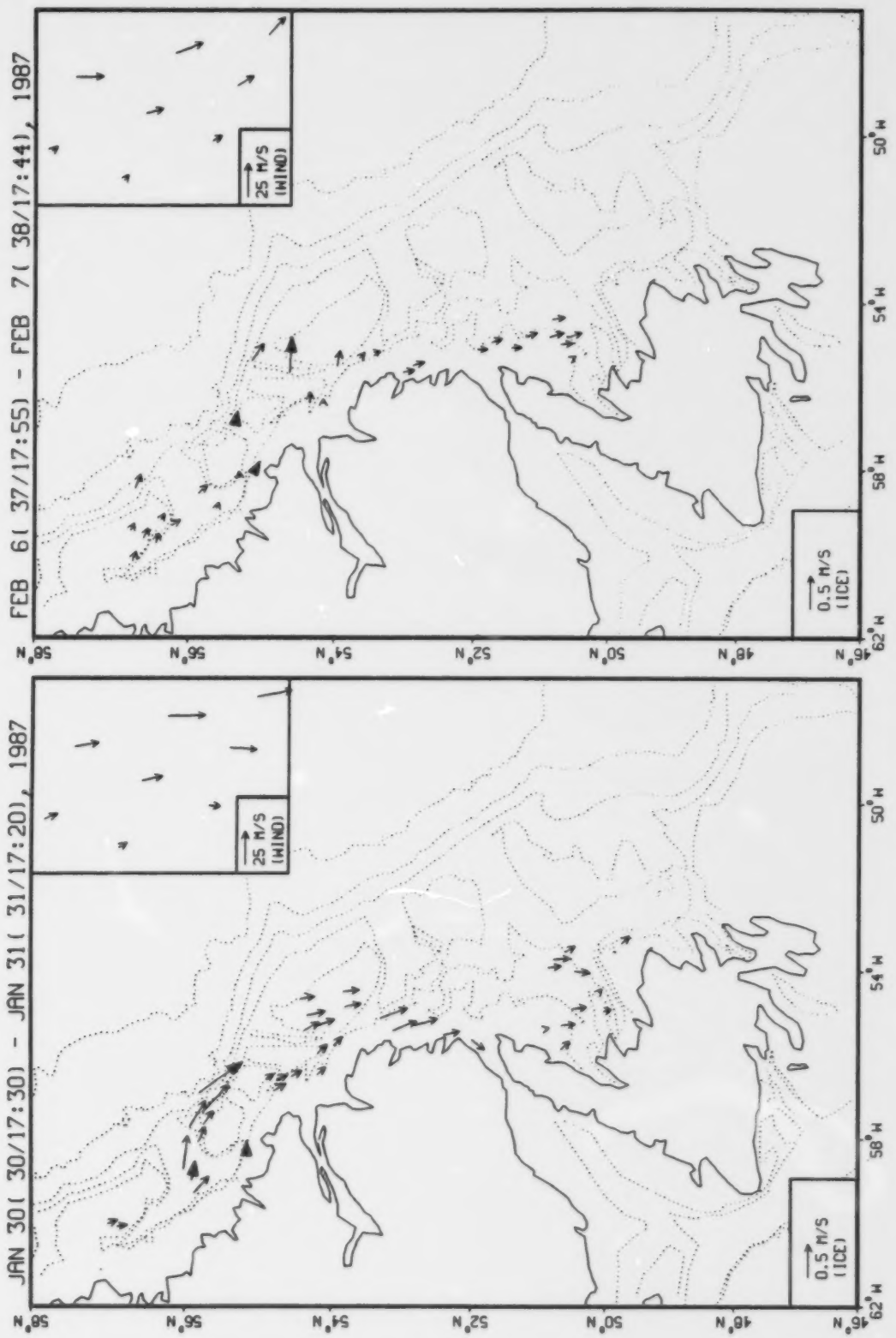
JAN 30( 30/17:30) - JAN 31( 31/17:20), 1987
25 M/S (WIND)
0.5 M/S (ICE)
FEB 6( 37/17:55) - FEB 7( 38/17:44), 1987
25 M/S (WIND)
0.5 M/S (ICE)
58°N
56°N
54°N
52°N
50°N
48°N
46°N
62°W
58°W
54°W
50°W

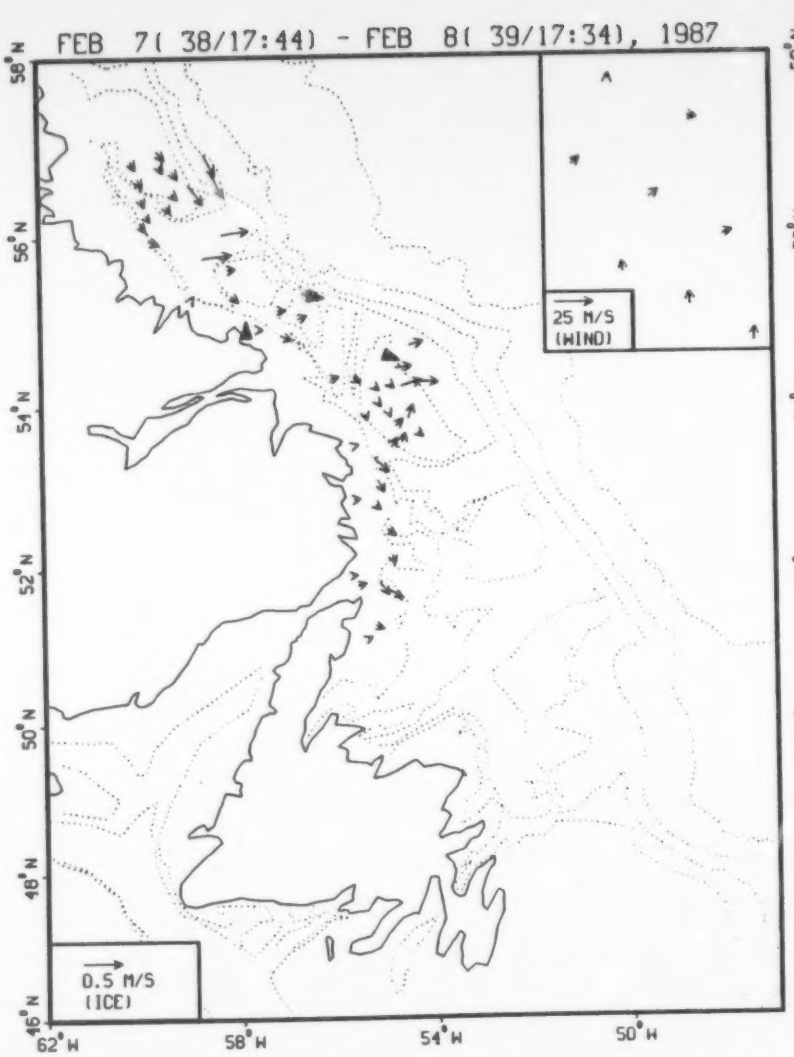
FEB 7( 38/17:44) - FEB 8( 39/17:34), 1987
25 M/S
(WIND)
0.5 M/S
(ICE)
58°N
56°N
54°N
52°N
50°N
48°N
46°N
62°W
58°W
54°W
50°W

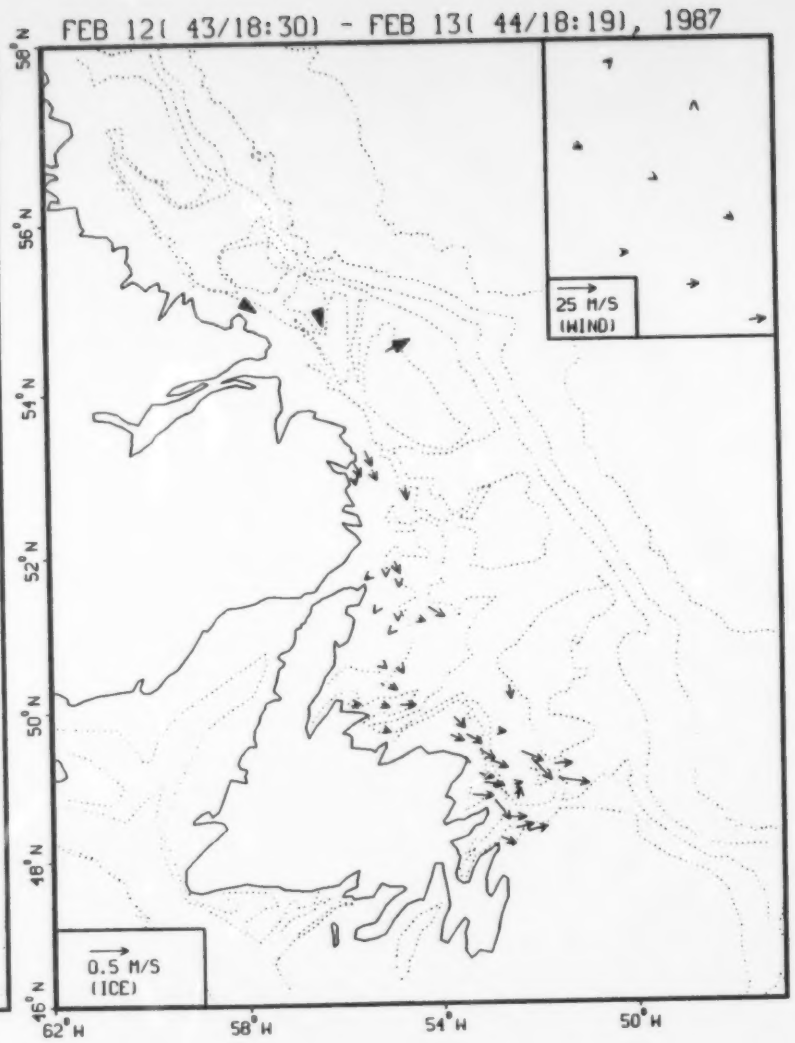
FEB 12( 43/18:30) - FEB 13( 44/18:19), 1987
25 M/S
(WIND)
0.5 M/S
(ICE)
58°N
56°N
54°N
52°N
50°N
48°N
46°N
62°W
58°W
54°W
50°W

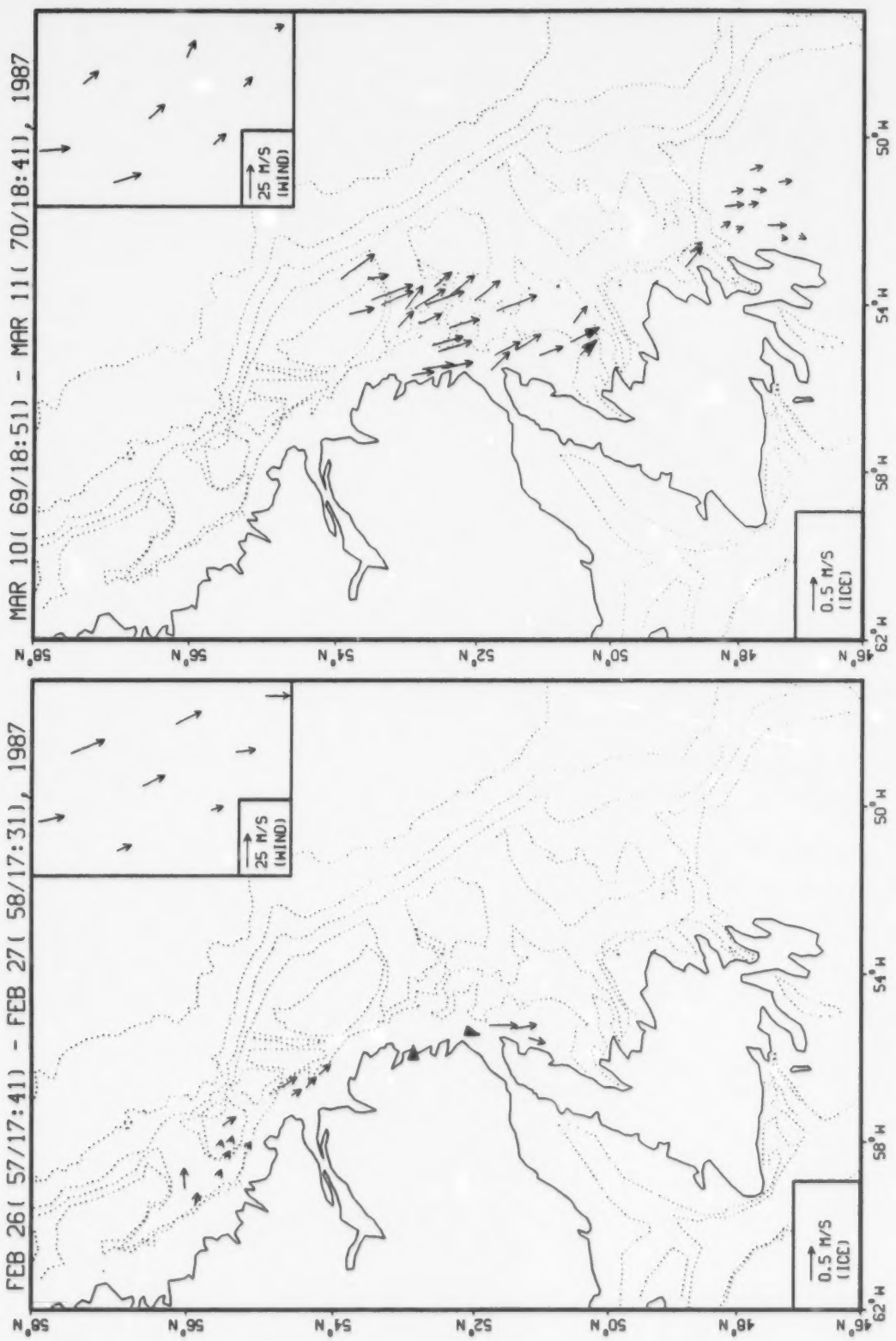
FEB 26( 57/17:41) - FEB 27( 58/17:31), 1987
MAR 10( 69/18:51) - MAR 11( 70/18:41), 1987
25 M/S (WIND)
0.5 M/S (ICE)
58°N
56°N
54°N
52°N
50°N
48°N
46°N
62°W
58°W
54°W
50°W

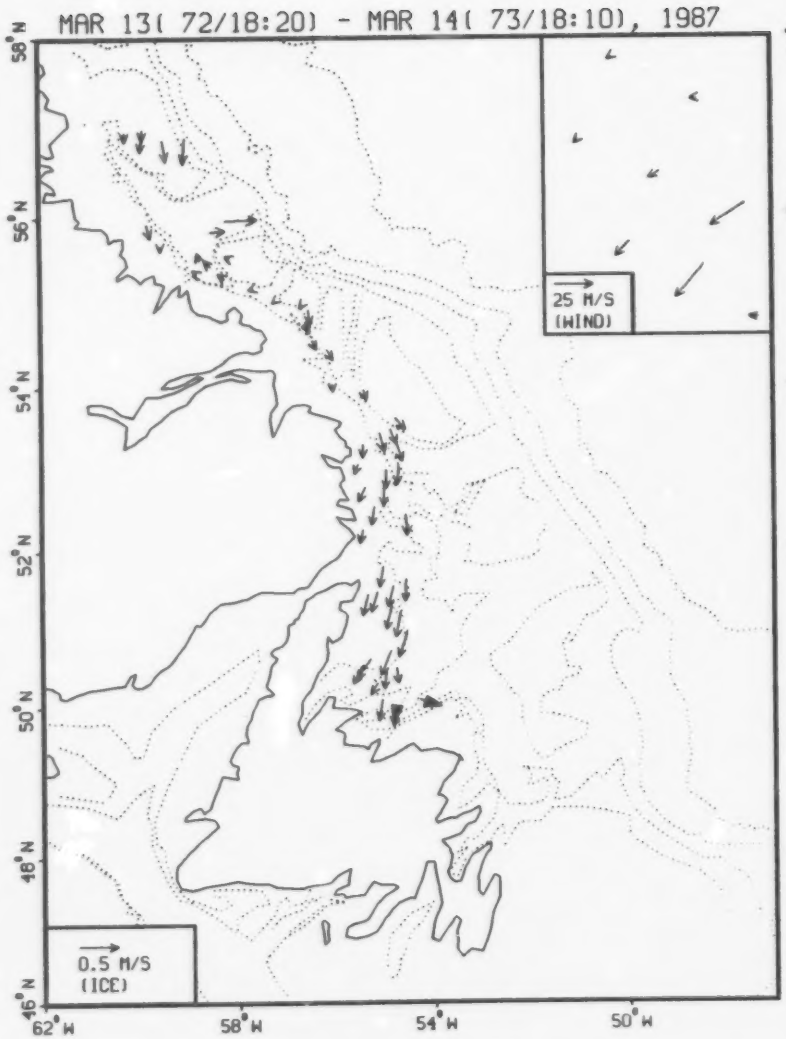
MAR 13( 72/18:20) - MAR 14( 73/18:10), 1987
25 M/S
(WIND)
0.5 M/S
(ICE)
58°N
56°N
54°N
52°N
50°N
48°N
46°N
62°W
58°W
54°W
50°W

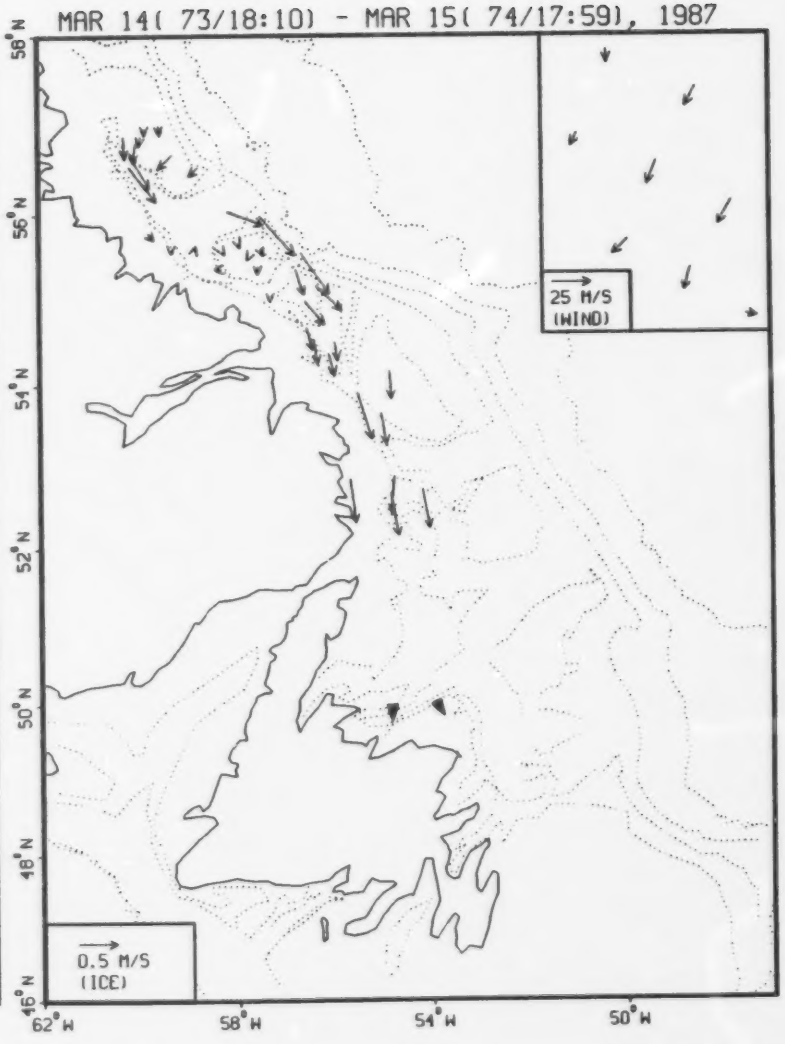
MAR 14( 73/18:10) - MAR 15( 74/17:59), 1987
25 M/S
(WIND)
0.5 M/S
(ICE)
58°N
56°N
54°N
52°N
50°N
48°N
46°N
62°W
58°W
54°W
50°W

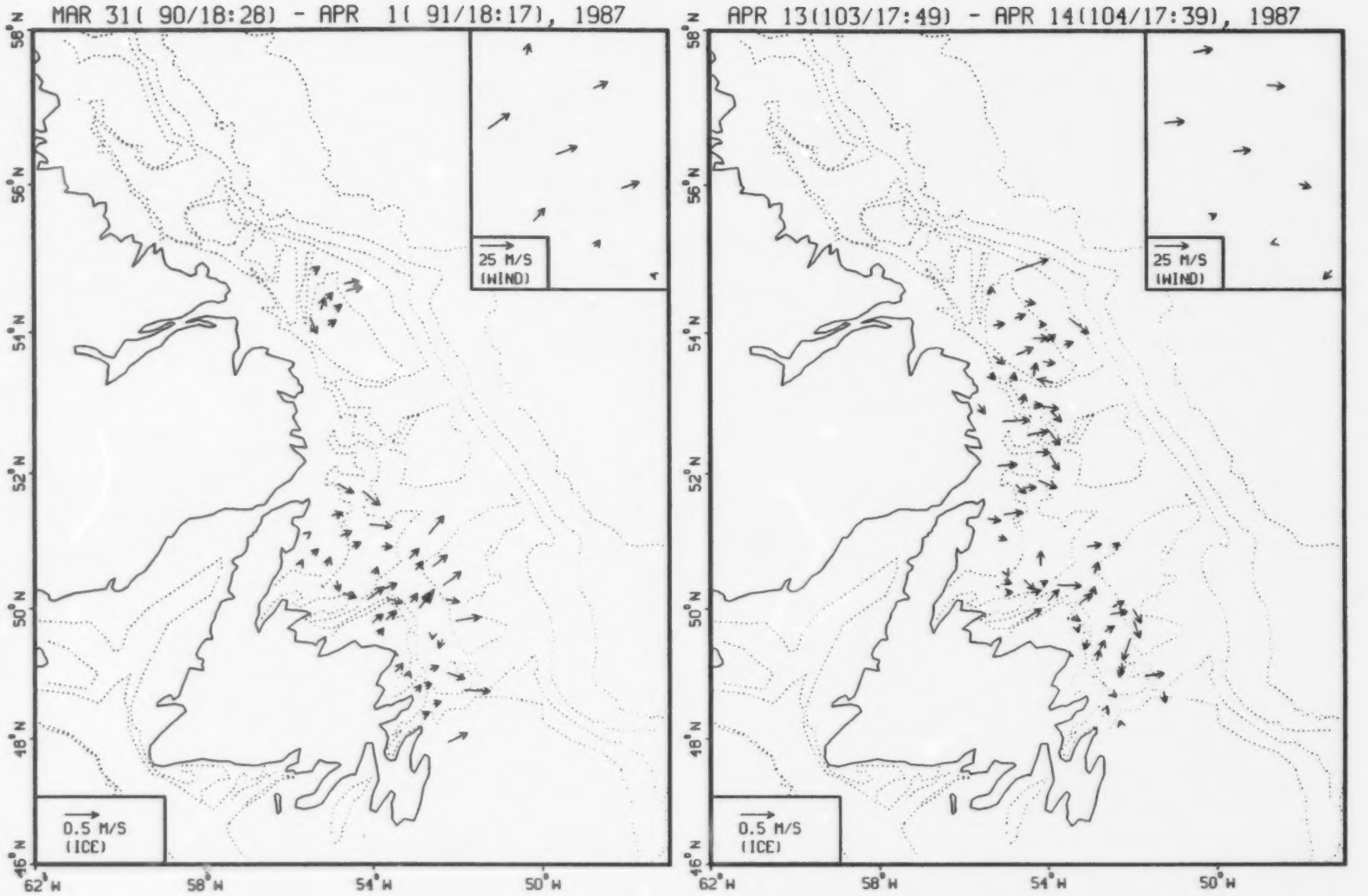
MAR 31( 90/18:28) - APR 1( 91/18:17), 1987
APR 13(103/17:49) - APR 14(104/17:39), 1987
25 M/S
(WIND)
0.5 M/S
(ICE)
58°N
56°N
54°N
52°N
50°N
48°N
46°N
62°W
58°W
54°W
50°W

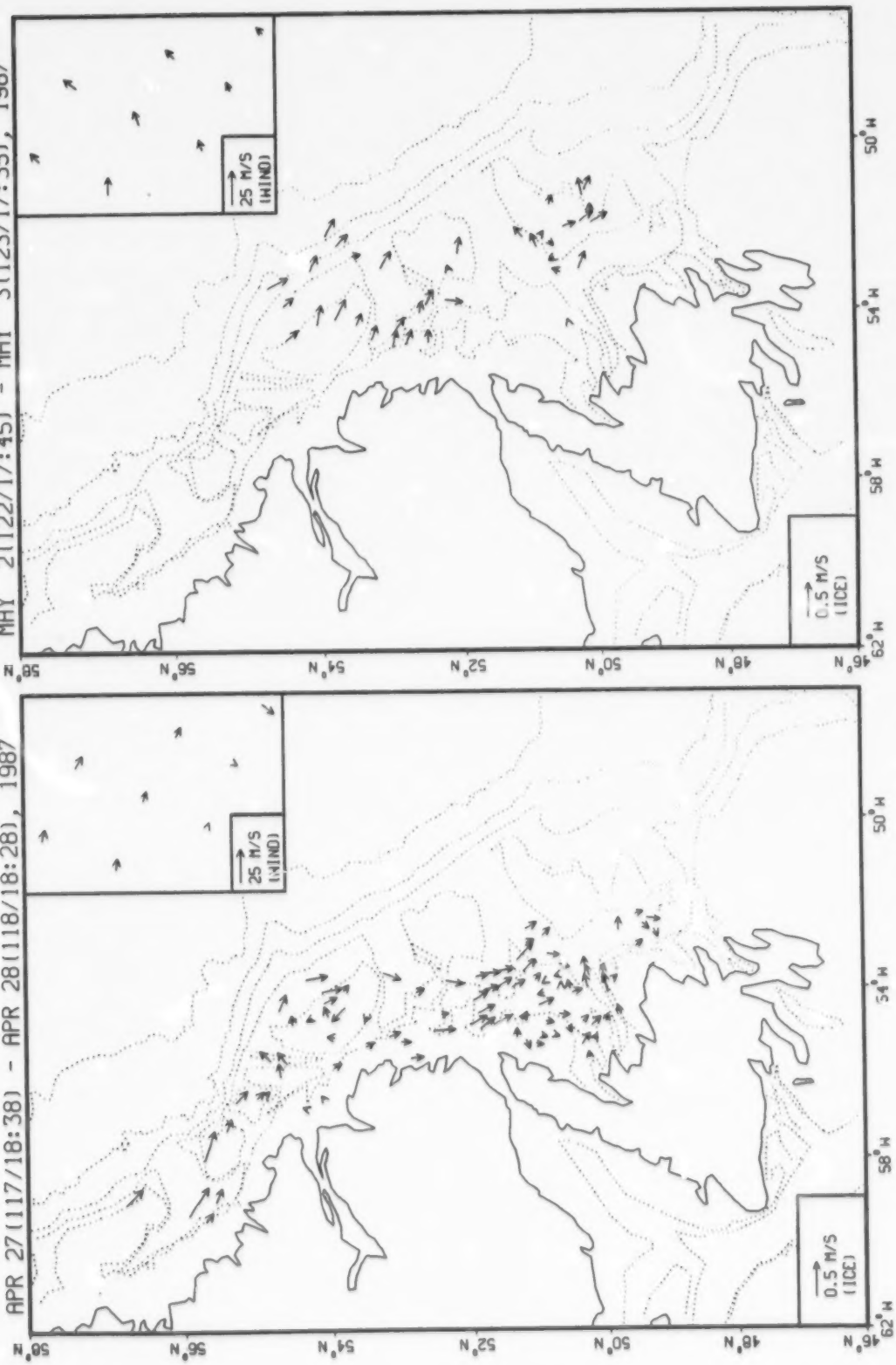
APR 27(117/18:38) - APR 28(118/18:28), 1987
25 M/S (WIND)
0.5 M/S (ICE)
MAY 2(122/17:45) - MAY 3(123/17:35), 1987
25 M/S (WIND)
0.5 M/S (ICE)
46°N
48°N
50°N
52°N
54°N
56°N
58°N
62°W
58°W
54°W
50°W

Appendix B. Examples of satellite imagery (1984-1987), approximately 500 km by 500 km. Figures B(1-12) show visible imagery off southern Labrador, centred at 54.5°N, 56°W, while figures B(13-20) show visible imagery east of Newfoundland, centred at 49.5°N, 52°W. Figures B(21-24) show infrared imagery from 1984, centred at 57.0°N, 54.0°W, with the visible imagery superimposed. The 200, 300, 1000, 2000, and 3000 m contours are plotted on all images.

B1

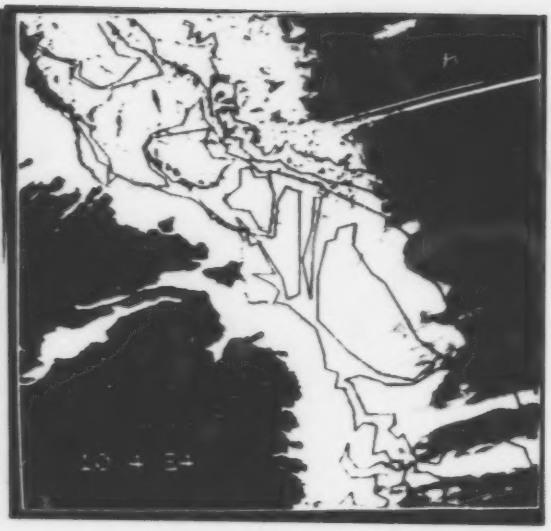

B2

B3

B4

B5

B6

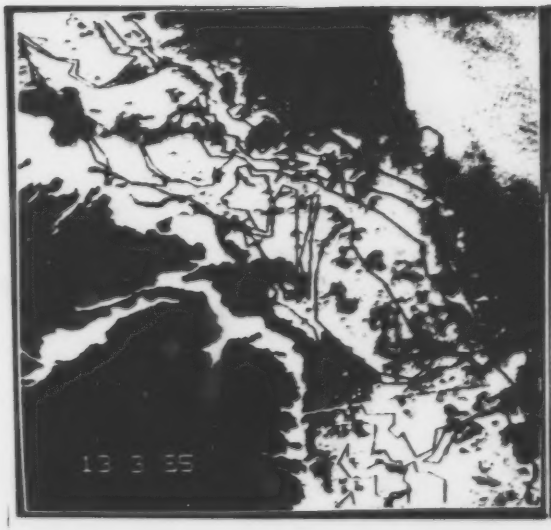


B7

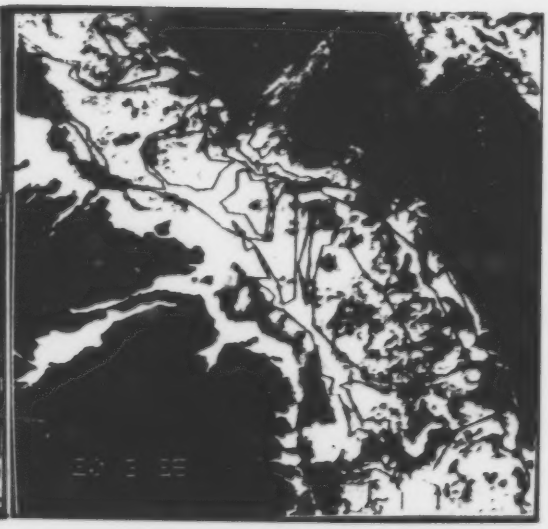

B8

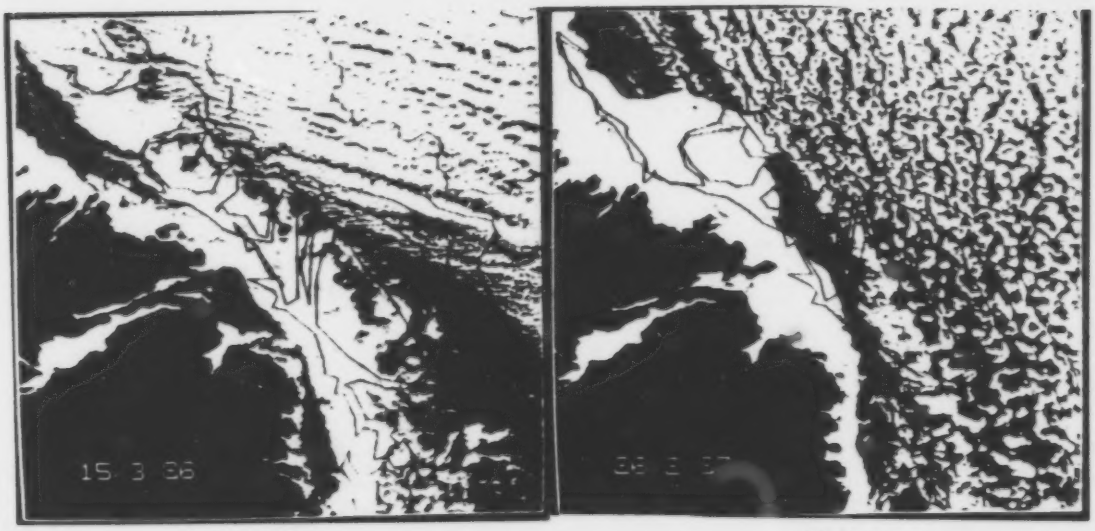


B9 B10

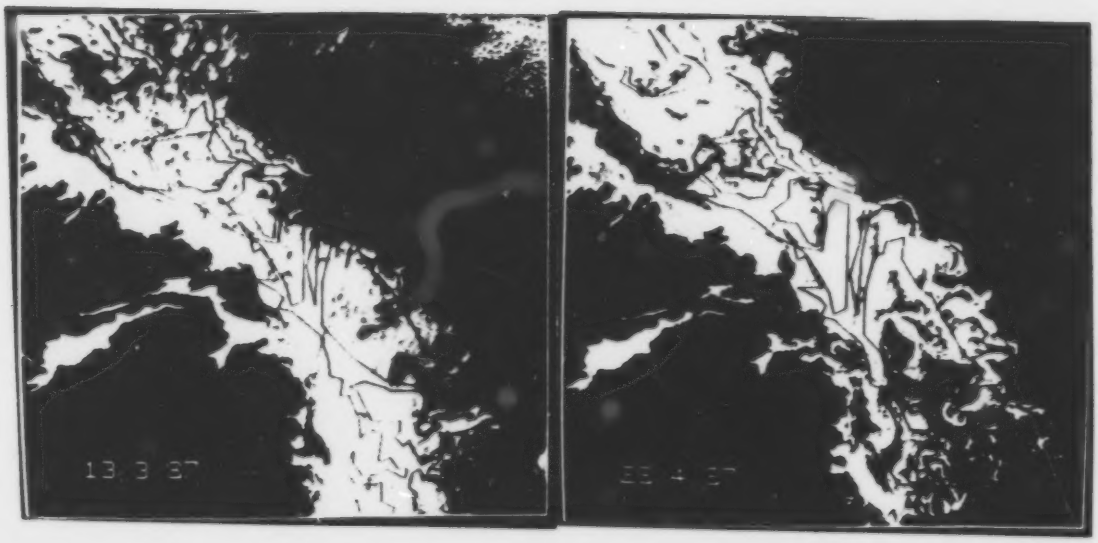


B11 B12

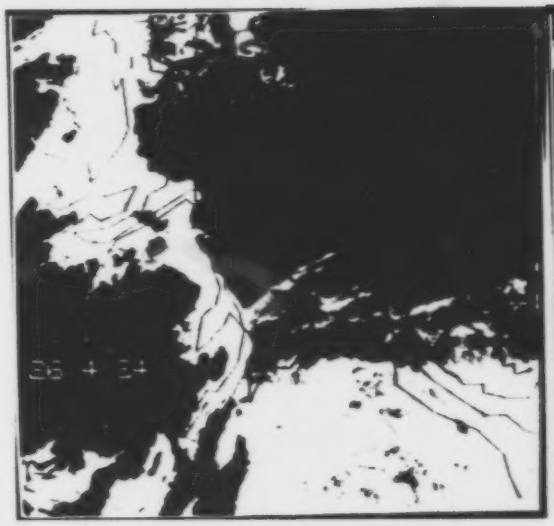

B13

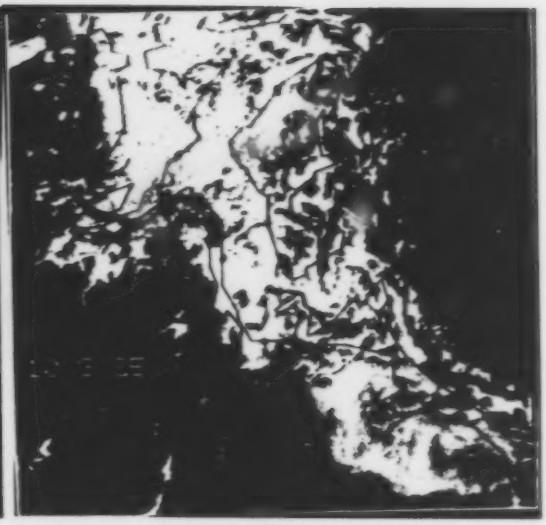

B14

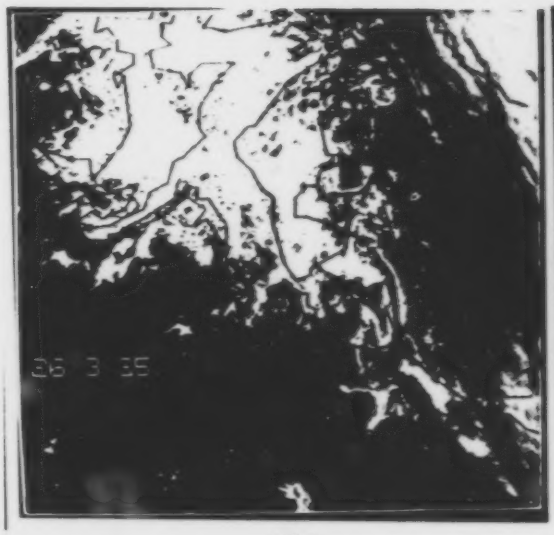

B15

B16

B17

B18

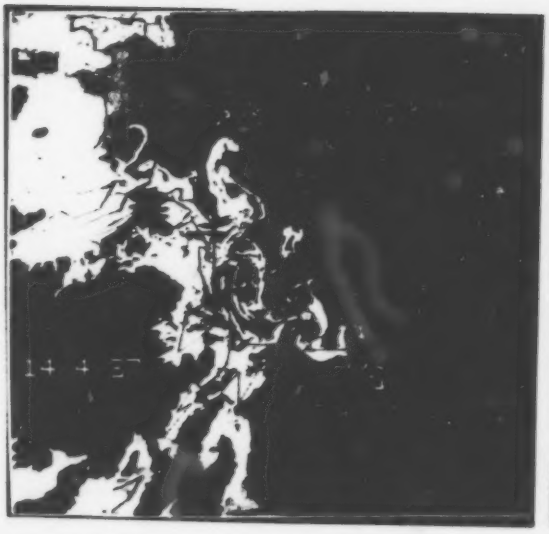

B19

B20

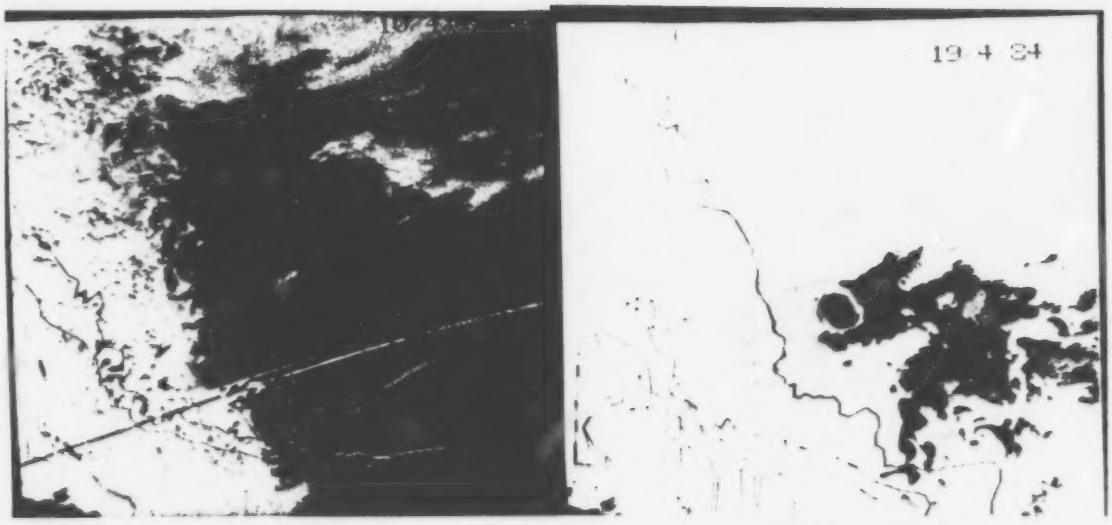

B21




B22

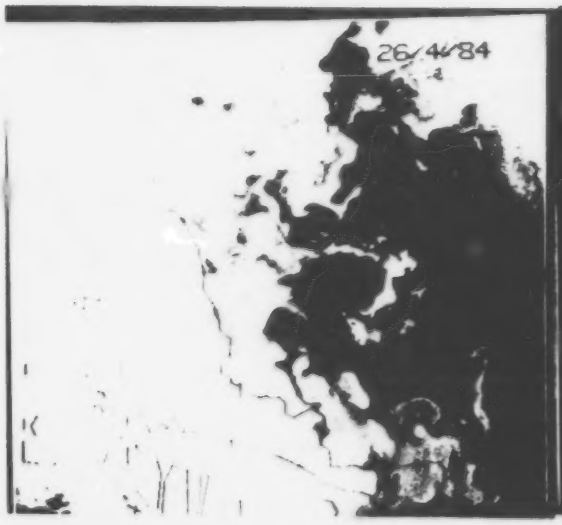


B23

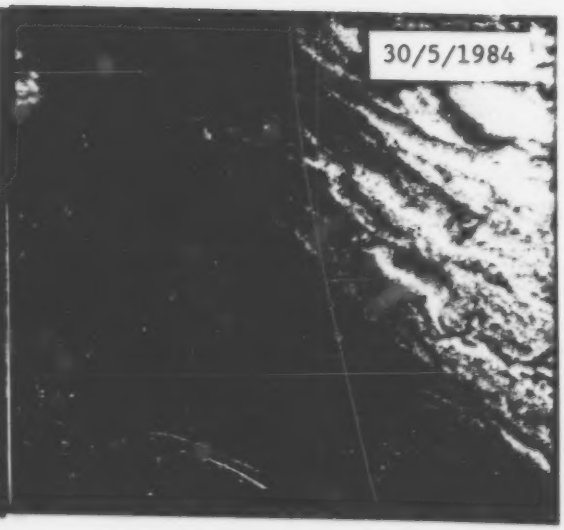


B24

Appendix C. Geostrophic winds at 52.8°N, 54.7°W (1984-1987), from late January to late May. The dates corresponding to the image pairs are indicated.

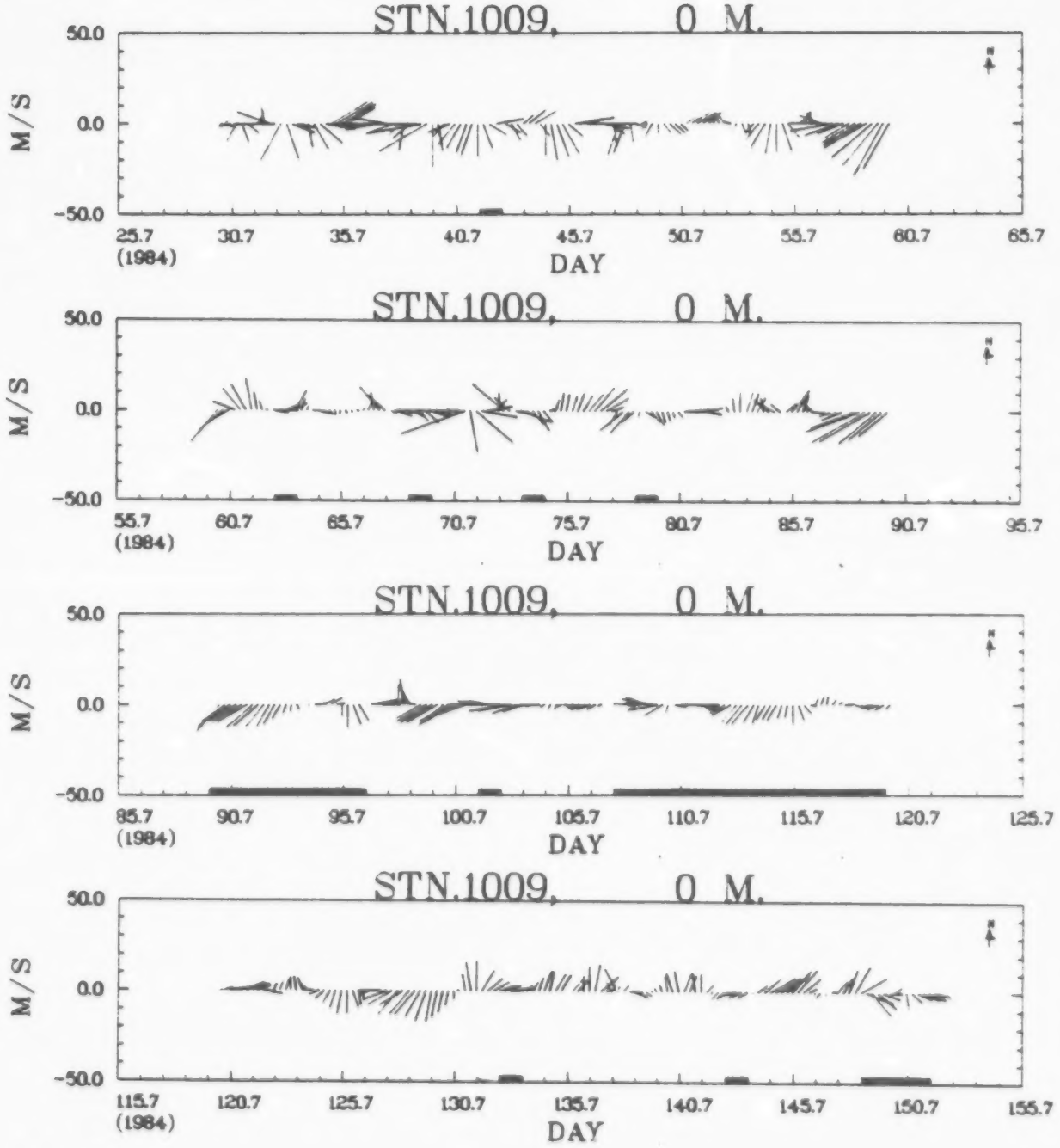
STN.1009, 0 M.
50.0
0.0
-50.0
M/S
25.7
(1984)
30.7
35.7
40.7
45.7
50.7
55.7
60.7
65.7
DAY
STN.1009, 0 M.
50.0
0.0
-50.0
M/S
55.7
(1984)
60.7
65.7
70.7
75.7
80.7
85.7
90.7
95.7
DAY
STN.1009, 0 M.
50.0
0.0
-50.0
M/S
85.7
(1984)
90.7
95.7
100.7
105.7
110.7
115.7
120.7
125.7
DAY
STN.1009, 0 M.
50.0
0.0
-50.0
M/S
115.7
(1984)
120.7
125.7
130.7
135.7
140.7
145.7
150.7
155.7
DAY

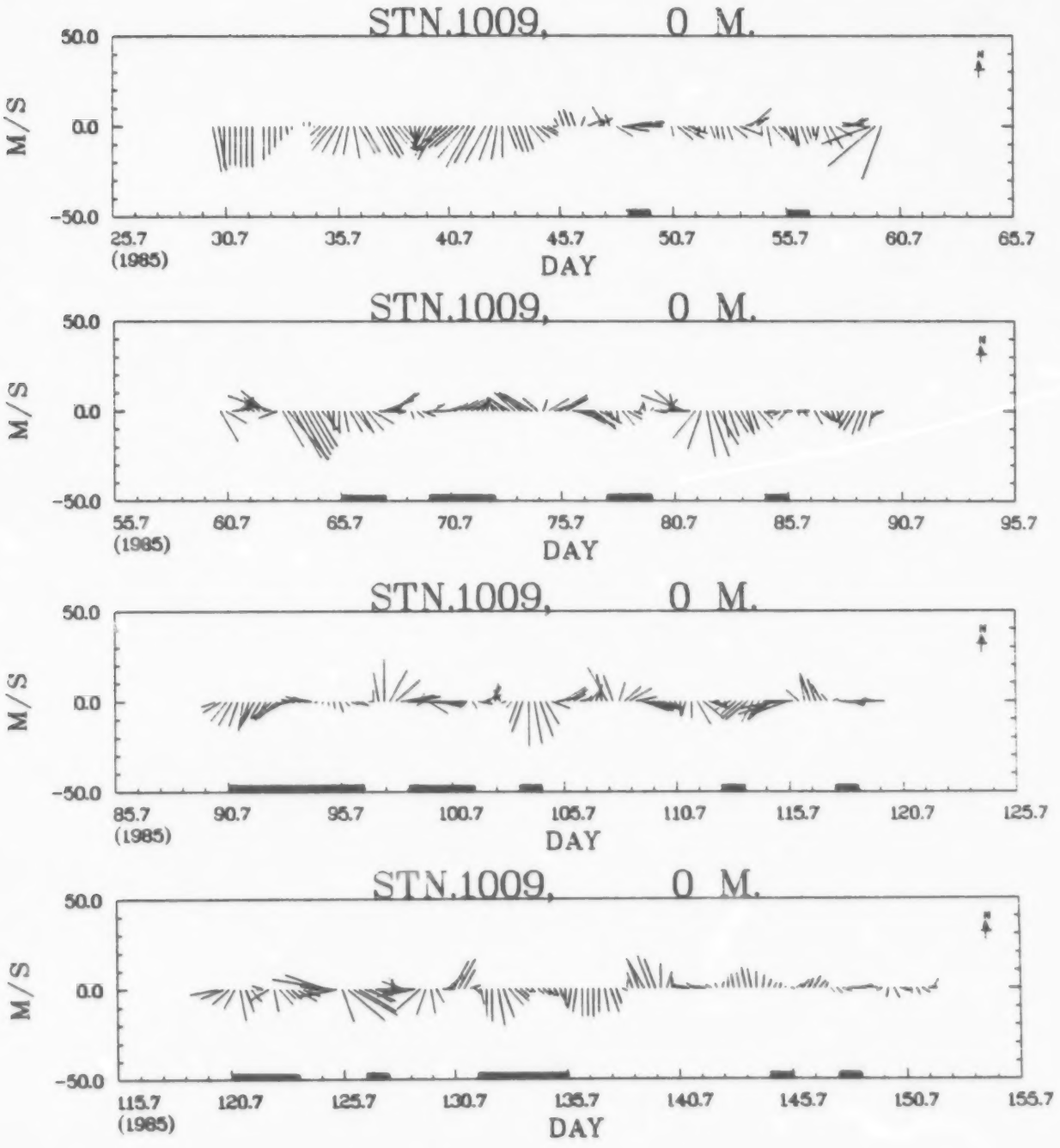
STN.1009, 0 M.
50.0
0.0
-50.0
M/S
25.7
(1985)
30.7
35.7
40.7
45.7
50.7
55.7
60.7
65.7
DAY
STN.1009, 0 M.
50.0
0.0
-50.0
M/S
55.7
(1985)
60.7
65.7
70.7
75.7
80.7
85.7
90.7
95.7
DAY
STN.1009, 0 M.
50.0
0.0
-50.0
M/S
85.7
(1985)
90.7
95.7
100.7
105.7
110.7
115.7
120.7
125.7
DAY
STN.1009, 0 M.
50.0
0.0
-50.0
M/S
115.7
(1985)
120.7
125.7
130.7
135.7
140.7
145.7
150.7
155.7
DAY

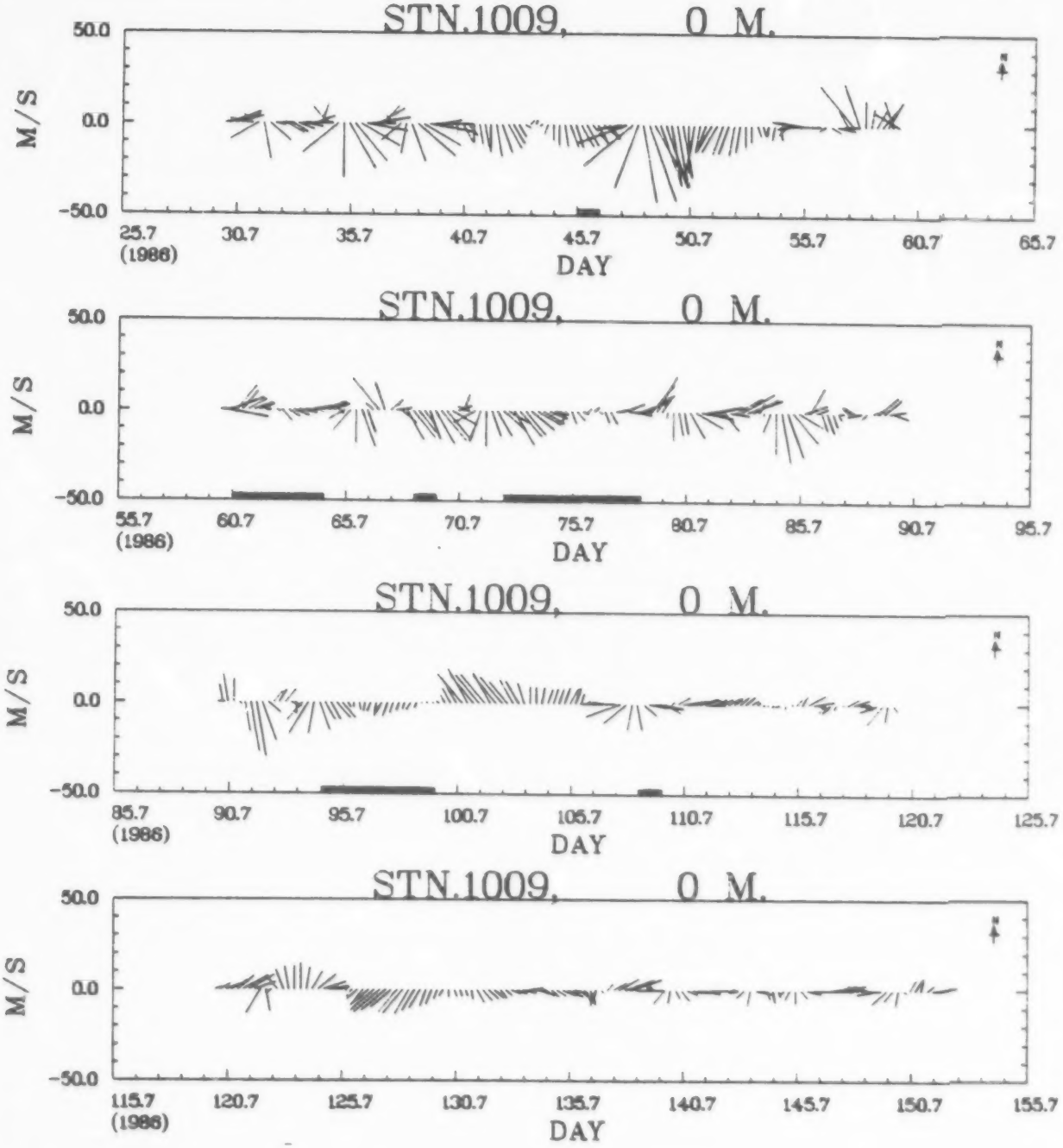
STN.1009, 0 M.
50.0
0.0
-50.0
M/S
25.7
(1986)
30.7
35.7
40.7
45.7
50.7
55.7
60.7
65.7
DAY
STN.1009, 0 M.
50.0
0.0
-50.0
M/S
55.7
(1986)
60.7
65.7
70.7
75.7
80.7
85.7
90.7
95.7
DAY
STN.1009, 0 M.
50.0
0.0
-50.0
M/S
85.7
(1986)
90.7
95.7
100.7
105.7
110.7
115.7
120.7
125.7
DAY
STN.1009, 0 M.
50.0
0.0
-50.0
M/S
115.7
(1986)
120.7
125.7
130.7
135.7
140.7
145.7
150.7
155.7
DAY

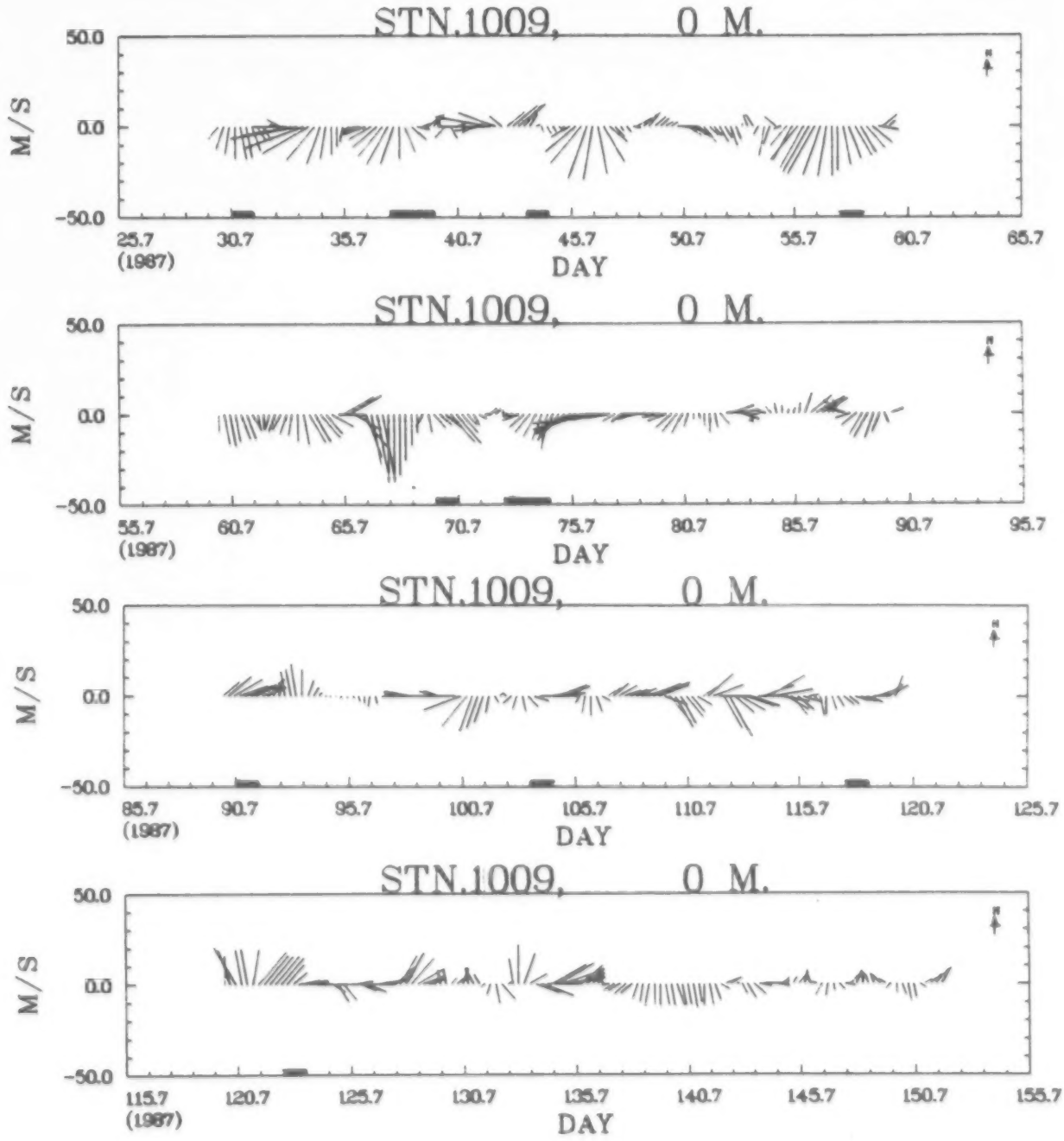
STN.1009, 0 M.
50.0
0.0
-50.0
M/S
25.7
(1987)
30.7
35.7
40.7
45.7
50.7
55.7
60.7
65.7
DAY
STN.1009, 0 M.
50.0
0.0
-50.0
M/S
55.7
(1987)
60.7
65.7
70.7
75.7
80.7
85.7
90.7
95.7
DAY
STN.1009, 0 M.
50.0
0.0
-50.0
M/S
85.7
(1987)
90.7
95.7
100.7
105.7
110.7
115.7
120.7
125.7
DAY
STN.1009, 0 M.
50.0
0.0
-50.0
M/S
115.7
(1987)
120.7
125.7
130.7
135.7
140.7
145.7
150.7
155.7
DAY